UNIVERSIDADE FEDERAL DE SANTA MARIA
CENTRO DE TECNOLOGIA
CURSO DE GRADUAÇÃO EM ENGENHARIA AEROESPACIAL

Augusto Cargnin Morcelli

INVESTIGATION OF THE PITCHING MOMENT COEFFICIENT INFLUENCE ON INDIVIDUAL PITCH CONTROL OF THREE-BLADED HORIZONTAL AXIS WIND TURBINES

Santa Maria, RS
2020

Augusto Cargnin Morcelli

INVESTIGATION OF THE PITCHING MOMENT COEFFICIENT INFLUENCE ON INDIVIDUAL PITCH CONTROL OF THREE-BLADED HORIZONTAL AXIS WIND TURBINES

Trabalho de Conclusão de Curso apresentado ao Curso de Graduação em Engenharia Aeroespacial da Universidade Federal de Santa Maria (UFSM, RS), como requisito parcial para obtenção do grau de **Bacharel em Engenharia Aeroespacial**.

ORIENTADOR: Prof. Carlos Eduardo de Souza

Santa Maria, RS
2020

Augusto Cargnin Morcelli

INVESTIGATION OF THE PITCHING MOMENT COEFFICIENT INFLUENCE ON INDIVIDUAL PITCH CONTROL OF THREE-BLADED HORIZONTAL AXIS WIND TURBINES

Trabalho de Conclusão de Curso apresentado ao Curso de Graduação em Engenharia Aeroespacial da Universidade Federal de Santa Maria (UFSM, RS), como requisito parcial para obtenção do grau de **Bacharel em Engenharia Aeroespacial**.

Submetido em setembro de 2020:

Carlos Eduardo de Souza, Dr. (UFSM)
(Presidente/Orientador)

Giuliano Demarco, Dr. (UFSM)

Humberto Pinheiro, Dr. (UFSM)

Ricardo Morim, Me. (UFSM)

Santa Maria, RS
2020

AGRADECIMENTOS

Àqueles que me cuidaram desde o berço e apoiam todas as minhas iniciativas, Mãe, Carol e Paulo, agradeço do fundo do meu coração por serem a mais sólida base que eu poderia ter para edificar a minha vida.

Agradeço pela orientação do professor doutor Carlos Eduardo de Souza, o qual acompanhou-me desde o início da graduação, constantemente exigiu o melhor de mim e, com sua paciência e didática, conseguiu conduzir-me enquanto eu desbravava o mundo fascinante da aerodinâmica e das turbinas eólicas.

Aos laços de amizade construídos e firmados dentro e fora do ambiente acadêmico, agradeço pelas muitas vezes que me sustentaram, motivaram e inspiraram a prosseguir. Em especial, estendo meus agradecimentos aos colegas Alan Pitthan, Fortunato Neto, Jonas Muller, José Carlos Zart, Luiz Henrique Soares e Nícolas Musskopf por tornarem minha experiência na graduação muito mais agradável. Que alcemos voos cada vez mais altos, juntos.

Faço questão de agradecer a todos os professores e servidores que passaram pela minha trajetória acadêmica. Também, deixo aqui registrado meu agradecimento a Universidade Federal de Santa Maria enquanto instituição e, claro, seu principal mantenedor: o pagador de impostos.

Por fim, agradeço ao meu companheiro que só se faz visível quando enxergo com o coração. Obrigado, Pai. Espero deixar-te orgulhoso.

RESUMO

INVESTIGAÇÃO DA INFLUÊNCIA DO COEFICIENTE DE MOMENTO AERODINÂMICO NO CONTROLE INDIVIDUAL DE PASSO DE TURBINAS EÓLICAS DE EIXO HORIZONTAL E TRÊS PÁS

AUTOR: Augusto Cargnin Morcelli
ORIENTADOR: Carlos Eduardo de Souza

A crescente demanda por energias renováveis impulsiona a exploração do vento no Brasil e no mundo. Esse mercado demanda das fabricantes turbinas e equipamentos cada vez mais duráveis, eficientes e maiores para captar mais energia do vento. Uma das consequências do aumento no tamanho dos aerogeradores é o aumento na intensidade e assimetria dos carregamentos estruturais no rotor. A redução desses carregamentos é sempre visada a fim de diminuir custos de manutenção e conferir maior durabilidade. O controle individual de passo das pás de turbinas eólicas apresenta-se como uma alternativa para redução de cargas ao longo de sua estrutura. Os efeitos desse tipo de controle de passo podem ser verificados através de simulações computacionais. Entretanto, simulações pouco detalhadas e com dados incompletos podem levar a predições ruins dos efeitos que ocorrem em uma turbina real, causando resultados e análises imprecisos. Logo, esse trabalho consiste em uma investigação sobre a influência do coeficiente de momento aerodinâmico em um controle individual de passo em simulações de turbinas eólicas de eixo horizontal e três pás realizadas no OpenFAST. Visto que o módulo aerodinâmico desse software requer coeficientes de sustentação, arrasto e momento de -180° até +180° e os dados fornecidos foram computados para uma pequena quantidade de ângulos de ataque, os modelos de correção de Du-Selig e Eggers e extrapolação de Viterna foram usados para tratamento de dados antes das simulações. Também, visto que o IPC utilizado não leva em consideração o momento torsional na raiz das pás para calcular os carregamentos no cubo da turbina, novas equações de transformação de coordenadas foram desenvolvidas, implementadas e testadas. Seguindo as recomendações da IEC 61400 Part 13, as principais variáveis analisadas nesse trabalho são os momentos na raiz das pás e momentos de arfagem e guinada do rotor. Os resultados das simulações indicaram que levar em considerar o coeficiente de momento aerodinâmico e implementar equações mais gerais não levaram a mudaçnas significativas nos momentos *edgewise* e *flatwise* da raiz das pás, tampouco nos momentos de arfagem e guinada do rotor, logo, não impactaram não dinâmica do controlador. Entretanto, o momento de torsão foi significativamente afetado ao considerar o coeficiente de momento nas simulações. Como isso pode impor restrições a um projeto de controle de passo, sugere-se introduzir esse coeficiente nos próximos estudos com o controle individual de passo para que resultados mais realistas sejam obtidos das simulações aerodinâmicas, mais espaço se abra para melhorias e um controlador ainda mais robusto.

Palavras-chave: Turbina Eólica. Aerodinâmica. Controle Individual. Passo. OpenFAST.

ABSTRACT

INVESTIGATION OF THE PITCHING MOMENT COEFFICIENT INFLUENCE ON INDIVIDUAL PITCH CONTROL OF THREE-BLADED HORIZONTAL AXIS WIND TURBINES

AUTHOR: Augusto Cargnin Morcelli
ADVISOR: Carlos Eduardo de Souza

The growing demand for renewable energy drives wind exploration in Brazil and worldwide. This market calls wind turbines manufacturers for longer-lasting, more efficient and larger structures and equipment to harness more energy from the wind. A size growth consequence is the increase in intensity and asymmetry of rotor structural loads. Load reduction is always aimed to low the maintenance cost and increase durability. Individual pitch control (IPC) of wind turbine blades emerged as an alternative to reduce loads along the turbine structure. The effects of this type of pitch control can be verified through computational simulations. However, poorly detailed simulations with missing data can lead to bad predictions of the effects on a real turbine, causing imprecise results and analysis. Thus, this work aims to investigate the influence of the aerodynamic pitching moment coefficient on an individual pitch control in simulations of horizontal axis and three-bladed wind turbines performed in OpenFAST. As this software aerodynamic module requires lift, drag and pitching moment coefficients from -180° to +180° and the data provided was computed only for a short range of angles of attack, Du-Selig and Eggers correction and Viterna extrapolation models were used to process the data before simulations. Also, as the utilized IPC did not take into account the blade root torsion moment during hub loads calculation, new coordinates transformation equations were developed, implemented and tested. Following recommendations from IEC 61400 Part 13, the main variables analyzed in this work are blade root, tilt and yaw rotor moments. The simulation results indicated that accounting pitching moment coefficient and implementing more general equations did not lead to significant change in edgewise, flatwise blade root bending moments and tilt and yaw rotor moments, thus not affecting significantly the controller dynamics. However, the torsional blade root moment was largely affected by taking pitching moment coefficient into account. As this may impose constraints to the pitch system design, it was suggested to introduce this coefficient in the next individual pitch control studies to obtain more realistic results from aerodynamic simulations, open up space for more improvements and an even more robust controller.

Keywords: Wind Turbine. Aerodynamics. Individual Pitch. Control. OpenFAST.

LIST OF FIGURES

LIST OF TABLES

LISTA DE SÍMBOLOS

C_l	2D lift coefficient (-)
C_d	2D drag coefficient (-)
C_m	2D pitching moment coefficient (-)
C_n	2D normal force coefficient coefficient (-)
C_t	2D tangent force coefficient (-)
c_p	Power coefficient (-)
v_∞	Undisturbed wind velocity (m/s)
v_{rel}	Relative wind velocity (m/s)
ρ	Flow density (kg/m^3)
P_W	Maximum available energy of the wind (W)
λ, TSR	Tip speed ratio (-)
Ω	Rotor speed or blade angular velocity (RPM)
R_{tip}	Rotor radius (m)
RMx	Blade root edgewise bending moment (kN.m)
RMy	Blade root flatwise bending moment (kN.m)
M_{tilt}	Rotor tilt moment (kN.m)
M_{yaw}	Rotor yaw moment (kN.m)
α, AoA	Angle of attack (°)
α_0	Zero lift angle of attack (°)
α_S	Stall condition angle of attack (°)
c	Airfoil chord (m)
β	Blade pitch angle (°)
θ	Local twist angle (°)
ψ	Azimuth angle (°)
ϕ	Yaw angle (°)
$\mathbf{RM_{b1}}$	Total root moment of blade 1 (kN.m)
$\mathbf{C_{b1h}}$	Coordinates transformation matrix from blade 1 to the hub (-)
$\mathbf{M_{h1}}$	Blade 1 root moment contribution for hub loading (kN.m)
$\mathbf{M_h}$	Total hub load caused by blades root moments (kN.m)

CONTENTS

1 INTRODUCTION

1.1 MOTIVATION

As a means to avoid the use of fossil fuels, more sophisticated tools are being created to increase the efficiency and low the cost of renewable energy generation. The downward trend in cost of wind and solar energy gathering is opening more space for these renewable options. Nowadays, the total installation cost global average of onshore and offshore wind farms is respectively 1473 USD/kW and 3800 USD/kW, which is 24 and 18% cheaper than 10 years ago. Operational and maintenance (OandM) costs also dropped more than 50% in the last decade for onshore turbines, now ranging from 33 USD/kW to 56 USD/kW. These drops impacts the cost of wind energy generation, which the 2019 average value (levelized cost of energy, LCOE) were 0.053 USD/kWh and 0.115 USD/kWh for onshore and offshore wind farms, respectively. Currently in some parts of the world (including Brazil, India, Sweden, United States and others), new onshore wind energy farms projects are cheaper than the cheapest fossil fuel-powered generation power plants (IRENA, 2020b).

According to IRENA (2020a), IEA (2019b), IEA (2019a), the worldwide installed capacity and energy generation from renewable sources reached 2.5 TW by the end of 2019 and 6500 TWh in 2018. Out of this, wind energy holds a great share: approximately 0.62 TW (8.6% of the global installed capacity) and 1263 TWh (approximately 5% of the global electric energy generation). In Brazil, the wind energy installed capacity reached 15.4 GW in February 2020 (9% in the country) (ONS, 2020; EPE, 2019) and it contributes with 50 TWh (8.3%) to brazilian energy generation. Bringing these numbers to reality, the Complexo Eólico de Osório, with generation capacity of 318 MW, is capable of powering more than 450,000 houses annually (Enerfín do Brasil, 2019).

Besides already holding a considerable share, the installed capacity of wind energy in Brazil tends to keep growing. According to ABEEólica (2019), until 2024, considering the ongoing projects, Brazil will have more than 19 GW of installed capacity of wind energy (Figure 1.1).

The high capacity factors of Brazilian power plants must also be highlighted. In October 2019, the average capacity factor registered was about 55% (ONS, 2019). The major indexes are from the northeast wind power plants, which the average capacity factor of one of its plants reached 74% in the state of Maranhão. The other states of northeast do not stay behind, having an average capacity factor greater than 60% in the most of them. To compare with another countries, the 2018 annual average capacity factor of Europe were 24% (WINDEUROPE, 2018) and in the US, approximately, 45% (US DOE, 2017).

Figure 1.1 – Evolution and growth forecast of installed wind capacity in Brazil.

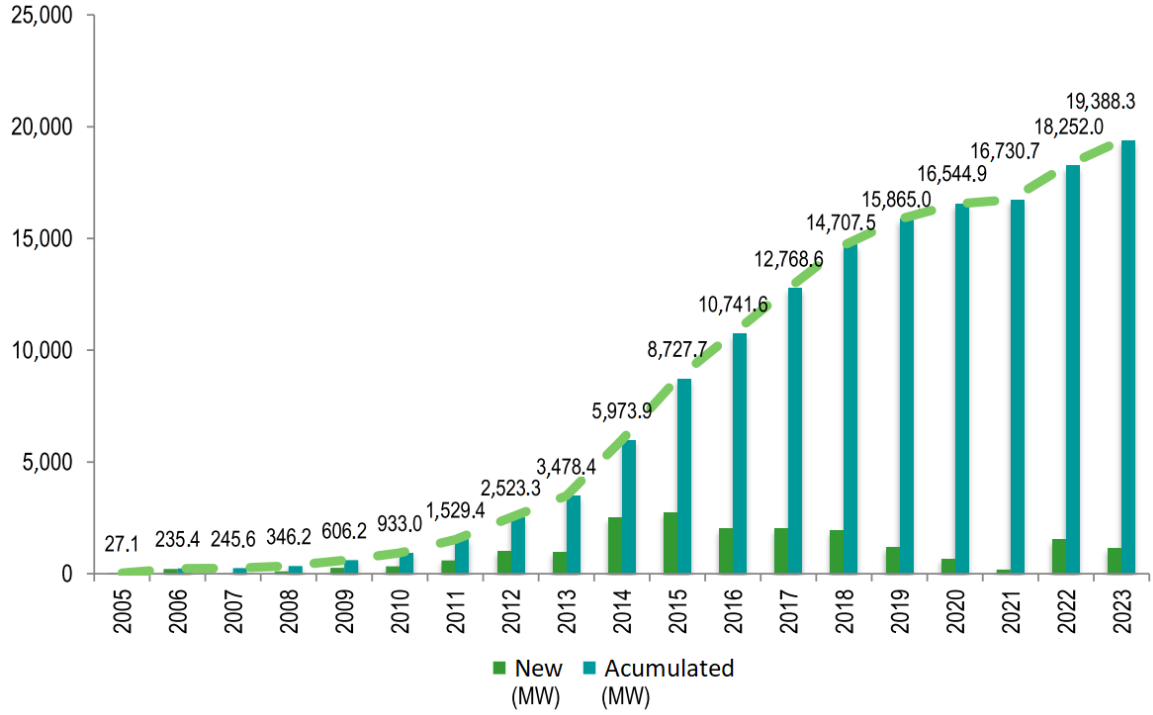

Source: Adapted from ABEEólica (2019)

There are several efforts of wind turbines (WTs) manufacturers and the academy to create, test and implement new systems to make turbines bigger, to raise the wind area covered by the rotor, more efficient, to harness more of the available energy, and longer-lasting. As turbines grow in size, asymmetrical loads intensity also increases, which raises maintenance cost and may low turbine lifespan. Components failure rate and downtime throughout annual operation (example seen in Figure 1.2) may also be affected by WT size increase. An alternative that emerged from these efforts to preserve the structure from higher loads is the individual pitch control (IPC) of wind turbine blades, firstly presented by Bossanyi (2003). Over the years, other models were presented, such as the IPC based on Robust Model Reference Adaptive Control (RMRAC), given by Morim (2019), Morim et al. (2019), and the IPC based on Sliding Mode Control (SMC), given by Xiao et al. (2013).

Implementation of new technologies generally are very costly. To low its cost and failure probability, researches are made initially with computer-aided engineering (CAE). Also, CAE tools are frequently used for design studies. Today, there are many software that are able to simulate a wind turbine. One of the most featured software for wind turbines simulation is OpenFAST, which stands for Fatigue, Aerodynamics, Structural and Turbulence, developed by the National Renewable Energy Laboratory (NREL). Its modular code structure makes it very flexible and gives it many uses. One of them is to substitute the control module given by the software to an user-made one.

Figure 1.2 – German wind turbines components reliability .

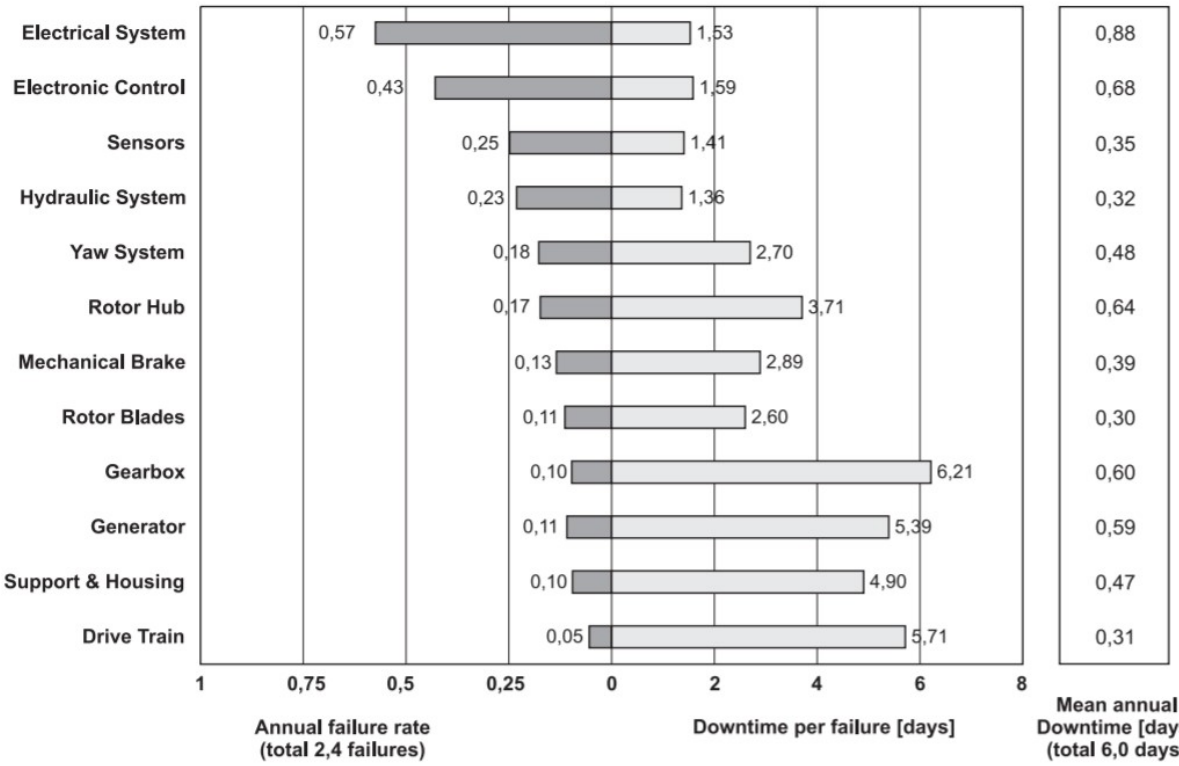

Source: Copied from Faulstich et al. (2011)

In the field of wind turbine models simulations, just like in real ones, aerodynamics is one of the most important modules. Therefore, it is necessary to have a proper set of aerodynamic data in the simulations to predict accurately the aerodynamic effects on a real turbine. The three main aerodynamic coefficients involved in aerodynamic forces and moments calculations are the lift, drag and pitching moment coefficients.

In OpenFAST simulations, it is possible to run aerodynamic calculations with or without the pitching moment coefficient. As an example of the possible impact of this coefficient, it is expected that its absence cause imprecise results of the torsional moment at the blade root. According to Manwell et al. (2010), this result is very important for the actual design of the control system mechanisms as it usually consists of electrical or hydraulic actuators.

1.2 OBJECTIVES

Therefore, this work primary objective is to investigate the influence of the pitching moment coefficient in an individual pitch control applied to a three-bladed horizontal axis wind turbine (HAWT). This work is done based on the framework defined by Morim (2019), Morim et al. (2019), in which the IPC was implemented but using a simplified aerodynamic model. As secondary objective, new blade root to hub coordinates transformation were developed, implemented and tested to analyze any impact on the turbine and IPC dynamics.

2 LITERATURE REVIEW

A consequence of increasing size and flexibility of wind turbine blades is the increase of the aeroelastic effects intensity. Interested in these effects, Wang et al. (2016) discuss the advantages and disadvantages of the most commonly used software in wind turbine simulation and review the main methods of aerodynamic and structural modeling and analysis of the blades cross sections, main aspects of aeroelastic modeling. The most used methods can be seen in Figure 2.1 in the form of a flowchart. The software that the article gathers to evaluate can be seen in Table 2.1, which also shows which method of aerodynamic and structural modeling is used in each of these.

Figure 2.1 – Main methods of wind turbines modelling.

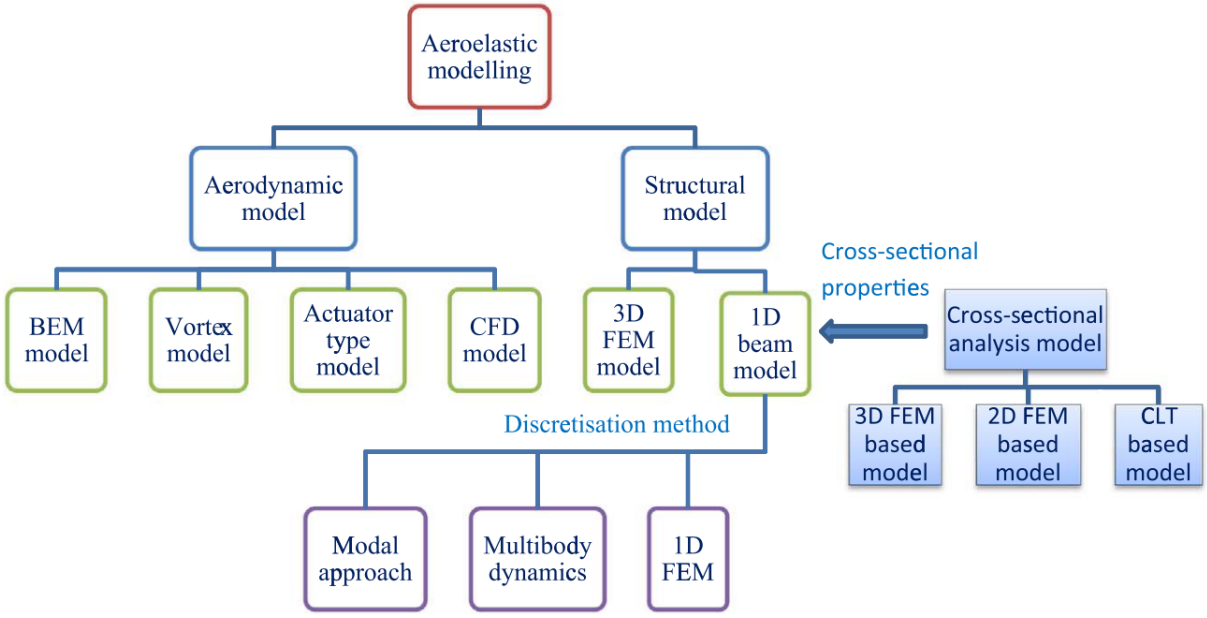

Source: Copied from Wang et al. (2016)

Table 2.1 – Overview of aeroelastic models used in wind turbine simulation software.

Name	Structural part		Aerodynamic part	Requires blade cross-sectional properties?
	Blade representation	Discretization method		
ADAMS/WT	1D beam	MBD	BEM	Yes
OpenFAST	1D beam	Modal approach	BEM	Yes
FLEX5	1D beam	Modal approach	BEM	Yes
GAST	1D beam	1D FEM	Free-wake vortex	Yes
GH-Bladed	1D beam	Modal approach	BEM	Yes
HAWC2	1D beam	MBD	BEM	Yes
PHATAS	1D beam	1D FEM	BEM	Yes

Source: Adapted from Wang et al. (2016)

Wang et al. (2016) concluded that the blade element momentum (BEM) and one-dimensional beam models are the ones that require less computational effort and present reasonably accurate results, which justifies most of the software using these two methods. Computational fluid dynamics (CFD) analysis and 3D finite elements make it possible to visualize the flow around the blades and structure stress distribution, very important information in a more detailed analysis, but with a much higher computational cost.

Among the software cited in Table 2.1, one of the most featured is OpenFAST. The US National Renewable Energy Laboratory (NREL) developed this software and still provides updates and documentation about its use, which is completely free. Recently, many changes have been made to the code structure and some modeling methods, mainly aerodynamic and structural, have been updated to decrease processing time and refine the results given by the program. Also, in 2017, NREL enabled an integrated development with the users community through the development platform GitHub (JONKMAN, 2018).

OpenFAST assumes a prominent role among other software for being completely open and modular, that is, the user can decouple parts of the code structure to execute independent module simulations. This software flexibility grants to its users many information, which can be used for many different purposes. For example, Liao et al. (2012) uses blade tip maximum deflection, calculated through OpenFAST, as one of the parameters to optimize blade mass distribution using a modified Particle Swarm Optimization (PSO) algorithm.

This WT simulation software has also been used in the analysis of offshore wind turbines. It has an internal hydrodynamics module called HydroDyn. But as any OpenFAST module can be replaced, Jose et al. (2018) coupled it to SIMDYN, a program developed by Marine Dynamics Laboratory capable of predicting the non-linear forces of fluids, in this case, ocean waves, which play a relevant role in parametric excitation problems.

Recently, according to Jonkman et al. (2017), NREL is developing a structural and performance analysis tool for wind farms which includes turbulence drag effects. The new software, which will be called "FAST.Farm", is already serving as a research source, mainly aimed to validation (JONKMAN et al., 2018). This article shows that the program has already been validated to single turbine and three wind turbines scenarios.

As Beltran et al. (2012) show, OpenFAST can be used to test different control laws in wind turbines. In that work, a Second-Order Sliding Mode was used in the generator to maximize output power. Another example can be seen in Morim (2019), in which an individual pitch control (IPC) of the blades was implemented to reduce turbine asymmetrical loads. One of the reasons why OpenFAST was chosen to perform the simulations in these works is because it has a friendly interface with MATLAB Simulink.

Active blade pitch control is the classification designated to individual and collective pitch controllers. This type of control can be used in conjunction with generator torque control to maximize wind energy harness below rated wind speed and restrain power above

this limit. IPC also have a significant impact on blade root and hub fatigue loads. Dr. Ervin Bossanyi studied and designed individual pitch controllers from the load reduction standpoint, aiming to mitigate asymmetrical loads caused by unequal wind incidence. Initial implementations based on Proportional Integral (PI) control achieved 20 to 30% fatigue load reduction. (BOSSANYI, 2000; BOSSANYI, 2003; BOSSANYI, 2005)

Since then, other IPC strategies were tested and adopted by other authors. Instead of using rotor loads as IPC inputs, Larsen et al. (2005) design a controller that considers local angle of attack and relative wind velocity measurements. Compared to a traditional collective pitch controller, the flow-based PI IPC was able to reduce more than 20% of rotor and blade root moments. Xiao et al. (2013) propose an SMC-based IPC to mitigate asymmetrical loads and concludes that it outperforms PI IPC, specially in turbulent wind conditions. Following a similar comparison, Morim (2019) presents a RMRAC-based IPC, which reduced fatigue loads in a wider frequency range and had a lower influence in rotor speed compared to a PI controller. Individual pitch control topic provide researches until today and further studies can be made about its capability of mitigating wind turbine loads. Later on this work, IPC mechanisms are detailed.

Another possibility for load reduction emerged from active pitch control coupling with active aerodynamic load control. An combination of these two methods is given by He et al. (2018), which couples an IPC to a trailing edge flap control (TEFC) to mitigate low and high frequency loads, respectively. Besides TEFC, other techniques were designed and tested to mitigate loads by influencing the aerodynamics around wind turbine blades. Some of them are summarized in a review proposed by Dam et al. (2008).

Although the use of OpenFAST is extensive, any software presents an error rate relative to experimental or real data from the system under study. Perez-Becker et al. (2020) does an aerodynamic modeling method comparison between OpenFAST (which uses BEM) and QBlade, a software developed by the Technical University of Berlin (TU Berlin). It concludes that, due to simplifications assumed by the method and by the various engineering corrections implemented to consider different effects (such as blade tip loss and oblique inflow), BEM can overestimate aerodynamic loads. An implemented effects comparison between BEM and the Lifting Line Free Vortex Wake-Method (LLFVW), used in QBlade, can be seen in Table 2.2, which ”I” means the feature is intrinsic to the method and ”EM” means the effect is considered due to an engineering model. It is observed that the LLFVW needs to make much less corrections through additional models compared to BEM. This reflects in simulation results, as LLFVW predicts 4% and 14% lower blade root and tower base moments. Therefore, when it comes to predicting fluid behavior and its interaction with the turbine structure, it results in a more accurate response than the obtained by BEM.

Another important aspect of aerodynamic wind turbine simulations is tower and nacelle influence. Santoni et al. (2017) investigated this by comparing the turbine wake results

in two different cases: considering and neglecting tower and nacelle in simulations. Figure 2.2 shows side (left column) and top (right column) views of the simulated turbine. Simulations (C) and (G) ignore tower and nacelle and the figure shows the turbulent kinetic energy for a tip speed ratio (λ, defined later in this work) of 6.

Table 2.2 – Comparison between BEM and LLFVW

Aerodynamic Phenomenon	**BEM**	**LLFVW**
Axial/Tangential induction	I	I
Radial induction	-	I
Tip- and root-loss	EM	I
Oblique inflow	EM	I
Turbulent wake state	EM	I
Wake memory effect	EM	I
Stall delay	EM	EM
Dynamic stall	EM	EM
Tower shadow	EM	EM

Source: Copied from Perez-Becker et al. (2020)

It can be noticed that the presence of tower and nacelle in the simulations influences the wake dynamics significantly, which plays an important role for aerodynamic loads calculation. High turbulence areas are generated around these structures and its influence propagates way beyond the turbine. Tower wake interacts with the one created by blade rotation, promoting tip vortex breakdown and increasing mean kinetic energy. Santoni et al. (2017) concludes that, specially for a wind farm where one turbine wake becomes the incoming wind of another, modeling tower and nacelle aerodynamics is crucial to obtain more accurate results.

Figure 2.2 – Color contours of turbulent kinetic energy in turbine side-view, (left column) and top-view (right column) with (D, H) and without (C, G) tower and nacelle.

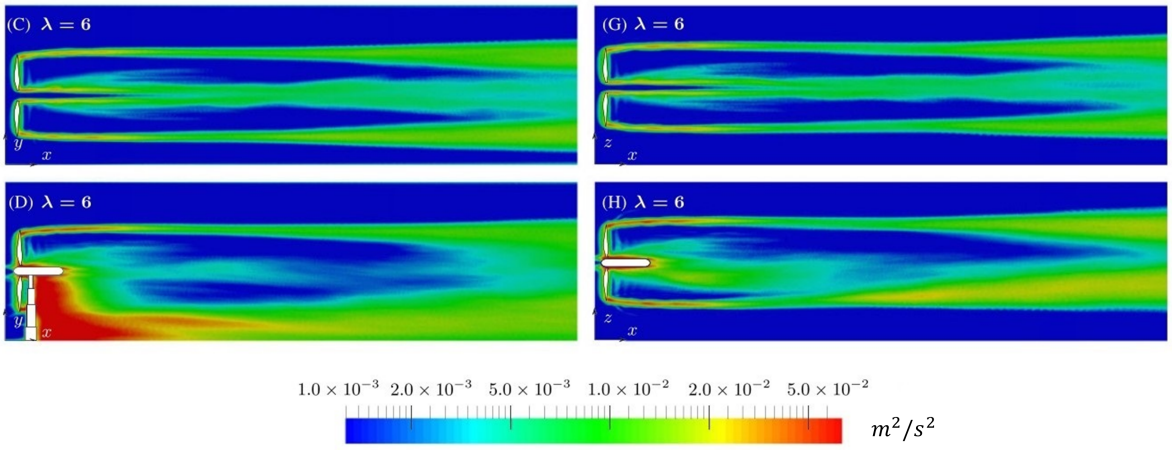

Source: Adapted from Santoni et al. (2017)

3 THEORETICAL REVIEW

The history behind wind turbines is very extensive. Burton et al. (2011) brings historical features briefly and Spera (2009) breaks it down from the different possible origins of windmills in ancient time to modern multi-MW (also referred as utility-scale) wind turbines. Since 1965, the study about windmills (and other types of mills, e.g. watermills), its historical, technical and cultural knowledge is called molinology.

The idea of harnessing the wind kinetic energy is not recent. Windmills consists basically of machines that convert this kinetic energy into mechanical energy in a shaft. Wind turbines adds one extra step, converting the mechanical energy in the shaft into electricity through an electrical generator. The wide use of these machines and the progress of modern physics, aerodynamics and science in general lead to studies about wind turbines theory, efficiency and other technical aspects.

3.1 BASIC CONCEPTS OF WIND TURBINES

Energy is the capacity to execute work. Power is the rate this work is done or that energy is transmitted. It is possible to calculate the available power of a wind flowing with a constant free stream velocity v_∞ perpendicular to a small area A_r, as it is demonstrated by Schaffarczyk (2014).

After a short time dt, this area moves shortly and constantly as $ds = v_\infty\, dt$. Thus, the volume created is $dV = A_r\, ds = A_r\, v_\infty\, dt$. Constant flow density can be assumed, which leads to $dm = \rho\, dV = \rho\, A_r\, v_\infty\, dt$. The differential form of kinetic energy is commonly calculated as $dE_{kin} = \frac{1}{2} dm\, v_\infty^2$. Power is commonly calculated as $P = dE/dt$. Thus, the power of a wind with velocity v and constant area A_r is

$$P_w = \frac{1}{2}\, \rho\, A_r\, v_\infty^3. \tag{3.1}$$

Equation 3.1 is the maximum available power in the wind that can be harnessed and, as Hansen (2015) mentions, this is very important because makes clear the relation between wind power and the cube of its velocity.

As it is the maximum available energy, it is known that is only possible to harness the maximum value in an ideal case. A real wind turbine can harness only a fraction of this value. The ratio between the actual power obtained and the ideal maximum power is called power coefficient c_p, defined as

$$c_p = \frac{P}{P_w} = \frac{P}{\frac{1}{2}\, \rho\, A_r\, v_\infty^3}, \tag{3.2}$$

which P is the actual power obtained. Without any consideration of design or wind con-

ditions, it is possible to determine the maximum value of the power coefficient, which is $c_{p,max} = 16/27 \approx 0.593$. This is derived from principles of conservation of mass and momentum, a study proposed by the German physicist Albert Betz in 1919. (HANSEN, 2015; BURTON et al., 2011; SPERA, 2009; SCHAFFARCZYK, 2014)

According to Hansen (2015), power coefficient of modern wind turbines reach around 85% of Betz limit. It is important to emphasize the difference between power coefficient and capacity factor. This is defined as the ratio between actual power generated and the maximum possible power the wind turbine or power plant could generate. The maximum possible power is the power extracted from the turbine operating with its nominal capacity without any stop. Capacity factors are usually measured by periods of time and are used to compare maintenance shut-down duration, failure rate and other operational parameters.

As almost all wind turbines use rotors to harness wind energy, its angular velocity (rotor speed, Ω), given in terms of RPM, is a very important information about the turbine operational state. Another very important parameter known as tip speed ratio (TSR, λ) relates the speed of the blade tip with the relative wind speed v_{rel},

$$\lambda = \frac{v_{tip}}{v_{rel}} = \frac{\pi \, \Omega \, R_{tip}}{30 \, v_{rel}}, \tag{3.3}$$

where R_{tip} is the radius of the rotor. It is necessary to multiply by a $\pi/30$ term to convert rotor speed from RPM to radians per second. Another important theoretical limit of wind turbines efficiency was written by the British aerodynamicist Hermann Glauert and published by Durand et al. (1935). His studies about propellers efficiency, takes into consideration the losses for low values of λ. Both cited limits can be seen in Figure 3.1.

In wind turbines load frequency analysis, it is very common to name the rotor speed (Ω) in radians per second or Hertz as 1P frequency (one cycle per rotor revolution). In other words, 1P cyclic loads or effects occur once per rotor revolution. This frequency serve as a benchmark to other effects that happens two or more times per revolution (2P, 3P, etc.).

It is interesting to state that many concepts and physical principles of wind turbine rotors are also applicable to aircraft propellers. Although the typical tip speed and use of this two technologies are very different (the first one decelerates the wind and the second one accelerates it to generate thrust), some of the aerodynamic phenomenons of wind turbines were first noticed and studied in propellers, such as tip speed ratio, stall delay and the tip-loss problem. The physical and mathematical description of propellers and wind turbines theory goes beyond the scope of this work. Other subjects such as rotor and actuator disk theory, induction factors, wake rotation and blade element theory are discussed in Manwell et al. (2010), Burton et al. (2011), Spera (2009), Schaffarczyk (2014).

3.1.1 Types

As Schaffarczyk (2014) and Manwell et al. (2010) explicits, and can also be seen in Figure 3.1, there are several wind turbine types. Focusing in the most common ones, two groups must be highlighted: horizontal (HAWTs) and vertical axis wind turbines (VAWTs).

HAWTs are the most common type. This name refers to the main shaft of the wind turbine being almost parallel to the ground surface, which is the opposite of VAWTs. Although this is a simple concept, misunderstandings were common as the old terminology usually defined the ”horizontal” or ”vertical” adjective referring to the blades rotation plane. (SPERA, 2009)

Another important classification is which orientation relative to the wind the rotor is generally facing: downwind or upwind turbines. According to the International Electrotechnical Commission (IEC) document, IEC 61400-1 (British Standards Institution, 2014), upwind orientation is the opposite of wind vector and downwind orientation points the same way as wind vector does. For wind turbine definition purposes, the rotor of upwind turbines receives the wind before it passes through the tower. In downwind turbines, it is the opposite. The tower impact in the flow, usually called tower shadow, must be considered for downwind turbines in the amount of power harnessed, blade aerodynamics, turbine dynamics and noise generation. According to Manwell et al. (2010), this type of turbine is typically noisier than upwind turbines.

Figure 3.1 – Wind turbine types and limits.

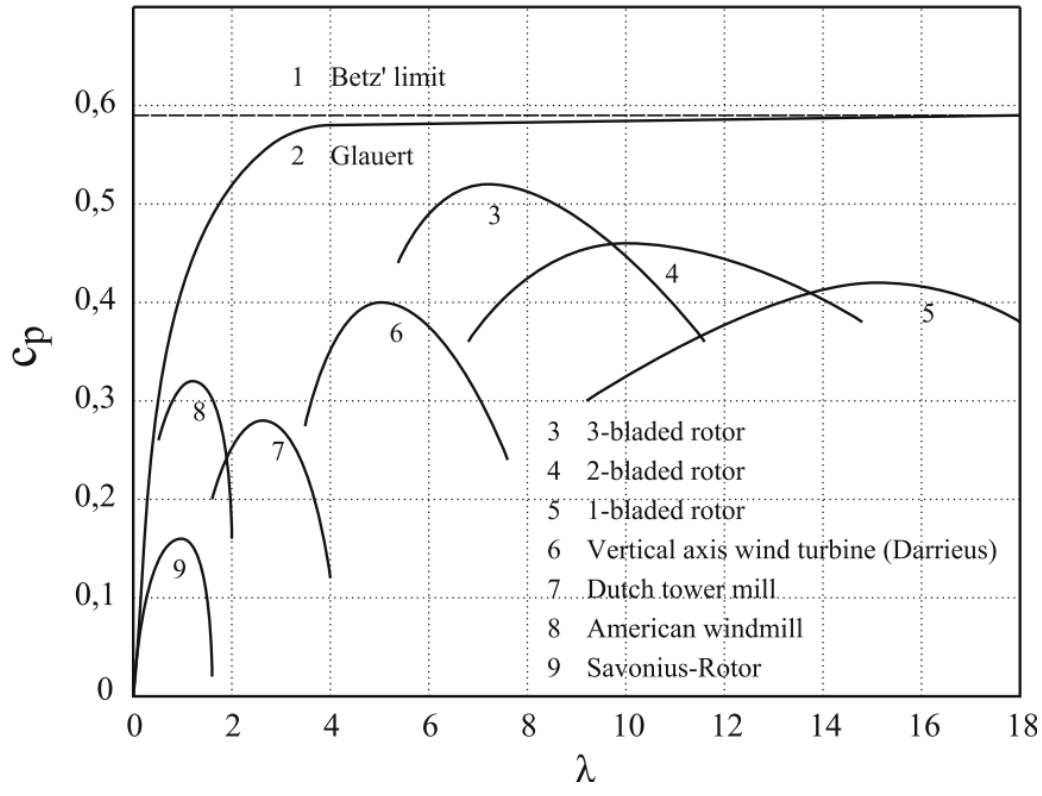

Source: Copied from Schaffarczyk (2014)

3.1.2 Main components

The wind turbine structure can be divided in different parts to be identified, manufactured and assembled. Along the wind turbines development history, many different designs were created. To avoid misinterpretation, the parts described in this section refers to modern utility-scale wind turbines, such as the GE 1.5sle.

The main component responsible for wind energy capture is the blade. Its geometry and aerodynamic shape is very connected to efficiency and its materials with durability. According to Manwell et al. (2010), composites, specifically fiberglass in polyester resin, dominates the selection for blade materials. The blades are attached to the hub, forming the rotor. The hub is made mostly from steel and, alongside with the blades, these are two of the most important components of wind turbines from the cost and performance point of view, as can be seen in Table 3.1. The turbine used as reference in this table is the NREL 1.5 MW 70 m diameter variable speed pitch regulated wind turbine.

Following the rotor, there is the drive train (Figure 3.2). This part of the turbine is responsible for converting the energy from mechanical to electrical. This is another set of movable components and usually consists basically of an low-speed shaft, speed-increasing gearbox, high-speed shaft and the electrical generator. The low-speed shaft, also referred as main shaft, is connected directly to the rotor and rotates with it in dozens of RPM. As the gearbox raises the rate of rotation to hundreds or thousands of RPM in the high-speed shaft, it transmits the mechanical energy to the electrical generator. More details about the drive train and its other components can be found in Manwell et al. (2010). According to Spera (2009), the main shaft is a critical component because of its structural (supports rotor weight, torque and lateral forces) and mechanical (energy transmission) functions, therefore all services, from design to maintenance, must be done very meticulously. Different electric generators can be used in wind turbines, but nearly all uses induction or synchronous AC generators. The choice of generator is primarily based on cost, power quality, power factor and torsional damping (MANWELL et al., 2010).

Recently, larger and offshore wind turbines manufacturers are adopting another option for the drive train: direct drive generators. This type of generators are connected to the rotor through a single shaft, which eliminates the necessity of gearbox. As gearbox failures in most wind turbines represent the longest downtime duration (FAULSTICH et al., 2011), eliminating this component may be vary advantageous, specially for offshore wind turbines in which maintenance access is difficult. But still, for many onshore wind turbines, this drive train option may not be viable due to the inherent increase in size and cost.

The nacelle connects the rotor to the tower and shelters the drive train, generator and yaw orientation system. It has an main frame (also known as bedplate) on which the shaft bearings are mounted. It is made up by welded and bolted steel sections to provide stiffness and static strength, rather than fatigue strength. The yaw orientation system (or yaw drive mechanisms) consists in sensors and one or more hydraulic or electric motors

which drives a pinion and a bull gear. This system is responsible for the alignment of the turbine with the wind. On the top of the nacelle, usually a cup or sonic anemometer and wind vane are the sensors that determine the intensity and direction of the wind and transmit this information to the yaw orientation system.

Figure 3.2 – Wind turbine traditional drive train arrangement.

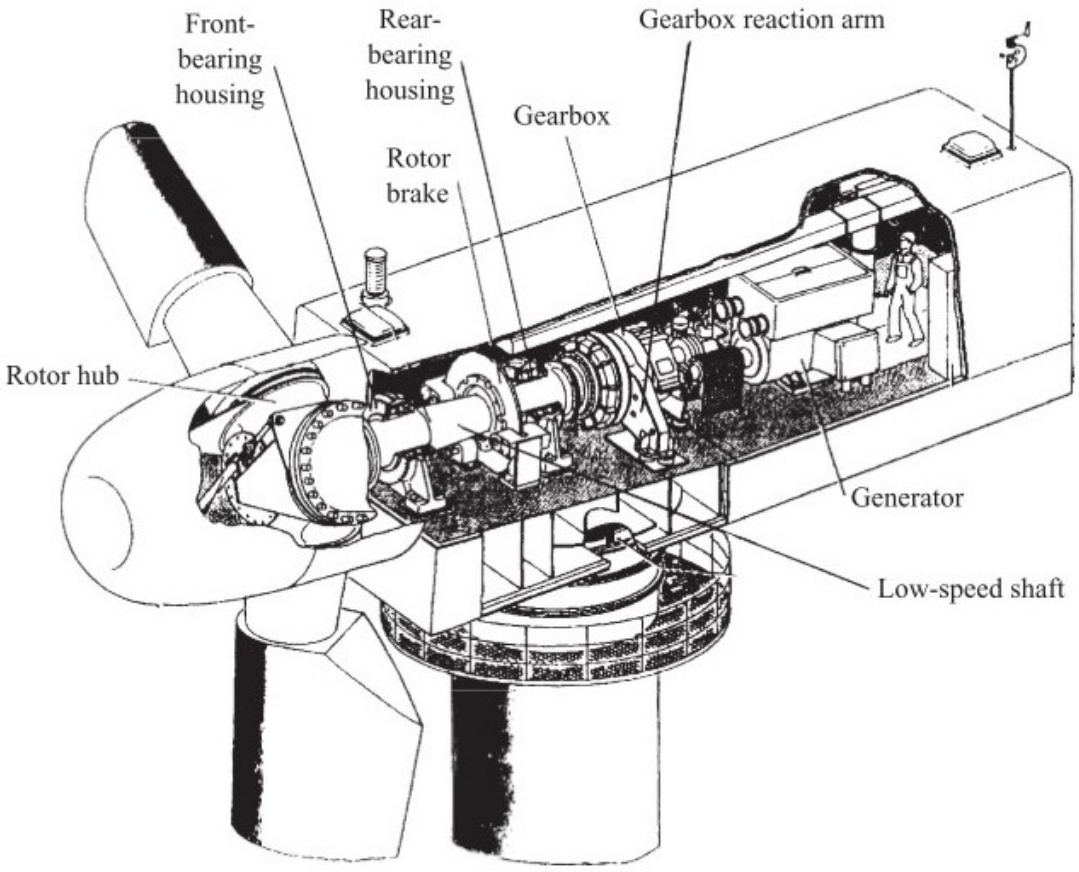

Source: Copied from Burton et al. (2011)

The tower supports the nacelle and is attached to the ground through the foundation. It elevates the rotor to the designed hub height, is the main access to the nacelle for maintenance and hosts power cables. The stiffness and dimensions of the tower structure, usually a cylindrical shell made by steel or reinforced-concrete, impacts in possible coupled vibrations between this component and the rotor. An indicator of relative rigidity is the ratio between fundamental system frequency and rotor speed. Three-bladed wind turbine towers with $f_{tower}/\Omega > 3$ are called stiff towers. When this indicator is less than one, its a soft-soft tower. Soft towers have an intermediate value. Soft-soft and soft towers are most commonly used. Besides having a ladder or elevator for upper components maintenance, the tower hosts many cables transporting power and operational data. Beneath the tower, there is an underground foundation that offers resistance to overturning and protects the soil around the turbine against rupture. Further information about offshore foundation can be found in Manwell et al. (2010).

Table 3.1 – NREL 1.5 MW 70 m diameter wind turbine components percentage cost relative to total machine cost.

Component	Percentage cost	Component	Percentage cost
Blades	11.4%	Yaw drive and bearings	1.5%
Hub	3.6%	Control system	2.7%
Pitch bearings and mechanisms	4.6%	Tower	12%
Low speed shaft and main bearings	2.5%	Brake and high speed shaft coupling	0.2%
Gearbox	11.6%	Foundation	3.6%
Generator	7.4%	Assembly and installation	3.2%
Variable speed electronics	9%	Transportation	3.9%
Nacelle	8.9%	Electrical and grid connections	14.2%

Source: Copied from Burton et al. (2011)

3.1.3 Operation regions

The operation of a wind turbine is strongly wind dependent. Due to mechanical and electrical losses, there is a minimum wind speed to start the turbine rotation and power generation. Also, the high structural loads caused by intense winds makes necessary to set a maximum wind speed for operation. This lower and upper limits of the wind speed are called cut-in (v_{in}) and cut-out (v_{out}) speeds, respectively. Operational wind speed range varies between those two limits. Another known parameter is the rated wind speed (v_r), at which the turbine reaches its rated power output. (BURTON et al., 2011)

WTs operation is commonly divided in 4 regions, shown in Figure 3.3. Over region 1, the wind speed varies from 0 to the cut-in speed, therefore, the rotation has not begun and there is no power generation. Region 2 of operation begins when wind intensity is greater than cut-in speed (minimal output power) and ends when the wind reaches rated speed and the turbine its nominal power output. During this phase, blades are in its optimal position to harness the maximum possible of the available energy. It is in region 3 that active rotor speed regulators are usually turned on, as the wind exceeds rated speed (v_r) and rotation must be controlled to maintain the turbine nominal power output. If the wind reaches higher velocities than the cut-out speed, the turbine operates in region 4, shutting off its rotation to avoid excessively high loads and structural damage. Some algorithms may be implemented in the WT in this region to harness some energy.

Figure 3.3 – Wind turbine operation regions.

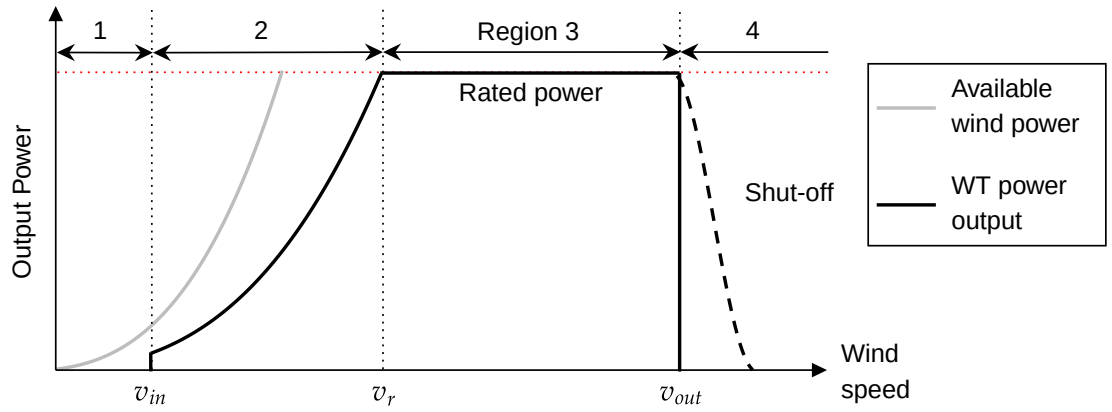

Source: Adapted from Morim et al. (2019).

3.1.4 Load measurement and monitoring

An important step of wind turbines certification process (see IEC 61400 Part 22) is to prove to certification bodies that the structures fulfill several design requirements and withstand various wind and load scenarios. This step is called load testing. Those requirements and scenarios are well described in IEC standard 61400 Part 1: Design requirements (British Standards Institution, 2014). Also, the standard part that covers load measurements is IEC Part 13: Measurement of mechanical loads (British Standards Institution, 2016). Load tests can be made through software or mechanical measurement in field testing to demonstrate that the calculated loads of the designed turbine were correctly estimated and match the real loads that the turbine will experience. The mandatory loads to be evaluated in this kind of test are determined by IEC and can be seen in Table 3.2. Tilt and yaw rotor moments are visually demonstrated in Figure 3.9 and the blade root moments can be seen in Figure 3.10.

Strain gauge bridges are recommended by IEC to measure blade root and rotor tilt and yaw and bending moments. Other recommendations regarding test instrumentation, such as positioning and cross-sensitivity avoidance, can be seen in the mentioned standard. Power performance, sound emission and other tests are also part of wind turbines certification process, but are not covered in this work (see IEC 61400 Part 1, 11, 12, 14 and 21).

Another theme related to load measurement is load monitoring. This can be used for active load control, short and long-term forecast of future wind turbine condition. Structural parameters observation aiming to to detect structure behavior change and damage is also known as structural health monitoring (SHM). According to Ciang et al. (2008), other benefits of SHM include remote supervision and diagnosis, avoidance of catastrophic failures, reduced maintenance cost and data gathering to improve future WT designs.

Many different sensors are used to monitor blade loads and fill control and prediction algorithms with data. Cooperman and Martinez (2015) makes a review over the many sensors used for load control, in which it describes two categories: inflow and structural. Inflow sensors measure wind variations before it reaches the turbine blades and cause the aerodynamic load itself. This provides information to the control system to predict incoming loads through correlation models and gives more time to actuators change blade position to low this loads. This opens up to inaccuracy and instability. Structural sensors, on the other hand, measure the actual load and can be very precise, but by the time the blade position is changed, it may be too late to alleviate high loads.

Table 3.2 – Fundamental load quantities in test measurements of WTs with rated power output equal or lower than 1.5 MW.

Load quantities
Blade root edgewise bending moment (RMx)
Blade root flatwise bending moment (RMy)
Rotor tilt moment (M_{tilt})
Rotor yaw moment (M_{yaw})
Rotor torque (M_x)
Tower base normal bending moment (M_{tn})
Tower base lateral bending moment (M_{tl})

Source: Copied from British Standards Institution (2016)

Wind turbine sensors requirements include resistance to harsh environment condition (rain, snow, dirt, lightning, etc.) and reliability due WTs common 20+ years lifespan, hard access to some wind farms (e.g. located in mountains) and wind turbine spots, specially the blade. Also, minimal sensor size and weight is aimed. Some structural sensors used to monitor loads for active load control purposes are:

- Metallic strain gauge;
- Piezoelectric strain sensor;
- Fiber optic intensity-based sensor;
- Fiber Bragg gratings (FBG);
- and Rayleigh backscattering.

Further information about each listed sensor can be found in Cooperman and Martinez (2015). Finally, another branch of structural health monitoring is identification of blade damage and mass asymmetry. Different methods and sensors are cited in Ciang et al. (2008). Also, besides presenting a review of blade damage detection methods, Li et al. (2015) talks about scenarios and types of blade damage.

3.2 BASIC BLADE AERODYNAMICS

This section is a brief review to establish basic concepts and will be restrained to 2D aerodynamics. For a more detailed description of aerodynamic theories and phenomena, see Hansen (2015), Anderson (2016), Bertin and Cummings (2013), Katz and Plotkin (2001).

Airfoil is a very common body shape in aerodynamic studies. It is usually found on airplane wings or wind turbine blades cross sections. Some of its geometric properties are: chord (c), chord line, leading edge and trailing edge (Figure 3.4). The position of the body relative to the 2D flow is measured by its angle of attack (α, AoA). It is the angle between the airfoil chord line and the relative wind velocity vector.

The flow of air around an airfoil generates a static pressure distribution along the body. This distribution depends highly on the airfoil shape and its angle of attack. Also, the air passing around a body suffers resistance due to the flow viscosity and surface roughness. This resistance results in a shear stress distribution. By integrating static pressure and shear stress distribution, it is possible to reach the total pressure force. By convention, the resultant force is decomposed into two components: perpendicular and parallel to the relative flow. The first one is called lift (L) and the second one drag (D). The pressure and shear stress generates a moment that acts to rotate the airfoil, the pitching moment (M). Figure 3.4 also shows the positive orientation of these forces and moment. Conventional airfoil generates a negative pitching moment, lowering the angle of attack (also know as "nose-down" effect).

Figure 3.4 – Airfoil geometric definitions and aerodynamic forces and moment.

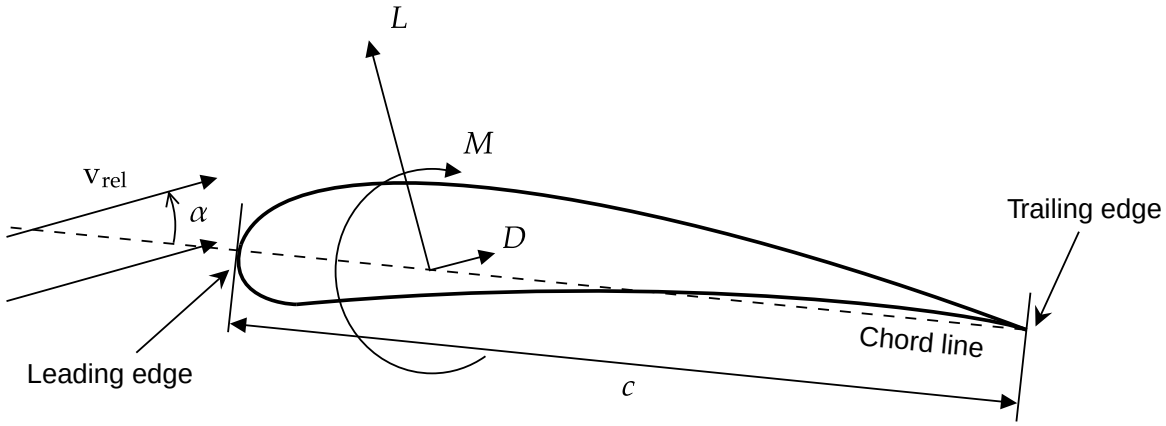

Source: Adapted from Manwell et al. (2010)

Aerodynamic forces and moments are always related to the relative wind density (ρ) and its velocity (v_{rel}) squared. These values are part of the dynamic pressure definition, which is $q = \rho v_{rel}^2/2$. Also, aerodynamic loads are related to a reference area, which is substituted in 2D aerodynamics by the chord value times an unitary length, and finally, to aero-

dynamic coefficients (C_l, C_d and C_m), which are function of the angle of attack, Reynolds and Mach numbers. The Mach number relates the flow velocity to the local speed of sound, given by $Ma = v_{rel}/a_\infty$. It allows to determine if the flow is subsonic, transonic or supersonic. Physically, Reynolds number is described as a measure of the ratio between inertial and viscous effects in a fluid, which is given by $Re = \rho v_{rel} c/\mu$, where c is a characteristic length (in 2D aerodynamics, the chord) and μ the flow viscosity coefficient. It allows to determine whether the flow is laminar, transitional or turbulent. Both Mach and Reynolds number are very important dimensionless parameters in fluid mechanics (ANDERSON, 2016). Therefore, lift, drag and pitching moment distributions (per unit span) along an airfoil are given by

$$L' = C_l \, q \, c, \tag{3.4}$$

$$D' = C_d \, q \, c, \tag{3.5}$$

$$M' = C_m \, q \, c^2. \tag{3.6}$$

For a complete 3D body, such as an airplane wing, aerodynamic coefficients are indicated with capital letters. As seen in Equations (3.4), (3.5) and (3.6), knowing aerodynamic forces, moment, air properties and airfoil chord, it is possible to calculate the aerodynamic coefficients values for a certain angle of attack. That is the principle behind wind tunnel testing. A wind tunnel balance sense forces and moments acting on an airfoil (or any other body) when air passes through it. Also, AoA is used as a reference angle to compare different airfoils and its coefficients.

Usually airfoils are designed in such a manner that increasing the angle of attack also increases the lift coefficient, hence lift force, until a certain maximum lift point is reached. Beyond this point, increasing α actually decreases lift. This phenomenon is called aerodynamic stall. Commonly, the stall AoA is situated between 15° and 20°.

3.2.1 Fundamental angles

In wind turbine blades, the relative wind vector is the sum of the wind vector and the blade section rotational speed, i.e., tangential speed vector, related to the rotational speed, as can be seen in Figure 3.5.

As the direction of the relative wind is related to the tangential speed, it changes for every blade section. The further the blade section is, relative to its root, the greater the tangential speed is. Also, as the wind is not uniform, the wind itself can change significantly at different parts of the blade. Then, it is important to define an angle that does not changes with the relative wind speed. That is the pitch angle (β). Pitch is the angle between the

rotational plane (also named as rotor plane) and the chord line of the blade section. Some wind turbines control the pitch angle actively (see section 3.3). By changing the blades pitch angle in a way that it reduces the angle of attack, the lift coefficient is also reduced, and hence it is possible to change the rotational speed of the rotor to avoid structural overloading. This process is usually called blade feathering. The blade pitch angle at 90° is called full feather position and represents the blade tip airfoil chord parallel to the shaft.

Assuming a constant wind speed along the blade, it is possible to see that, due to the low tangential speed near the blade root, the angle of attack at that section would be higher. Higher angles of attack lead to higher aerodynamic loads acting on the structure. To mitigate this effect, twist is implemented to make the angle of attack constant along the blade. The twist angle (θ) is higher near the blade root. Therefore, it is easier to observe the blade pitch angle near the blade tip.

Figure 3.5 – Definition of blade and section angles.

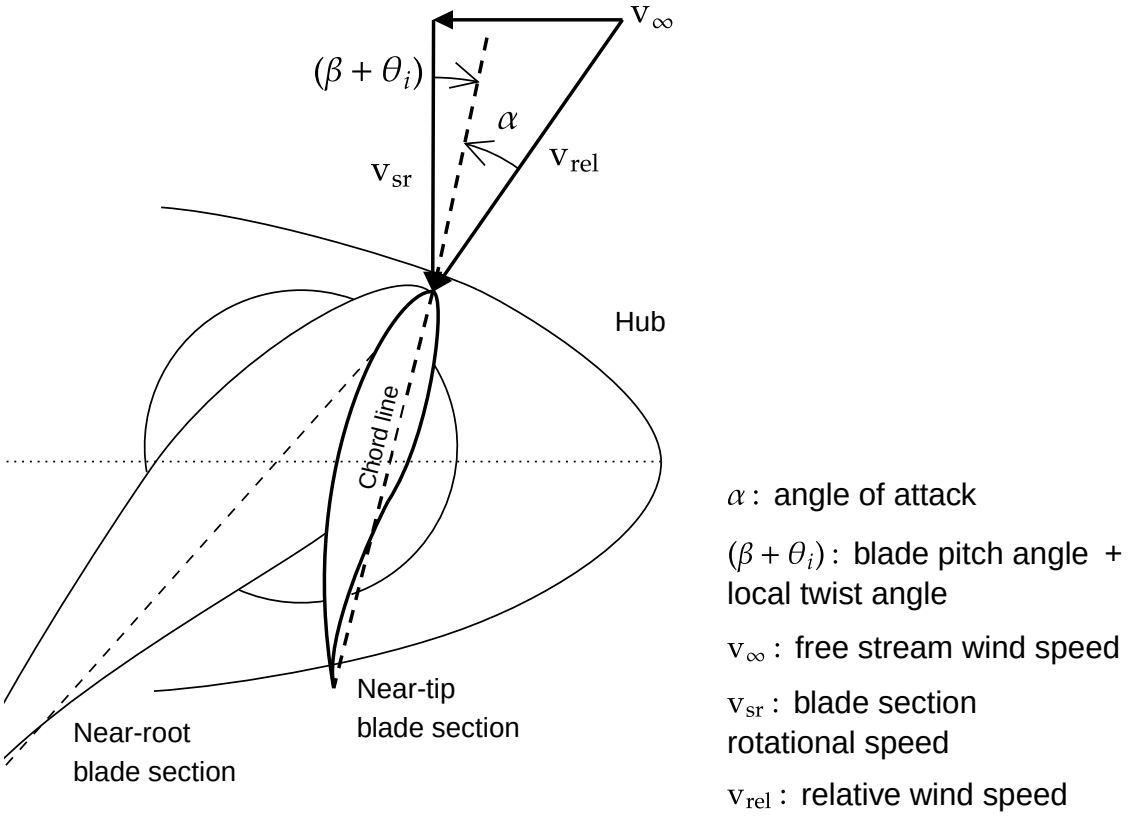

Source: Author.

As the blades rotates, it is also important to define an angle that describes its rotational position. That is the azimuth angle (ψ). It is the angle between the direction that the blade is pointing (blade axis) and the upward direction and is measured positively clockwise.

Over the time, as the wind direction changes, it is necessary to measure the position of the WT with respect to the incident wind or an inertial frame. Thus, yaw (ϕ) is the angle between the direction the rotor is pointing (rotor axis) and the incoming wind and

turbine angle (ϕ_{turb}) is the angle between an arbitrary reference (N) and the rotor axis. To optimize turbine power generation, the rotor plane must be parallel to the wind vector. To accomplish this, the yaw orientation system controls the nacelle to make the yaw angle zero and correct horizontal misalignment. Finally, to measure the rotor plane angle with respect to the upward direction, tilt (τ) is used. In other perspective, it is the angle between the rotor shaft and a generic vertical plane parallel to the ground surface, positive in the clockwise orientation. This angle changes rotor aerodynamics, power output and tower shadow, having positive impacts when properly designed to do so, according to Wang et al. (2019). Also, in wind farms, tilt and yaw control may be used to change wake characteristics and improve overall power production of aligned turbines as Annoni et al. (2017) states. Usually, wind turbines are designed with positive tilt angles to avoid blade tip impacts with the tower by increasing their distance (tower clearance). Now that these two angles have been formerly presented, it is easier to understand that tilt and yaw moments presented earlier consists in the rotor loads that act in the direction to change tilt and yaw angles.

Figure 3.6 – Definition of blade azimuth (ψ), turbine (ϕ_{turb}), yaw (ϕ) and tilt (τ) angle.

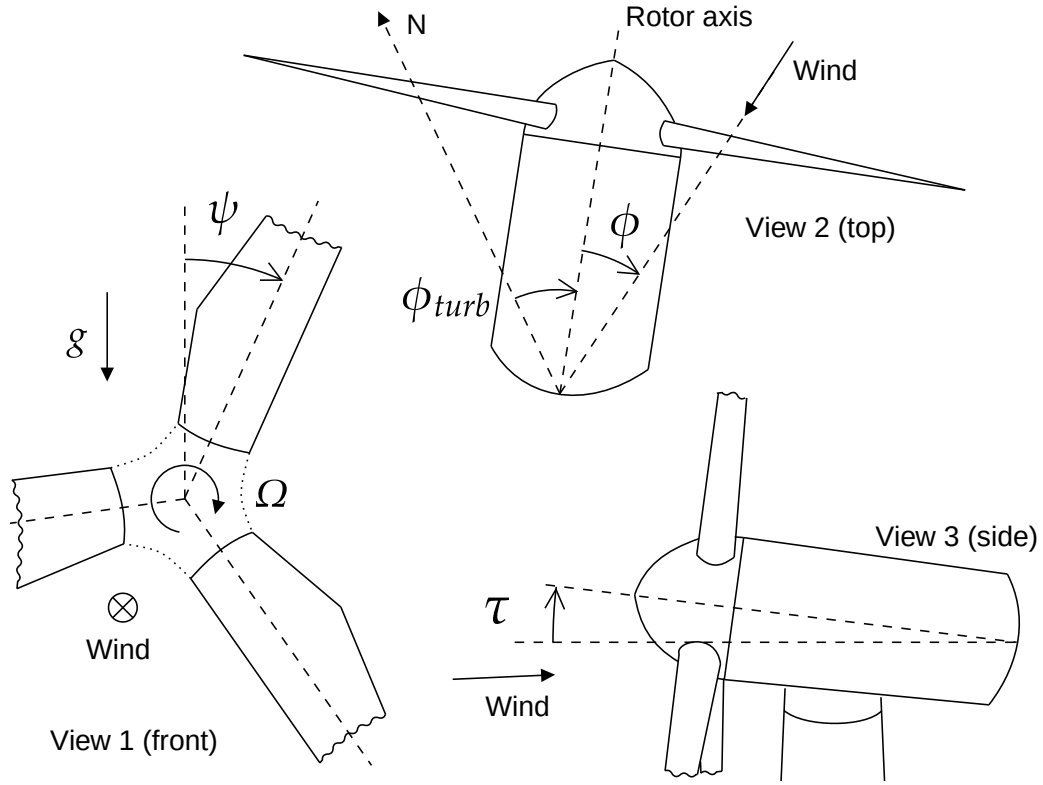

Source: Author

3.3 TURBINE CONTROL SYSTEMS

In wind turbines, control systems play a very important role in the operational integration of the different systems and are responsible for many crucial functions of the turbine. Besides automation of many processes (1), control systems usually aim to preserve vari-

ous components integrity (2) and improve harness efficiency (3). According to Burton et al. (2011), these three functions can be summarized in three different categories: supervisory control (1), safety systems (2) and closed loop control (3).

Supervisory control is the system in charge of turbine operational state changes. For example, when the turbine is in standby due to low wind intensity and the wind velocity surpasses cut-in speed, supervisory control will trigger a sequence of turbine mechanisms to start rotation. On top of supervisory control, safety systems act as a backup in the case of emergency shut-offs, when the main system is failing to change the turbine operational state.

Subsequently, closed loop controllers usually aim to adjust a components state (i.e. position, velocity, etc.) relative to a certain ideal curve or limiting parameter. Some examples of this category are generator torque control, yaw misalignment correction, power output and rotor speed regulation.

There are two main power and rotor speed regulators regarding blades: passive stall and active pitch control. The first one consists basically in using the post-stall low lift and high drag forces to compensate the increase in wind speed by lowing rotor speed, hence limiting output power. This makes any position change in the blades unnecessary, as the blade pitch angle is fixed in a way that the power generation is maximized for a certain wind speed, making it one of the simplest way of power control. Alternatively, active pitch control is more complex. This system, typically allocated inside the hub and nacelle, is made basically out of sensors, controllers and actuators. It takes action in operation region 3 (wind speed above rated) and it rotates some parts or the entire blades around its own axis changing pitch angle in order to change aerodynamic forces. Besides power and rotor speed control, this can be used to maintain certain rotor loads in a defined envelope to preserve the structure. In active pitch control, pitch angle typically varies from 0° to 90° (full feather position) and can also serve as aerodynamic brake. (BURTON et al., 2011)

Active pitch control mechanisms control blades collectively (collective pitch control, CPC) or individually (individual pitch control, IPC). An example of these two options can be visualized in Figures 3.7 and 3.8. CPC usually act through a single push-rod connected to each blade by mechanical linkage, but it may also work through individual actuators for each blade receiving the same controller command. On the other hand, as individual pitch controllers send to each blade actuator a specific target blade position, it can only work with individual actuators. When the pitch control system is composed by this type of actuation, IPC can work in parallel with CPC by making the fine adjustments of each blade pitch angle.

Both CPC and IPC may have hydraulic or electric actuators and need devices to transmit power from the non-rotating nacelle to the rotating hub. Rotary hydraulic joints and slip rings can be used for transmitting, respectively, hydraulic or electric power to the hub. Every pitch control mechanism has to be able to return the blades to feather position with backup energy sources in the case of emergency shut-off. In this situations, electric and

hydraulic actuators commonly rely respectively on batteries and accumulators. According to Burton et al. (2011), a blade pitch change rate of 5 or more degrees per second is found adequate.

Figure 3.7 – Hydraulic collective pitch actuation system.

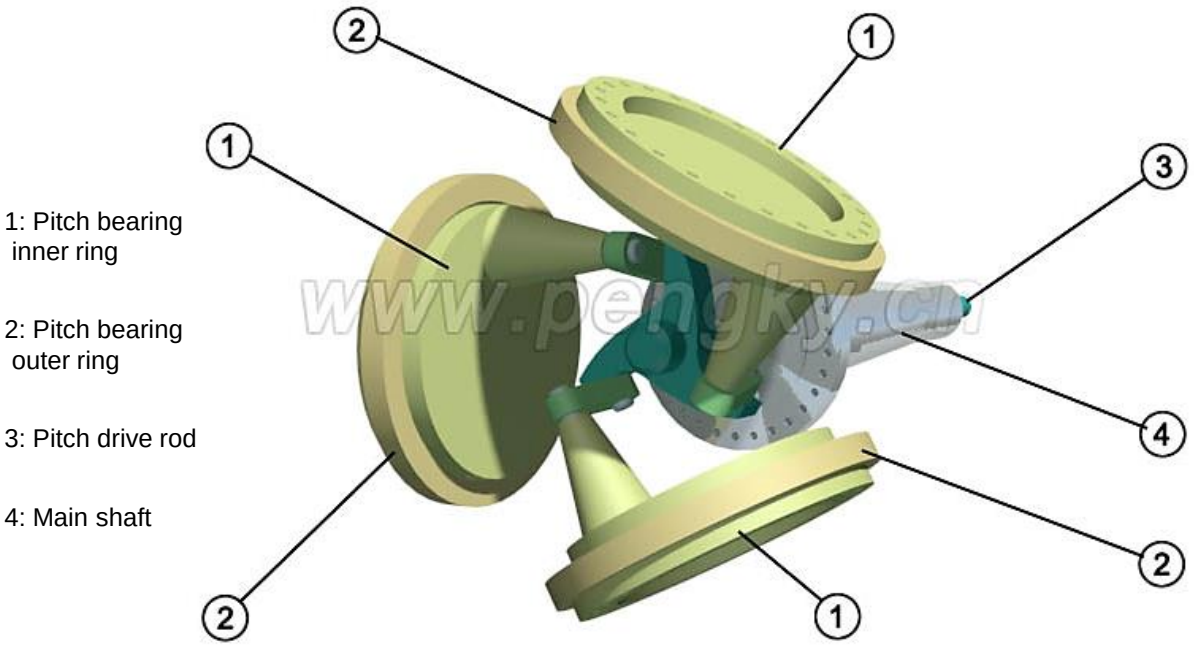

Source: Adapted from Peng K Y (2009)

Figure 3.8 – Electric individual pitch actuation system.

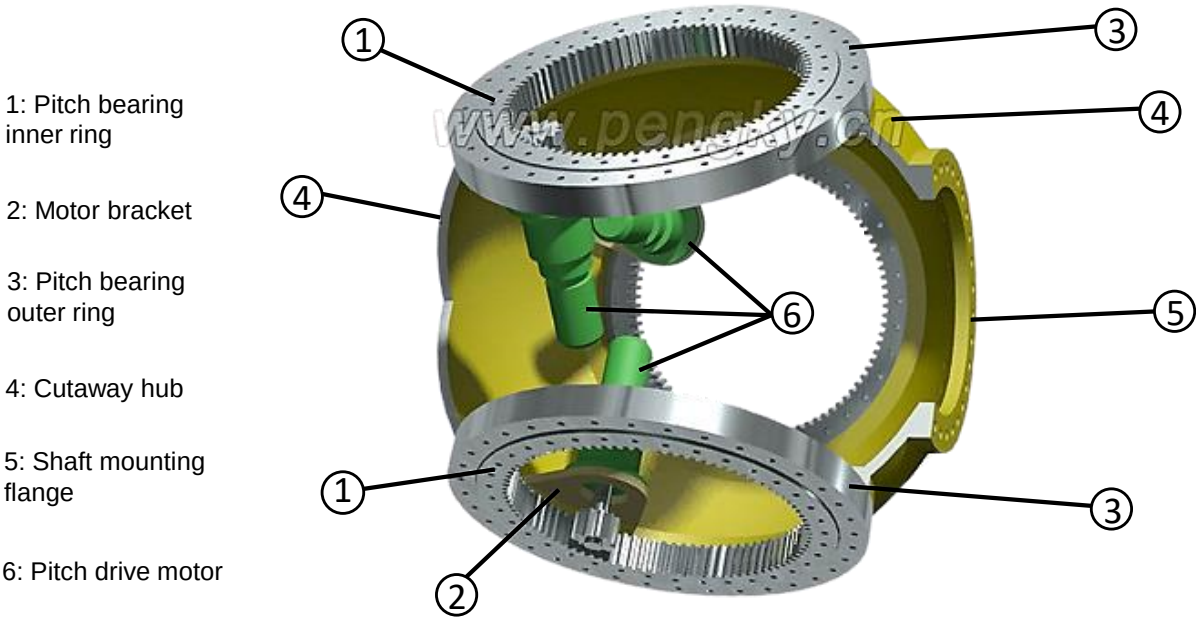

Source: Adapted from Peng K Y (2009)

Individual pitch controllers, such as the one given by Morim (2019), also serve as a means to reduce blade asymmetrical loads caused by unequal wind distribution along the rotor area. Employing active load control and load monitoring, it is also possible to install the same turbine in locations with a wider wind range, expanding viable wind farm sites. Besides active pitch control, another system that can reduce loads is the active aerodynamic load control. Device examples for this system are microtabs, microjets, plasma actuators, trailing edge flaps and morphing wing trailing edge (DAM et al., 2008).

3.4 REFERENCE FRAMES

The coordinates systems were adopted according to IEC 61400-13 (British Standards Institution, 2016) and OpenFAST documentation (NREL, 2019) definitions for upwind horizontal axis three-bladed wind turbines. Firstly, the tower base reference frame is presented (Figure 3.9). Its origin is fixed at the center of the connection between the structure and the ground foundation or support platform. The $\vec{z_T}$ points upwards, in the opposite orientation of the gravitational force. The $\vec{x_T}$ points downwind and $\vec{y_T}$ completes the right-handed coordinates system.

Besides being a component that rotates, the chosen hub reference frame adopted in this work is stationary. The non-rotating hub coordinates system is static relative to the rotor and can also be seen in Figure 3.9. When the azimuth angle of blade 1 is zero, the $\vec{z_h}$ points to its tip, but this axis do not follow its movements. Also, it is orthogonal to the rotor axis. The $\vec{x_h}$ is aligned to the rotor axis and points downwind. The $\vec{y_h}$ is orthogonal to the $x_h - z_h$ plane and completes the right-handed coordinates system.

The rotor shaft reference frame also do not follow the rotation of the rotor, but it follows the yaw and tilt movement of the turbine. The origin of this system is the intersection of the rotor shaft center with the plane that follows $\vec{z_T}$ and cuts the tower in half. The $\vec{x_s}$ is aligned with the rotor shaft and points downwind, $\vec{y_s}$ is orthogonal to $\vec{x_s}$ and points to the left side of the turbine looking downwind. Finally, $\vec{z_s}$ is orthogonal to the $x_s - y_s$ plane and completes the right-handed coordinates system pointing upwards.

The blade coordinates system is shown in Figure 3.10. This reference frame is fixed in the blade, i.e., it follows the pitch and rotational movement (around $\vec{x_s}$) of the blade. Its origin is the intersection between the root plane and the pitch movement axis. The $\vec{z_b}$ points to the blade tip and is aligned with the pitch movement axis. The $\vec{y_b}$ points to the blade trailing edge and is aligned with the chord line at the zero-twist blade station. The $\vec{x_b}$ is orthogonal to the $y_b - z_b$ plane and completes the right-handed coordinates system pointing downwind. In the same figure, it is possible to see edgewise, flatwise and torsional blade root moments.

Figure 3.9 – Tower base and non-rotating hub reference frame.

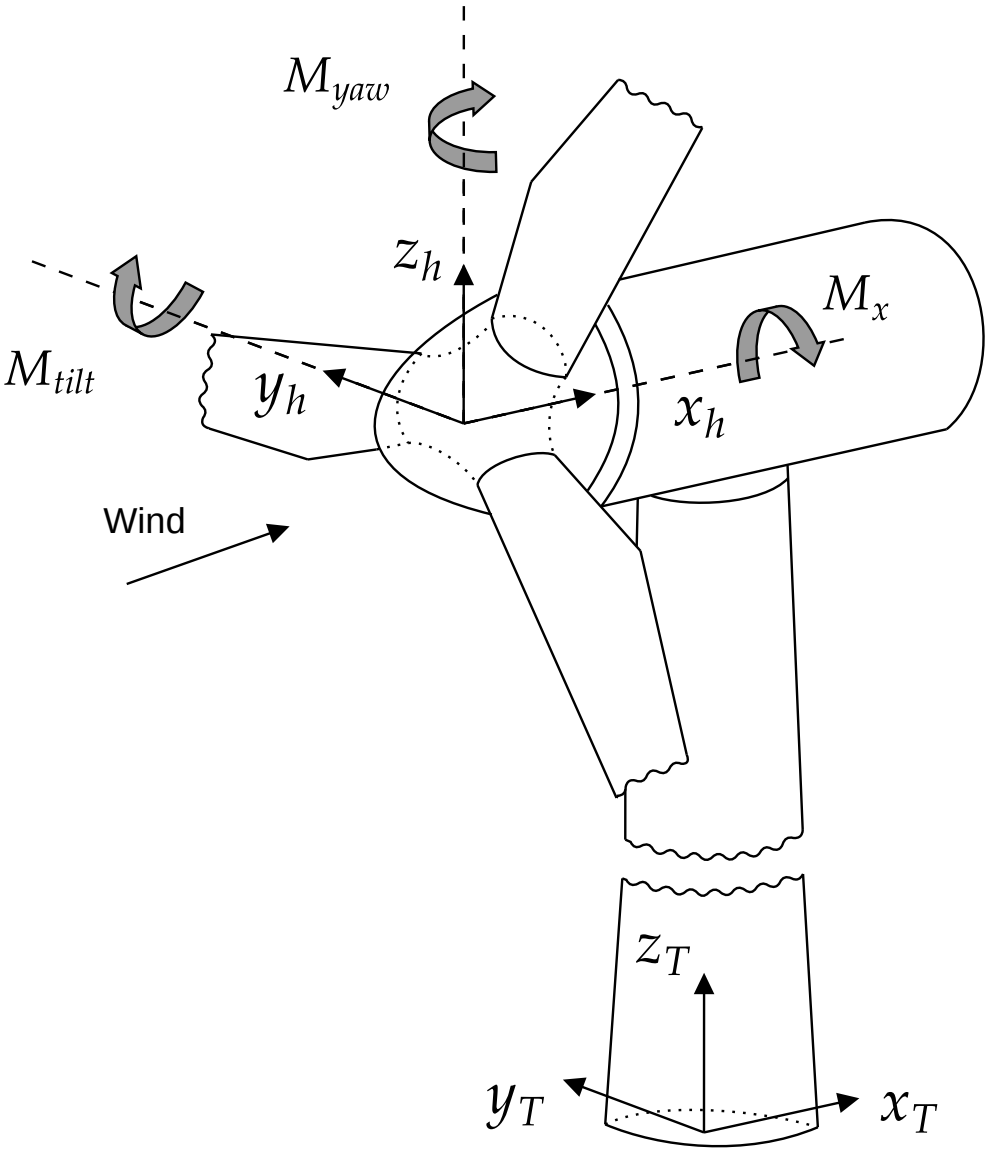

Source: Adapted from Rooij (2001)

3.4.1 Coordinates transformation

In structural dynamics problems, usually more than one reference frame is used, e.g., body reference frame and inertial reference frame. In this cases, such as aircraft and spacecraft flight mechanics, it may be necessary to convert the coordinates of a vector from one reference frame to another. This is also the case of wind turbines.

In this work, it was necessary to convert blade root loads, written in the blade reference frame, to the rotor reference frame, to be able to compute rotor loads. The reference frames adopted in this work are presented in the next chapter. To do this coordinates transformation, a combination of planar rotations was used.

Figure 3.10 – Blade reference frame.

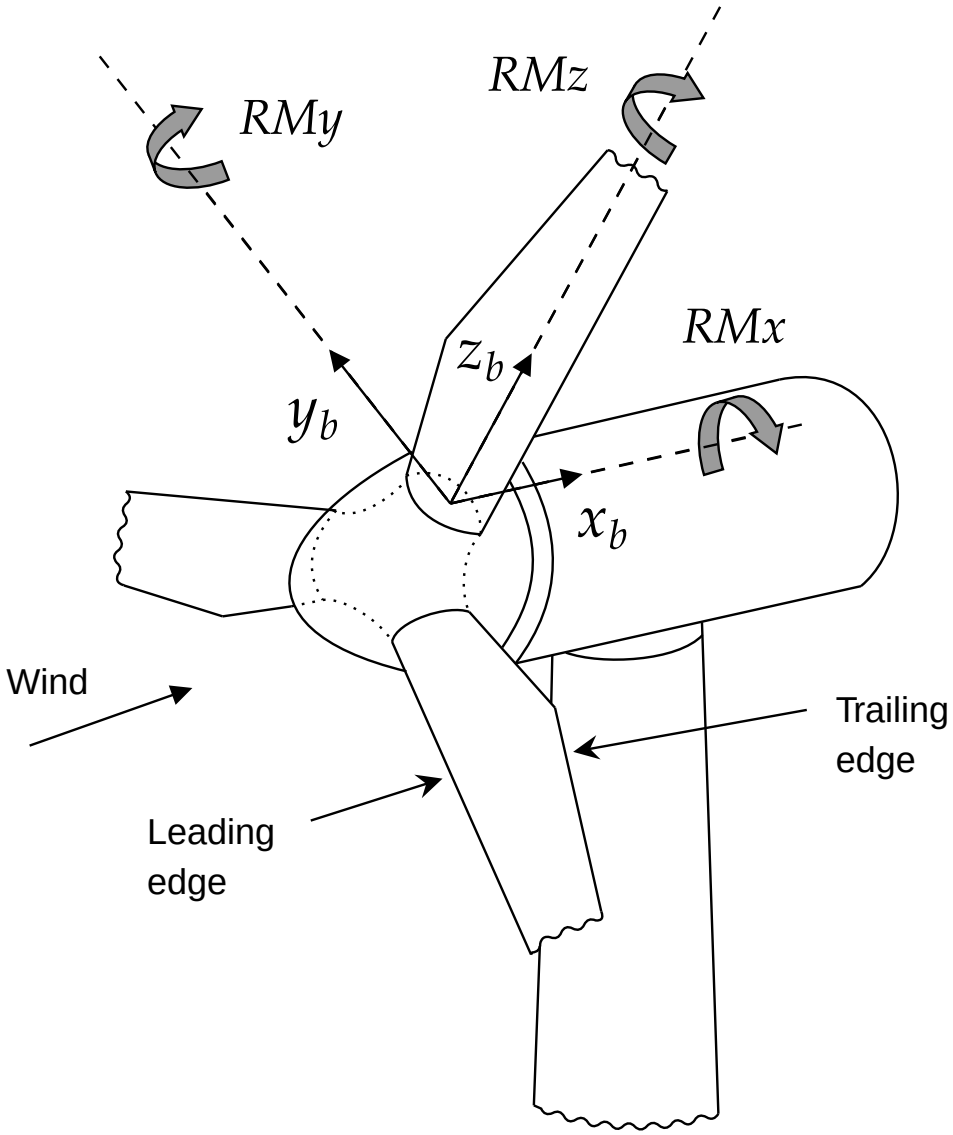

Source: Adapted from Rooij (2001)

This is the simplest form of rotation operation, and consists in the reference frame rotation about one of its axis or unit vectors (BAUCHAU, 2011). The operators, which are a result of simple trigonometry, can be geometrically visualized in Figure 3.11 and are mathematically given by the following matrices

$$\mathbf{C_1}(\gamma_a) = \begin{bmatrix} 1 & 0 & 0 \\ 0 & \cos(\gamma_a) & \sin(\gamma_a) \\ 0 & -\sin(\gamma_a) & \cos(\gamma_a) \end{bmatrix}, \tag{3.7}$$

$$\mathbf{C_2}(\gamma_b) = \begin{bmatrix} \cos(\gamma_b) & 0 & -\sin(\gamma_b) \\ 0 & 1 & 0 \\ \sin(\gamma_b) & 0 & \cos(\gamma_b), \end{bmatrix}, \tag{3.8}$$

$$\mathbf{C_3}(\gamma_c) = \begin{bmatrix} \cos(\gamma_c) & \sin(\gamma_c) & 0 \\ -\sin(\gamma_c) & \cos(\gamma_c) & 0 \\ 0 & 0 & 1 \end{bmatrix}. \tag{3.9}$$

Figure 3.11 – Planar rotations.

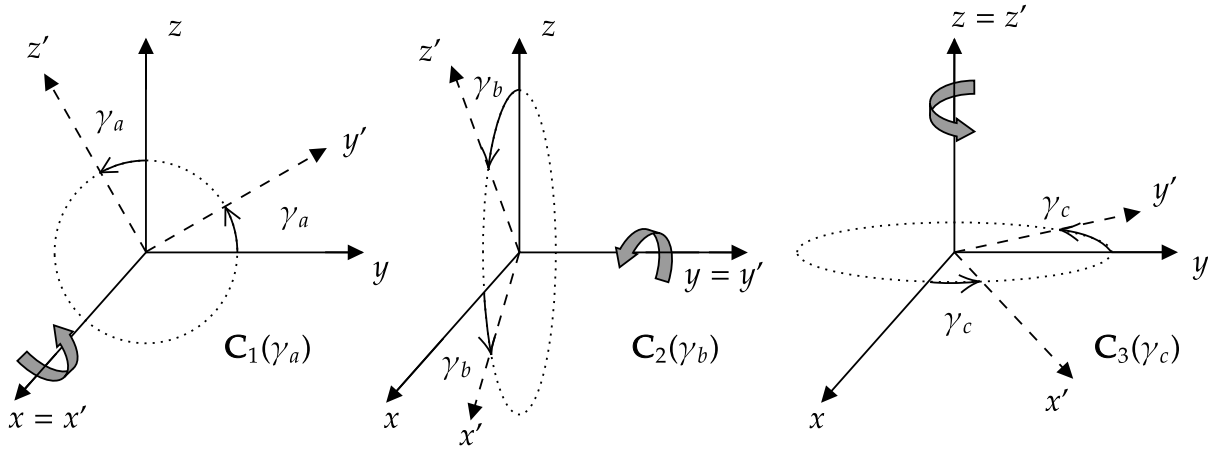

Source: Author

Equation (3.7) represents a rotation of positive γ_a degrees around the x axis. Equations (3.8) and (3.9) can be interpreted the same way. The indexes 1, 2 and 3 represents the axis x, y and z, respectively, or their intermediates in case of successive rotations. The sign of the rotation angle is defined according to the right-hand convention. Note that, in this work, bold letters are used to distinguish matrices from scalar variables.

3.4.2 Successive rotations

Coordinates transformation usually accounts more than one planar rotation around different axis. As long as successive rotations are not made around the same axis, the final matrix rotation equation development is achieved by the inner product of each planar rotation in the inverse order that they are made.

Every rotation creates an intermediate system of coordinates until the final rotation is concluded. For nomenclature purposes, the initial one is $(\vec{x}\,\vec{y}\,\vec{z})$. After the first rotation, the new reference frame is identified as $(\vec{x'}\,\vec{y'}\,\vec{z'})$ and so on. As an example, the 321 sequence of rotation, commonly used in aircraft flight mechanics, consists of an initial rotation about z-axis, followed by an intermediate rotation about y' and a final rotation about x''. Its mathematical expression is given by

$$\mathbf{C_{321}} = \mathbf{C_1} \cdot \mathbf{C_2} \cdot \mathbf{C_3}. \tag{3.10}$$

3.5 AERODYNAMIC CORRECTION MODELS

Correction models are a manner to include unaccounted effects into aerodynamic coefficients to reduce error in aerodynamic loads calculation. Two of these effects are stall delay and dynamic stall. The stall delay phenomenon was also first noticed during aircraft propeller blade studies. Otherwise called Himmelskamp effect, it basically consists of a delay effect on flow detachment (stall) caused by rotation, which changes the C_l-α curve and maximum lift coefficient. Further information about this phenomenon may be found in Breton (2008). Dynamic stall is an unsteady aerodynamic phenomenon caused by a dynamic variation of angle of attack near the stall region, which leads to fluctuations in the aerodynamic forces and coefficients. This effect is described in more details by VISBAL (1991).

3.5.1 Du-Selig and Eggers corrections

The Du-Selig corrections consists in an algorithm to modify 2D lift and drag aerodynamic coefficients to take into account the 3D stall delay effect that happens in wind turbines (DU; SELIG, 1998). Thus, the corrected set of aerodynamic coefficients are given by

$$C_{l,c} = C_l + f_L(C_{l_P} - C_l) \tag{3.11}$$

and

$$C_{d,c} = C_d - f_D(C_d - C_{d_0}) \tag{3.12}$$

in which $C_{l_P} = C_{l\alpha}(\alpha - \alpha_0)$, α_0 is the angle of attack when $C_l = 0$, C_{d_0} is the drag coefficient at $\alpha = 0$ and $C_{l\alpha}$ is the lift curve slope. The values of f_L and f_D are given by

$$f_L = \frac{1}{2\pi}\left[\left(\frac{1.6(c/r)}{0.1267}\right)\frac{a-(c/r)^{\frac{R_{tip}\,d}{\Lambda r}}}{b+(c/r)^{\frac{R_{tip}\,d}{2\Lambda r}}} - 1\right] \tag{3.13}$$

and

$$f_D = \frac{1}{2\pi}\left[\left(\frac{1.6(c/r)}{0.1267}\right)\frac{a-(c/r)^{\frac{R_{tip}\,d}{2\Lambda r}}}{b+(c/r)^{\frac{R_{tip}\,d}{2\Lambda r}}} - 1\right], \tag{3.14}$$

where

$$\Lambda = \frac{\Omega R_{tip}}{\sqrt{v_{rel}^2 + (\Omega R_{tip})^2}} \tag{3.15}$$

as Ω is the rotational speed of the blade in RPM, R_{tip} is the blade length, (c/r) is the ratio of the local chord to the local radius of the blade, Λ is a modified tip speed ratio and v_{rel} is the relative wind velocity in meters per second. In the lack of empirical information, the

correction factors a, b and d can be set to 1. After aplying this correction, unknown lift and drag coefficients can be found through the model presented below.

Eggers correction aims to correct 2D aerodynamic normal (C_n) and tangent (C_t) force coefficients to better predict side forces and rotor center of thrust (EGGERS et al., 2003). Normal and tangent forces are also derived from the aerodynamic resulting force. While lift and drag are, respectively, perpendicular and parallel to the relative wind, normal and tangent forces are perpendicular and parallel to the chord line. Thus, the angle between lift and normal is the angle of attack. The same goes for drag and tangent force.

As the model corrects the pair C_n and C_t, this changes must be incorporated into lift and drag coefficients. In the absence of 2D aerodynamic normal and tangent force coefficients, both can be estimated as

$$C_n = C_l \cos(\alpha) + C_d \sin(\alpha) \tag{3.16}$$

$$C_t = C_l \sin(\alpha) - C_d \cos(\alpha). \tag{3.17}$$

In this work, a coupling between Du-Selig and Eggers is used. Using the C_l correction, given by Equation (3.11), and the 2D aerodynamic data, it is possible to define

$$\Delta C_L = C_{l,c} - C_l. \tag{3.18}$$

This definition is used to correct the drag coefficient as given by Eggers, so that:

$$\Delta C_D = \Delta C_L \left[\frac{\sin(\alpha) - 0.12\, cos(\alpha)}{\cos(\alpha) + 0.12 \sin(\alpha)} \right] \tag{3.19}$$

$$C_{d,c2} = C_d + \Delta C_D. \tag{3.20}$$

To apply 3D corrections to lift and drag coefficients of rotating sections, Equations (3.11) and (3.20) can be used.

3.5.2 Viterna method

The Viterna Method is a post-stall model used to extrapolate aerodynamic coefficients obtained by wind tunnel tests or numerical algorithms (e.g. XFOIL) for a wider range of angles of attack. The proper formulation is found in Viterna and Janetzke (1982). The unknown lift and drag coefficients then are given by

$$C_{l,ex} = A_1 \sin(2\alpha) + A_2 \frac{\cos^2(\alpha)}{\sin(\alpha)} \tag{3.21}$$

and

$$C_{d,ex} = B_1 \sin^2(\alpha) + B_2 \cos(\alpha). \tag{3.22}$$

In the above equations, the parameters A_1 and B_1 are given by

$$A_1 = \frac{C_{d,max}}{2} \tag{3.23}$$

and

$$B_1 = C_{d,max} \tag{3.24}$$

where $C_{d,max}$ is the drag coefficient at $\alpha = 90°$. In the lack of empirical information, this can be approximated for a blade aspect ratio (AR) that is finite with $AR \leqslant 50$ by

$$C_{d,max} \approx 1.11 + 0.18AR. \tag{3.25}$$

The value of A_2 and B_2 are given by

$$A_2 = \frac{(C_{l_S} - C_{d,max} \sin(\alpha_S) \cos(\alpha_S)) \sin(\alpha_S)}{\cos^2(\alpha_S)}, \tag{3.26}$$

$$B_2 = C_{d_S} - \frac{C_{d,max} \sin^2(\alpha_S)}{\cos(\alpha_S)} \tag{3.27}$$

as the subscript S means stall condition. Du-Selig, Eggers and Viterna algorithms presented in this section are consistent with each other and are implemented in an OpenFAST sheet called AirfoilPrep, which is free and available for this software users. In the present work, this was used to process data before simulations were executed. The model for C_m extrapolation implemented in AirfoilPrep is given by

$$\begin{cases} C_{m,ex} = C_{m,0} - \chi(C_l \cos(\alpha) + C_d \sin(\alpha)), \textit{ when } \alpha > 0 \\ C_{m,ex} = -C_{m,0} + \chi(-C_l \cos(-\alpha) + C_d \sin(-\alpha)), \textit{ when } \alpha < 0 \end{cases} \tag{3.28}$$

$$\chi = C_{m,ref} \tan(|\alpha| - 90) + 0.25, \tag{3.29}$$

where $C_m, 0$ is the C_m at zero lift angle, $C_{m,ref}$ is a correction parameter calculated using coefficients at the highest input angle of attack α_{hi}. Thus, it is determined by

$$C_{m,ref} = \frac{XM - 0.25}{\tan(\alpha_{hi} - 90)}, \tag{3.30}$$

$$XM = \frac{C_{m,0} - C_{m,hi}}{C_{l,hi} \cos(\alpha_{hi}) + C_{d,hi} \sin(\alpha_{hi})} \tag{3.31}$$

4 METHODOLOGY

To accomplish the objective of this work, new simulations using the same wind turbine model and validated framework given by Morim et al. (2019) were executed. It uses OpenFAST v2.1.0 framework coupled with an IPC through the "user-defined" option of pitch control (PC) in the OpenFAST control module (ServoDyn). The equations that were used to calculate the input parameters of the controller in the aforementioned work did not take into account the blade torsional root moment (RMz). Therefore, the coordinates transformation equations development was redone and is shown later on this chapter. In the absence of pitching moment coefficients, only lift and drag coefficients were considered in the simulations executed by Morim et al. (2019). In this work, new aerodynamic coefficients were estimated through correction models and an extra column containing obtained pitch moment coefficients were added in the airfoil files, which are linked to the aerodynamic module (AeroDyn). All other OpenFAST modules, such as the structural one (ElastoDyn) remained unchanged in most of the work, thus are not shown in Figure 4.1. A single parameter of the structural module was changed for a final investigation. Its name is "YawDOF" and it is a flag that enables or disables turbine yaw movements during OpenFAST simulations. The output file consist in a binary or text containing time series of parameters defined by the user for later post processing.

4.1 WIND TURBINE MODEL

Following Morim et al. (2019) methodology, the model chosen is the GE 1.5sle, with 1.5 MW nominal capacity and hub height of 80 meters. It was the most used utility-scale wind turbine in 2009 (GE Energy, 2009) and is one of the four megawatt-scale wind turbines installed at the National Wind Technology Center (NWTC) field-research site . More information about its technical data can be seen in the Table 4.1.

Table 4.1 – Additional GE 1.5sle turbine information.

Technical data			
Operating data		**Electrical interface**	
Rated power capacity	1500 kW	Frequency	50/60 Hz
Operation temperature range	-30ºC to +40ºC	Voltage	690 V
Survival temperature range	-40ºC to +50ºC	**Rotor and tower**	
Cut-in wind speed (v_{in})	3.5 m/s	Rotor diameter	77 m
Cut-out wind speed (v_{out})	25 m/s	Swept area	4657 m^2
Rated wind speed (v_r)	14 m/s	Hub heights	65/80 m

Source: Adapted from GE Energy (2009)

This wind turbine is already registered in OpenFAST files named as ”WP_VSP_WTurb” or ”Test13” in older software versions. This makes the preparation process of the simulation much easier, because it was already made by the software developers team.

4.2 IPC MODULE

The pitch control module implemented in the simulations and integrated in the framework through MATLAB Simulink is given by Morim (2019), Morim et al. (2019) and consists of an validated IPC based in the Robust Model Reference Adaptive Control (RMRAC), working in parallel with a collective pitch control (CPC). The objective of this controller is to minimize rotor tilt and yaw bending moments and blade root moments in the 1P frequency during region 3 of operation. These were defined according to IEC 61400-13 (British Standards Institution, 2016) fundamental loads, which presents the most critical ones for wind turbines structures in test measurements (see Table 3.2).

To accomplish the load reduction, the measured root moments RMx and RMy of each blade are converted from the blade coordinates system to the non-rotating hub reference frame through the Coleman Transformation at each time step. The present work proposes a change in this coordinates transformation by including RMz in the conversion. In the sequence, these loads are filtered by an low-pass filter, resulting in the inputs (calculated M_{tilt} and M_{yaw}) for the RMRAC. The outputs of the RMRAC controller are converted through the Inverse Coleman Transformation to result in the blade pitch correction for each blade at the current time step, which pass through final filters that model the dynamics of pitch control.

Figure 4.1 – OpenFAST flowchart with input data for present study and IPC framework.

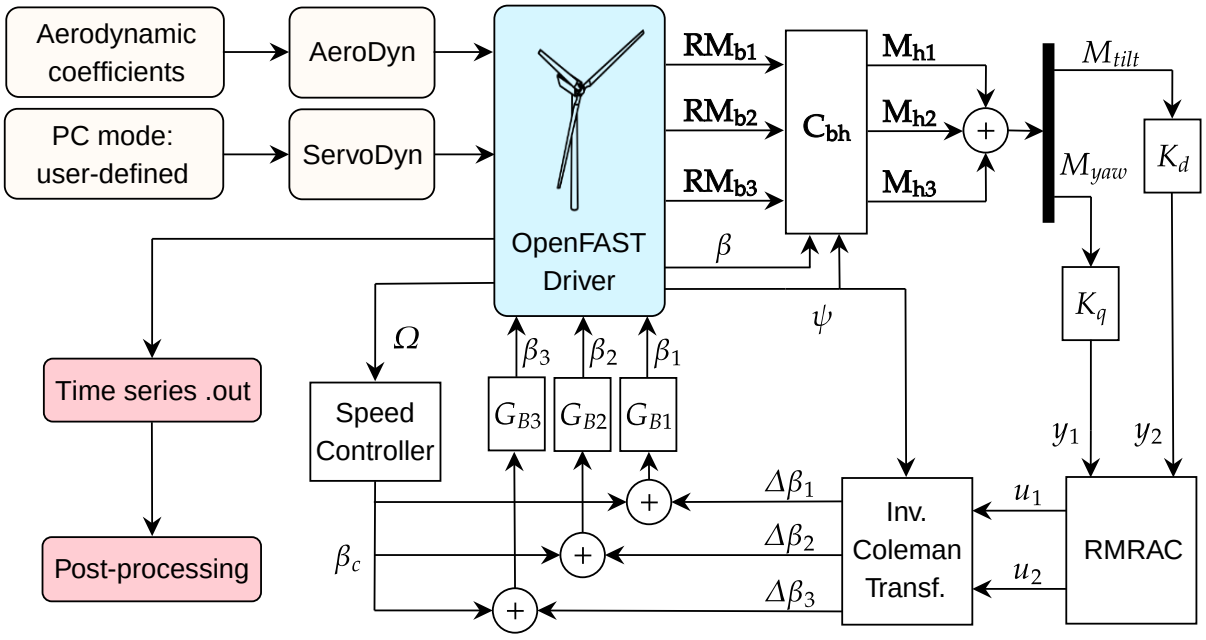

Source: Author

4.3 BLADE TO HUB COORDINATES TRANSFORMATION

The largest blade loads concentrate in the blade root and are usually measured or calculated in the blade reference frame (Figure 3.10). These loads are mechanically transferred to the hub, which is connected to the main shaft. Therefore, it is important to analyze the impact of the blade root loads in the shaft through coordinates transformation. This is a transformation from three rotating blades to two non-rotating components. In the literature, it is usual to find this named as Park's Transformation (or d-q axis transformation), when the subject is three-phase electrical machines, and Coleman Transformation, when the subject is helicopter or wind turbine rotors.

As Coleman Transformation only takes into account each blade azimuth angle, the blade pitch angle must also be considered before converting blade root loads to the hub. These two transformations may be seen as two successive planar rotations. The final matrices of rotation that describes the transformation from blade to hub reference frame are given by

$$\mathbf{C_{b1h}} = \mathbf{C_1}(-\psi_1) \cdot \mathbf{C_3}(\beta_1) = \begin{bmatrix} \cos(\beta_1) & \sin(\beta_1) & 0 \\ -\cos(\psi_1)\,\sin(\beta_1) & \cos(\psi_1)\,\cos(\beta_1) & -\sin(\psi_1) \\ -\sin(\psi_1)\,\sin(\beta_1) & \sin(\psi_1)\,\cos(\beta_1) & \cos(\psi_1) \end{bmatrix}, \tag{4.1}$$

$$\mathbf{C_{b2h}} = \begin{bmatrix} \cos(\beta_2) & \sin(\beta_2) & 0 \\ -\cos(\psi_1+120)\,\sin(\beta_2) & \cos(\psi_1+120)\,\cos(\beta_2) & -\sin(\psi_1+120) \\ -\sin(\psi_1+120)\,\sin(\beta_2) & \sin(\psi_1+120)\,\cos(\beta_2) & \cos(\psi_1+120) \end{bmatrix} \tag{4.2}$$

and

$$\mathbf{C_{b3h}} = \begin{bmatrix} \cos(\beta_3) & \sin(\beta_3) & 0 \\ -\cos(\psi_1+240)\,\sin(\beta_3) & \cos(\psi_1+240)\,\cos(\beta_3) & -\sin(\psi_1+240) \\ -\sin(\psi_1+240)\,\sin(\beta_3) & \sin(\psi_1+240)\,\cos(\beta_3) & \cos(\psi_1+240) \end{bmatrix}, \tag{4.3}$$

as ψ_1 is the azimuth angle of blade 1 and β_1, β_2 and β_3 are respectively the pitch angle of blades 1, 2 and 3 at the instant this calculation is made. Also, as the azimuth angle of the blade 1 is taken as a reference in the previous equations, Equations (4.2) and (4.3) accounts the equally spaced blades by adding respectively 120 and 240 degrees to the azimuth angle of blade 1.

The total root moment of blade 1 is given by

$$\mathbf{RM_{b1}} = \begin{bmatrix} RMx_{b1} \\ RMy_{b1} \\ RMz_{b1} \end{bmatrix}. \tag{4.4}$$

Total root moment of blades 2 and 3 follows an identical nomenclature. This equation takes into consideration all three components of the blades root moment. The equations implemented by Morim (2019) omit the moment around blade z_b-axis (RMz). Following this assumption, blade 1 edgewise and flatwise root moments are transformed to the hub coordinates through

$$\begin{cases} M_{d1} = (RMy_{b1}\ \cos(\beta_1) - RMx_{b1}\ \sin(\beta_1))\ \cos(\psi_1), \\ M_{q1} = (RMy_{b1}\ \cos(\beta_1) - RMx_{b1}\ \sin(\beta_1))\ \sin(\psi_1) \end{cases} \tag{4.5}$$

where M_{d1} and M_{q1} are the blade 1 contributions to hub loading around y_h and z_h-axis, respectively.. Blade 2 and 3 contributions are calculated by the same way. The sum of each blade contribution is the tilt (M_d) and yaw (M_q) rotor moment not considering the RMz.

To transform all three blade root moment components measured in the rotating blade reference frame to the non-rotating hub reference frame, an inner product is applied using Equations (4.1), (4.2) and (4.3) respectively in each blade root moment, such as

$$\mathbf{M_{h1}} = \mathbf{C_{b1h}} \cdot \mathbf{RM_{b1}}, \tag{4.6}$$

$$\mathbf{M_{h1}} = \begin{bmatrix} RMx_{b1}\ \cos(\beta_1) + RMy_{b1}\ \sin(\beta_1) \\ RMy_{b1}\ \cos(\beta_1)\ \cos(\psi_1) - RMx_{b1}\ \sin(\beta_1)\ \cos(\psi_1) - RMz_{b1}\ \sin(\psi_1) \\ RMy_{b1}\ \cos(\beta_1)\ \sin(\psi_1) - RMx_{b1}\ \sin(\beta_1)\ \sin(\psi_1) + RMz_{b1}\ \cos(\psi_1) \end{bmatrix}. \tag{4.7}$$

This is the blade 1 root moments contribution to the hub load considering the RMz. To calculate $\mathbf{M_{h2}}$ and $\mathbf{M_{h3}}$, the same procedure of Equation (4.6) is adopted. Finally, as each blade contributes to the hub loading, the total moment in the hub caused by each blade root moments is

$$\mathbf{M_h} = \mathbf{M_{h1}} + \mathbf{M_{h2}} + \mathbf{M_{h3}} = \begin{bmatrix} M_x \\ M_{tilt} \\ M_{yaw} \end{bmatrix}. \tag{4.8}$$

Besides the first component of Equation (4.8), which is the rotor torque, the second and third components, i.e. the moments around y_h and z_h-axis in the non-rotating hub reference frame respectively, are very important to wind turbine design as they are transmitted to the main shaft. The second component of $\mathbf{M_h}$ is named M_{tilt}, as it contributes to

change the turbine tilt angle, and the third one is named M_{yaw} for the same reason. In this work, Morim's equations were initially implemented and then were used to compare with the modified equations results.

4.4 AERODYNAMIC DATA PROCESSING

One of the OpenFAST aerodynamic module inputs is the aerodynamic coefficients of the blade airfoils. There are many wind turbine models and cases native to the software that are ready to be simulated in OpenFAST and all original data provided are complete. However, in some cases, there is a lack of information regarding aerodynamic coefficients. The wind turbine model chosen by Morim (2019) suffers from that lack of information, only having lift and drag coefficients available and lacking the pitching moment coefficients in the original files.

In this cases, NREL provides some aerodynamic coefficients at their website database (NREL, 2004), usually results of the Eppler code or wind tunnel experiments and computed for a short angle of attacks interval (usually -7° to 8°). The airfoils of the chosen wind turbine model are NREL S818 (near-root), S825 and S826 (near-tip) and its coefficients given by NREL data base can be seen in Figure 4.2. However, OpenFAST aerodynamic module requires a complete range of angles of attack from -180° to $+180^\circ$. This brought up the necessity to create new sets of aerodynamic coefficients compatible with the original ones.

In this work, the available data was corrected and extrapolated through a tool provided by NREL in OpenFAST native files named "AirfoilPrep". The aerodynamic corrections cited in the previous chapter (Du-Selig, Eggers and Viterna) are already implemented in this tool. Thus, it was used to generate a new set of aerodynamic coefficients based on the raw input data available in NREL database.

4.5 VARIABLES ANALYZED

The list of possible outputs of OpenFAST simulations is very extensive. The variables that were chosen in this work can be seen in the last part of each driver file present in appendix B.2 and their definition can be seen in a sheet provided by NREL to OpenFAST users called "OutListParameters". From all available variables, only those directly related to the present investigation will be discussed here.

Besides investigating any changes in the controller input variables (calculated M_{tilt} and M_{yaw}), as these are a decomposition of the root moments of each blade, it is also aimed to assess the influence of the C_m in the root moments RMx, RMy and RMz to better understand the effects of this coefficient, specially the last one, as its expected that the now accounted pitching moment will cause extra torsion in the blade. To avoid unnecessary repetition, only the blade 1 root moments will be shown.

Figure 4.2 – Database coefficients and airfoils of GE 1.5sle wind turbine model.

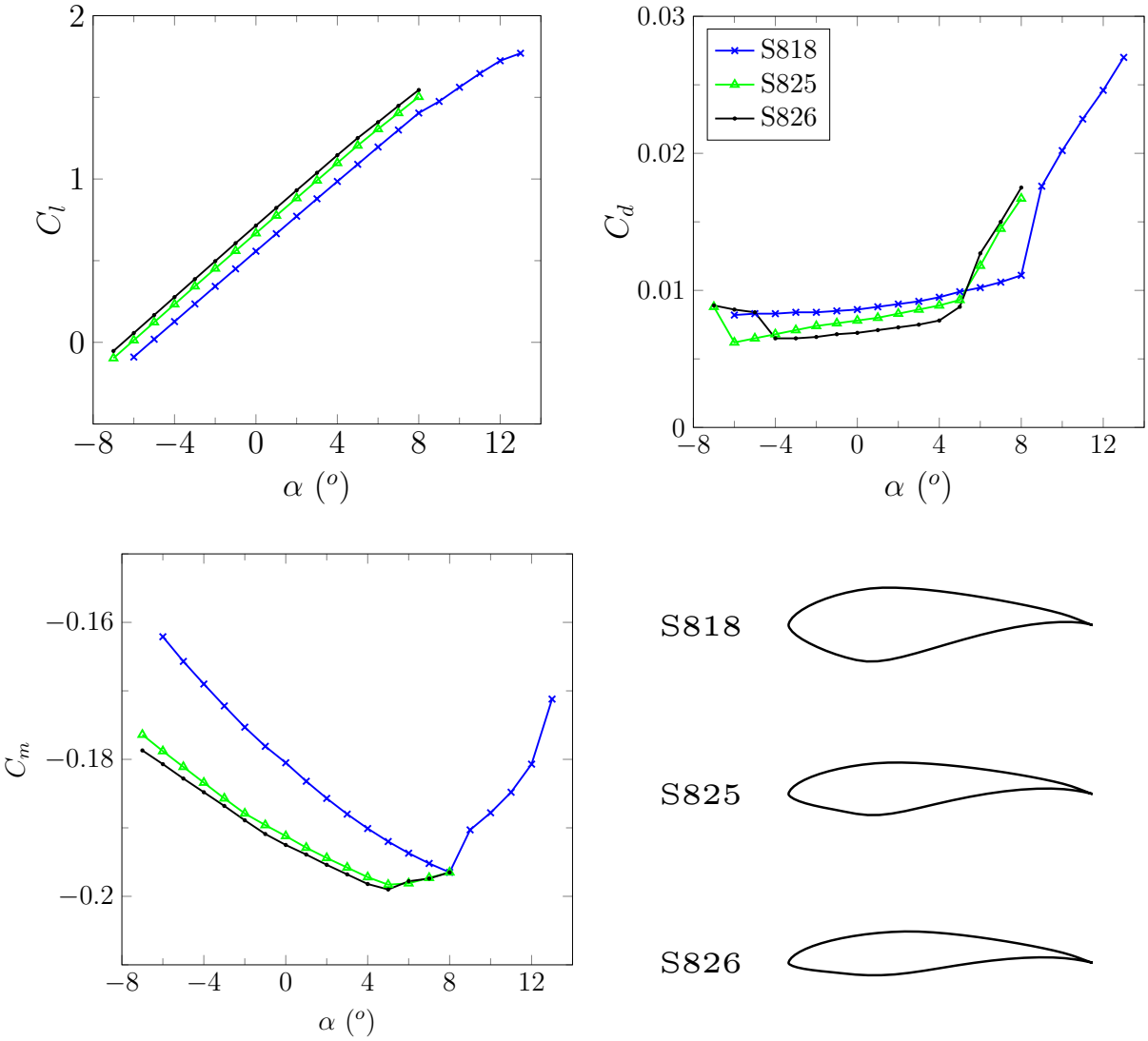

Source: Adapted from (NREL, 2004).

There are dozens of input parameters that are necessary to run OpenFAST simulations appropriately. The output is very sensitive to some of those parameters. The OpenFAST modules files containing information about all those parameters can also be seen in appendix B.2.

During this work, it was observed that in Morim (2019) simulations, the aerodynamic influence of the tower and nacelle was not taken into account and an important flag of the structural module (ElastoDyn) was turned off. This flag is called ”YawDOF” and it enables or disables yaw movements of the nacelle. When this flag is turned off, the nacelle remains fixed in a predefined angle set by the user and do not suffers any interference from the wind. As any change in the yaw dynamics of the turbine may affect the controller developed by Morim (2019), simulations were made to investigate any change in its functioning and the impact in the mentioned variables.

4.6 WIND INPUTS

OpenFAST provides a tool called "TurbSim" to generate new wind files with different characteristics. Two different wind profiles were used in the simulations. The chosen mean wind speeds (MWS) in X direction at hub height were 14.5 m/s and 18 m/s. The first wind profile is near the rated wind speed of the GE 1.5sle and has low turbulence index of 3%, so it is expected to the turbine work properly in these conditions. The second one, which was also used in Morim (2019) simulations, approximates the cut-out wind speed and has approximately 15% of turbulence index, so the turbine will experience higher loads and operate in a more severe condition. Therefore, for this last case, the turbine behavior may change significantly compared to the other. The X direction wind velocity at hub height can be seen in Figure 4.3. OpenFAST wind summary files can be seen in the appendix B.1 and B.2 .

Figure 4.3 – Chosen wind time series at hub height.

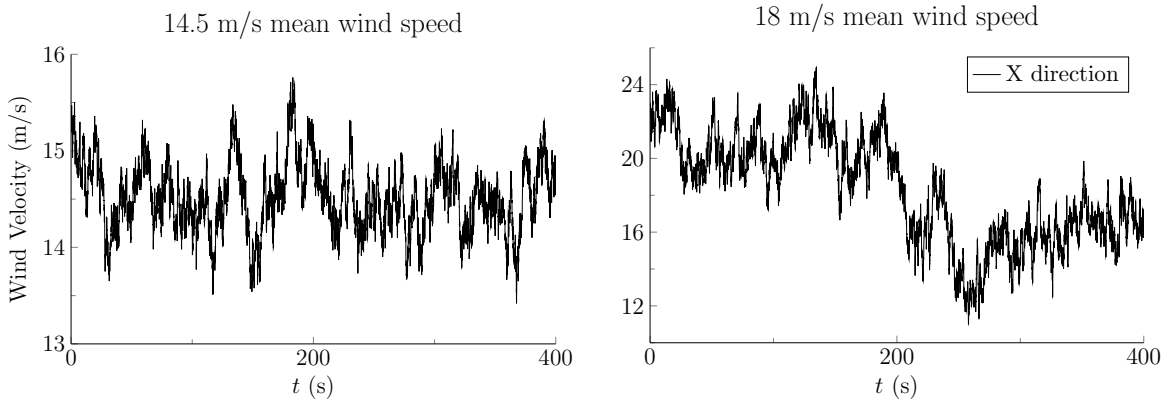

Source: Author.

4.7 POST PROCESSING

Few adjustments were necessary to analyze the data over time. As it is not the objective of this work to analyze transient behavior, the first 50 seconds of simulation were not considered in the analysis process. Besides plotting time domain data, Power Spectral Density (PSD) was used to analyze signals in frequency domain. PSD basically multiplies the Fast Fourier Transform (FFT) amplitude by its complex conjugate and divides it by the bin width for normalization. This prevents that any change in the amount of data points impact the amplitude of the result. Also, it is specially suitable to analyze data with a considerable amount of noise (low energy elements) because it highlights frequency components according to the signal energy distribution. Taking the signal average before applying PSD removes offsets and improve other frequencies visualization. In this work, the *pwelch* MATLAB function was used with a 50 s window time to compute the power spectral densities. Further information about it can be seen in MATLAB (2020), Hayes (1996).

5 RESULTS

The aerodynamic data processing results can be seen in the first part of this chapter. Also, four study cases are presented and, in each of these, the main findings are highlighted and further discussion is made. The first case study consists in comparing original and new coefficients simulation results to see if they produce similar results. Small difference in the main loads, turbine dynamics and blade pitch angle will show that they are compatible and the new coefficients are validated for further studies. Only then, the influence of the pitching moment coefficient shall be investigated in case study 2.

Equations implemented by Morim (2019) did not take into account the blade torsional root moment (RMz) in M_{tilt} and M_{yaw} calculations. Thus, cases 1 and 2 simulations were made using Equation (4.5) and case 3 consists in comparing this and the implementation of the Equation (4.7) developed in this work. Finally, the fourth case study is to investigate IPC robustness and possible C_m or modified equations impact in an alternative simulation condition by enabling yaw dynamics ("YawDOF" flag turned on). The impact in the controller, main loads and turbine dynamics will be analyzed.

The cases are summarized as

- Case 1: original vs new coefficients without C_m;
- Case 2: new coefficients without C_m vs new coefficients with C_m;
- Case 3: Morim's equations vs modified equations;
- Case 4: yaw dynamics enabled vs disabled.

The simulation results shown in the second part were achieved with the individual pitch controller code given by Morim (2019). Simulation conditions and wind profiles considered are presented in chapter 4. To spare space and allow comparisons between all three sets of coefficients, cases 1 and 2 results were plotted in the same figures. Time domain results are displayed only for a 20 seconds period of time to improve visualization and understanding. In the chosen time interval (110 to 130 s), both winds experience growing intensity change. As the mean turbine rotor speed remained 20 RPM in the simulations, 1P and 2P frequencies are approximately 0.33 Hz and 0.66 Hz, respectively, and were displayed in frequency domain analysis figures. The tilt and yaw rotor moments results were calculated from blades root moments.

5.1 AERODYNAMIC DATA CORRECTION

The correction process described in the last chapter was applied in the database coefficients. Both original and new data are listed in Appendix A and can be seen in Figure 5.1.

Figure 5.1 – Comparison between original and new lift and drag coefficients.

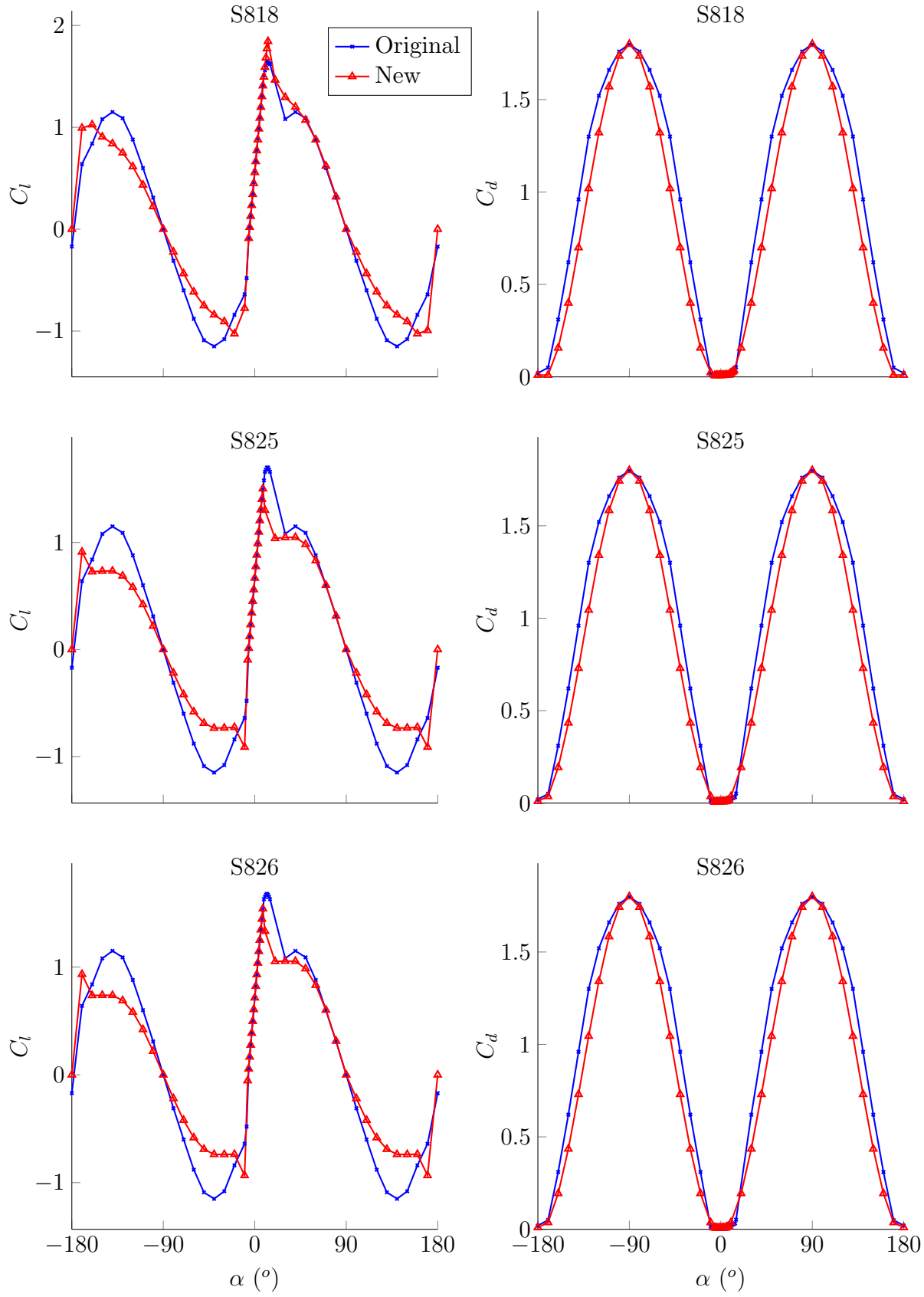

Source: Author.

Figure 5.2 – Obtained pitching moment coefficients.

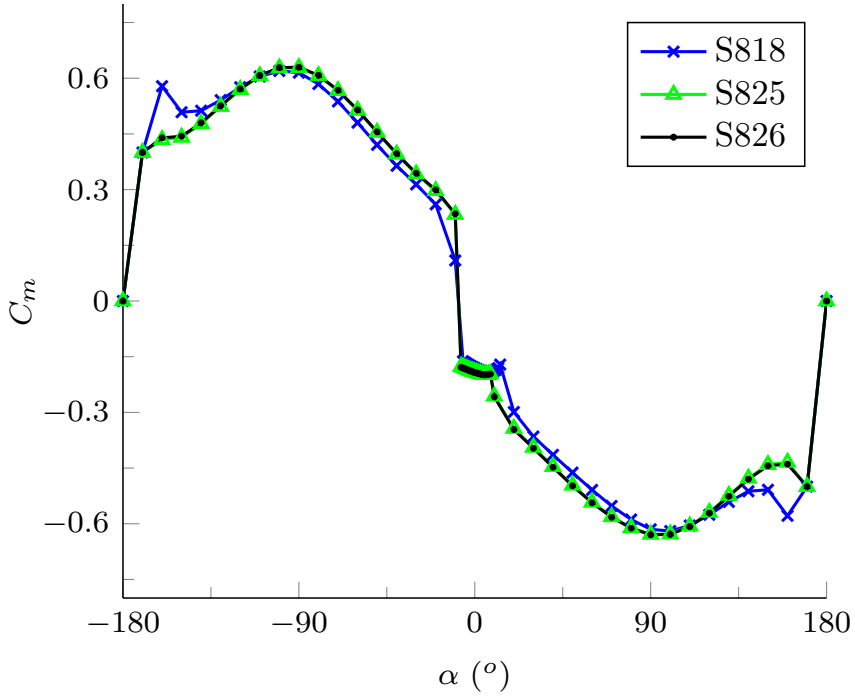

Source: Author.

Although only official information and tools from NREL were used in this process, the new C_l and C_d are not equal, but similar, to the original ones. For all three airfoil aerodynamic data, the maximum value of the drag coefficient at $\pm 90°$ is the same, but for other angles of attack values, the original C_d value is greater than the new one. The original and new lift coefficients are similar for small angles of attack ($\pm 15°$), but the discrepancy increases for $\alpha < -15°$ and $\alpha > 90°$. Higher differences noticed for negative angles of attack may be explained by the difficulty of aerodynamic coefficients correction models to predict accurately airfoil performance under these conditions.

Despite these differences, during usual operation, it was observed on simulation results that the angle of attack varies alongside the blade span from $-13.5°$ at the tip to $26°$ at the blade root, but most of the blade sections angle of attack is kept between $-3°$ and $9°$. Therefore, it is expected that adopting the new coefficients will not produce significant differences relative to original coefficients simulation results.

5.2 CASE 1: AERODYNAMIC DATA VALIDATION

Comparing original and new coefficients, regarding edgewise and flatwise blade root moments shown in Figure 5.3, minor differences were perceived. The most significant difference was noticed in the 14.5 m/s mean wind speed RMy_{b1} amplitude. Studying this variable in frequency domain (Figure 5.4), as both PSD signals are very similar, the visible time domain distinction is constant throughout the entire simulation. This was proved by applying

the average of the time domain signals and observing that they overlap. The low impact this intensity difference have on the IPC controller and the turbine dynamics can be seen in Figure 5.5. The magnitude of each blade root moment component must be highlighted. In 14.5 m/s MWS simulation, comparing 500 to -400 $kN.m$ and 950 to 700 $kN.m$ variation, for the given time interval, edgewise (RMx) component signal amplitude was greater than flatwise (RMy) component, but this one surpasses the other in load intensity. On the other hand, in 18 m/s MWS simulation, RMy amplitude varied from 900 to 0 $kN.m$, a greater variation relative to RMx.

Figure 5.3 – Blade 1 RMx and RMy in time domain for cases 1 and 2.

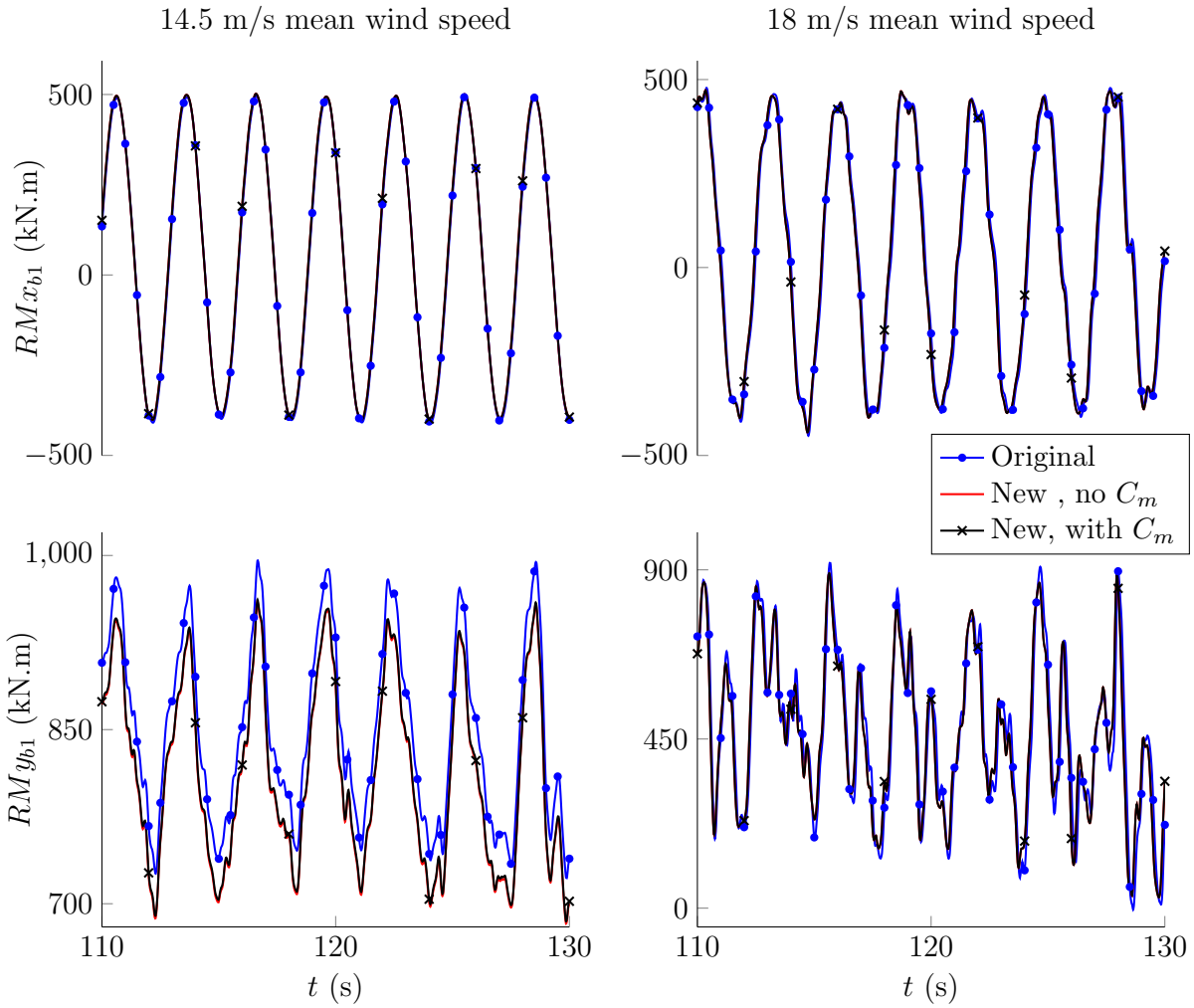

Source: Author.

Figure 5.4 – RMy for cases 1 and 2 in frequency domain (PSD).

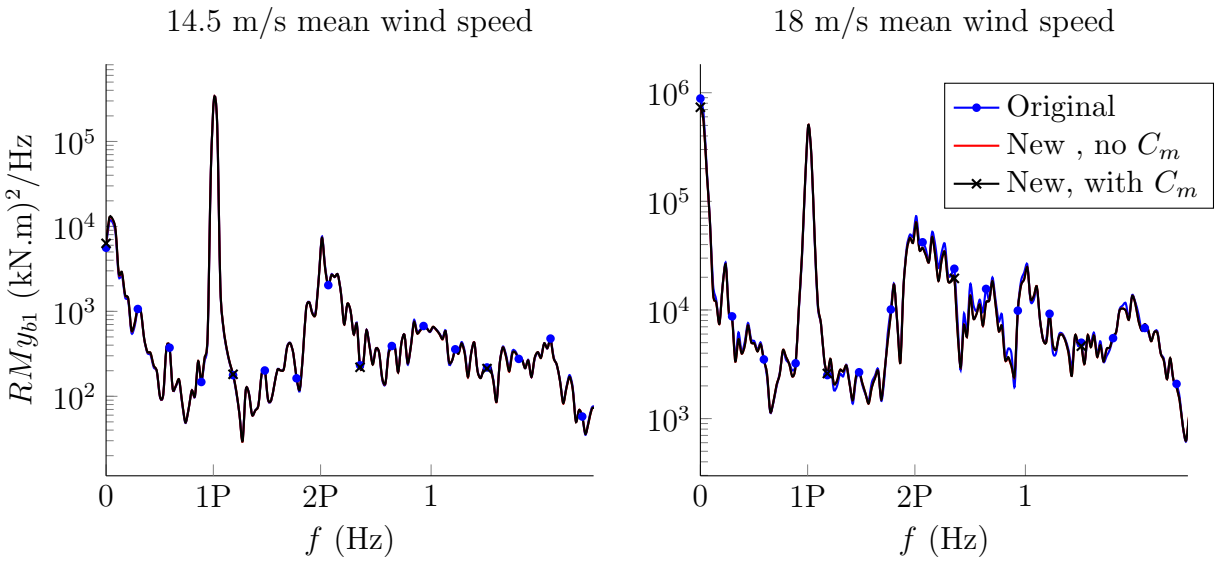

Source: Author.

Figure 5.5 – Blade 1 pitch for cases 1 and 2.

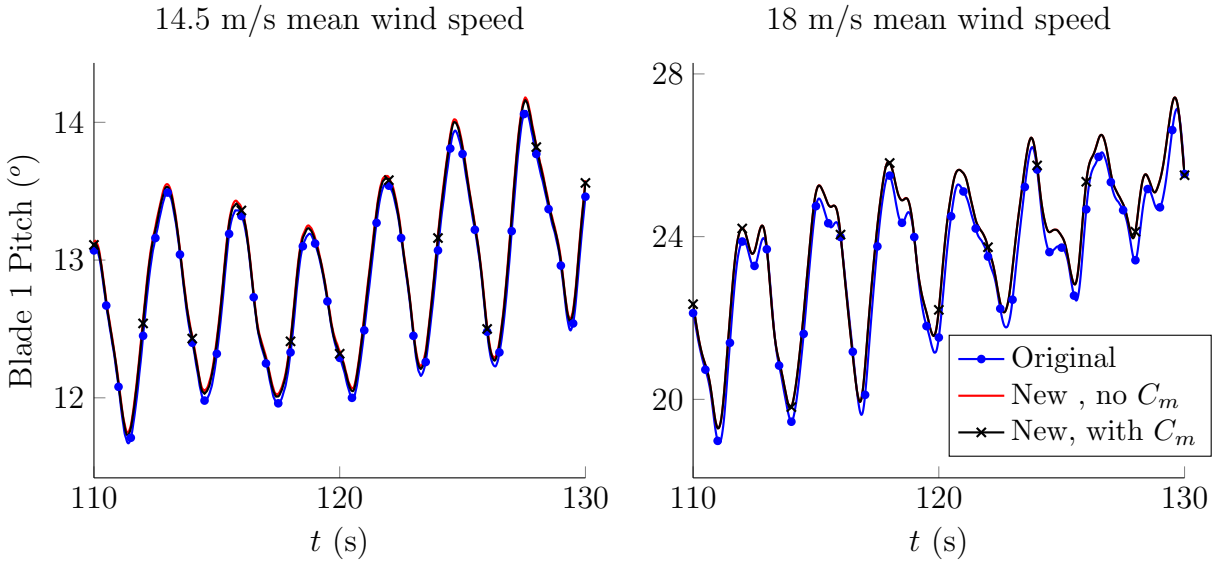

Source: Author.

As the wind velocity of the 18 m/s MWS increases from 18 to 24 m/s and the other wind varies from 13.5 to 15.5 m/s during the analysis time interval, this impacts local aerodynamics calculation. The significant RMy amplitude difference from one wind to another highlight the great role that aerodynamics plays in the flatwise blade root component. However, RMx intensity barely differs from one wind to another. This may be explained by the dominant effect of rotor speed in the edgewise blade root component, which is nearly constant in both simulations due the IPC actuation in blade position. This also causes the revolution-based loads to have very similar peaks in frequency analysis for both winds.

Regarding tilt and yaw rotor moments, small differences are noticed comparing the original and new set of coefficients overall results. The most notable difference is seen in peaks of the 18 m/s MWS result. This distinction can also be noticed in Figures 5.3 and 5.5. However, the signal amplitude difference does not imply in any overall turbine dynamics change. A frequency analysis showed that M_{tilt} and M_{yaw} peaks concentrate at 1 and 2 Hz. These are the 3P and 6P frequencies, which demonstrates the collective impact that each blade has on the load frequency at the hub. The high amplitude difference between 14.5 and 18 m/s wind results show the great impact that high intensity and turbulence winds have on tilt and yaw rotor moments.

Figure 5.6 – M_{tilt} and M_{yaw} for cases 1 and 2 in time domain.

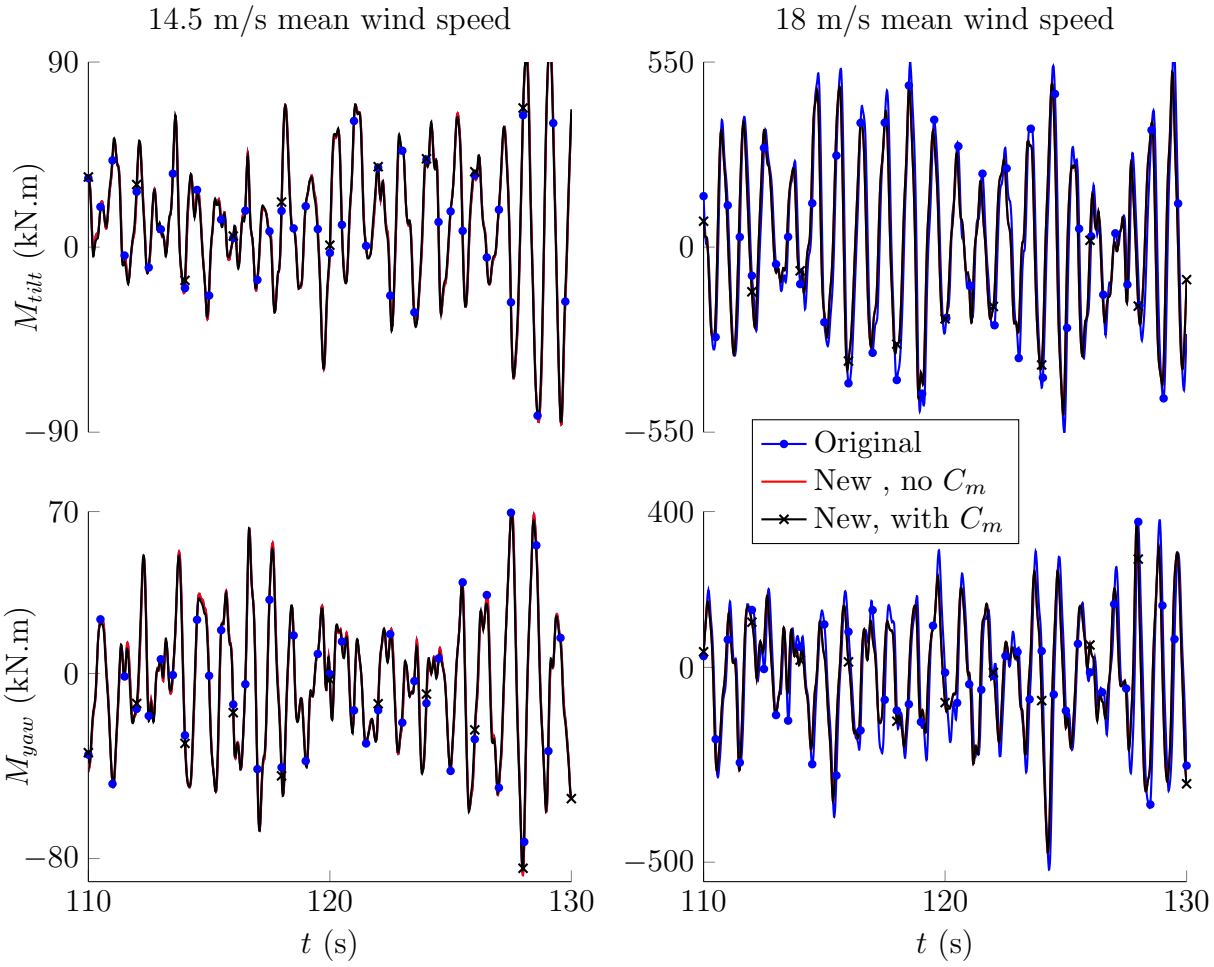

Source: Author.

Another interesting point is that the 18 m/s MWS has a different overall behavior compared to the other wind. This adds a more dominant effect into RMy frequency domain compared to the 1P frequency. This is also the case of RMz. Analyzing these variables in frequency domain, it is seen an increase in 0P (non-rotational) and 2P effects compared to the 14.5 m/s wind. Also, wind turbulence seems to impact greatly the simulation results as local aerodynamics play an important role in the blade root moments and turbine overall

behavior. Turbulence is one of the main causes for asymmetrical blade loads and this contributes for an increase in tilt and yaw rotor moments, as is shown in Figure 5.6.

Following the previous discussion, even with the near cut-out and higher turbulence wind speed, the results obtained using original or new aerodynamic coefficients were very similar. Therefore, after the previous results analysis, it is possible to conclude that, for the conditions considered, the coefficients are compatible and other case studies can be evaluated.

Figure 5.7 – Blade 1 RMz for cases 1 and 2 in time and frequency (PSD) domain.

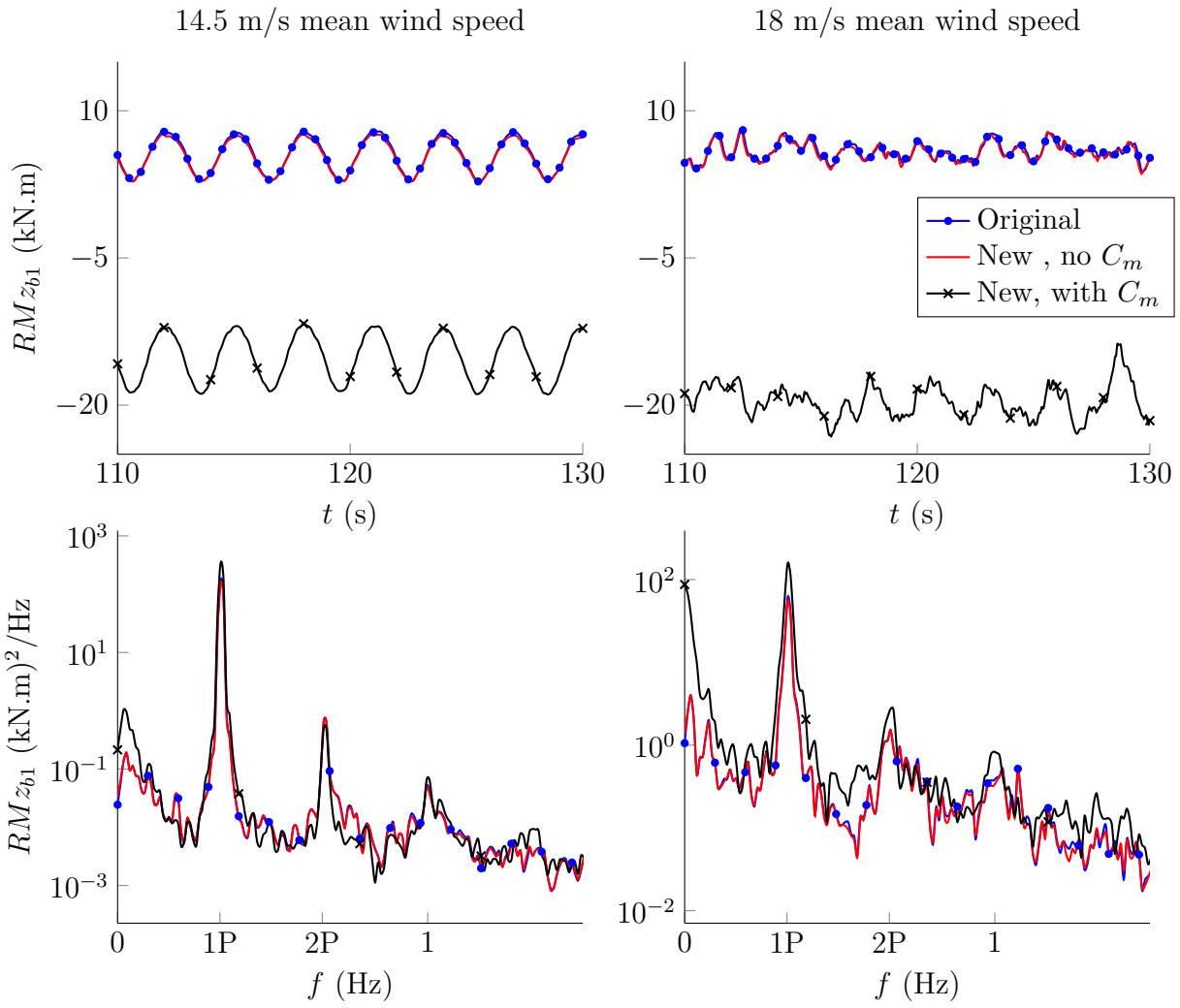

Source: Author.

5.3 CASE 2: C_m INFLUENCE

After new coefficients validation in the previous analysis case, it is possible to analyze the impact of pitching moment coefficient C_m on the IPC. As no great differences in turbine and controller overall dynamics were noticed in case 1, any significant change in results will be caused solely by the consideration of pitching moment coefficient.

Analyzing section 5.2 figures, most variables are not affected by the pitching moment coefficient consideration. However, Figure 5.7 explicit that accounting C_m plays a big role in the torsional moment at the blade root. Besides changing orientation, there is a load intensity increase of more than 50% in both considered winds. The 18 m/s wind also shows an even greater intensity and frequency change, indicating that C_m impact is even greater in higher intensity and turbulent winds.

OpenFAST uses BEM in its aerodynamic module, thus lift, drag and pitching moment are calculated locally for blade sections. As the C_m of the used airfoils are negative for positive angles of attack, it is expected that aerodynamic calculations that compute this coefficient generate negative RMz, i.e. a moment that tends to reduce the angle of attack. The simulations that does not account for the pitching moment generates positive torsion moment, which demonstrates the inaccuracy of this result. Positive values of RMz may be caused due to structural and inertial effects.

5.4 CASE 3: MODIFIED EQUATIONS INFLUENCE

This simulations were executed to measure the impact that modified equations implementation combined with the now considered pitching moment coefficient have in the IPC. Analyzing Figure 5.8, there is no great difference between the shown results.

Figure 5.8 – 18 m/s MWS M_{tilt}, M_{yaw} and pitch angle for case 3 in time domain.

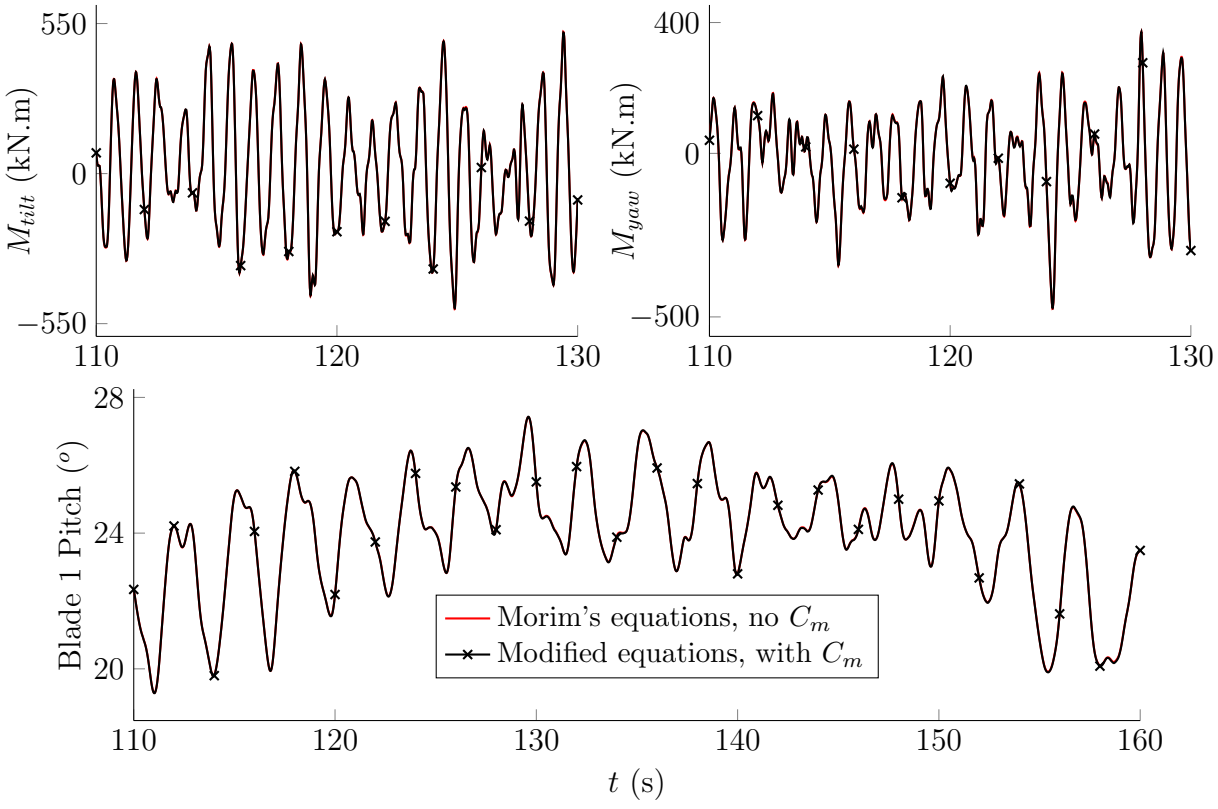

Source: Author.

This may be explained by the low magnitude of RMz compared to RMx and RMy, as can be seen in previous results. As tilt and yaw moments are calculated from blade root moments and this remained unchanged, only rotor moments were shown. Despite that, the turbine and controller dynamics remained unchanged. The higher turbulence and intensity wind caused a very similar conclusion, thus only one wind simulation results were shown.

Thus, it is possible to conclude that, for the conditions considered in this work, taking pitching moment coefficient into account and implementing the modified equations does not produce a significant result change in the IPC dynamics with its current configuration and gains. However, further study is required to investigate its impact in different and more severe winds and alternative turbine conditions.

5.5 CASE 4: YAWDOF ON VS OFF

As any change in the simulated yaw dynamics can produce significant differences in tilt and yaw rotor moments, thus impacting the controller, simulations were executed to study enabling OpenFAST "YawDOF" flag effects. Morim's equations were used and the three set of coefficients were simulated once again to compare their results and compatibility.

Analyzing Figures 5.9, 5.10 and 5.11, enabling yaw motion changed completely the turbine and controller dynamics relative to other simulations. When the "YawDOF" flag is turned on, yaw angle changes significantly due to wind incidence and turbine own dynamics. Also, its motion is uncontrolled because no yaw misalignment control was used. A great difference between original and new coefficients results is seen. It is also possible to notice a discrepancy between the results that take and do not take C_m into account.

According to NREL (2019), the skewed-wake correction model used in the aerodynamic simulations is invalid for very large (> 45 °) yaw errors. Hence, further investigation is necessary about the aerodynamic effects in this new condition, making any case 4 conclusion about the pitching moment coefficient influence on the IPC uncertain.

Figure 5.9 – 14.5 m/s MWS turbine angle for case 4 in time domain.

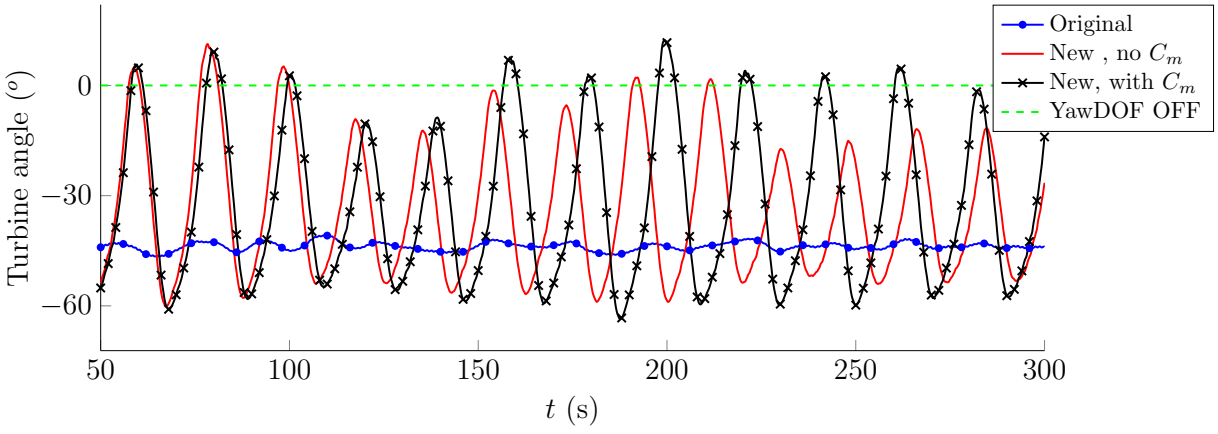

Source: Author.

Figure 5.10 – 14.5 m/s MWS blade 1 pitch and root moments for case 4 in time domain.

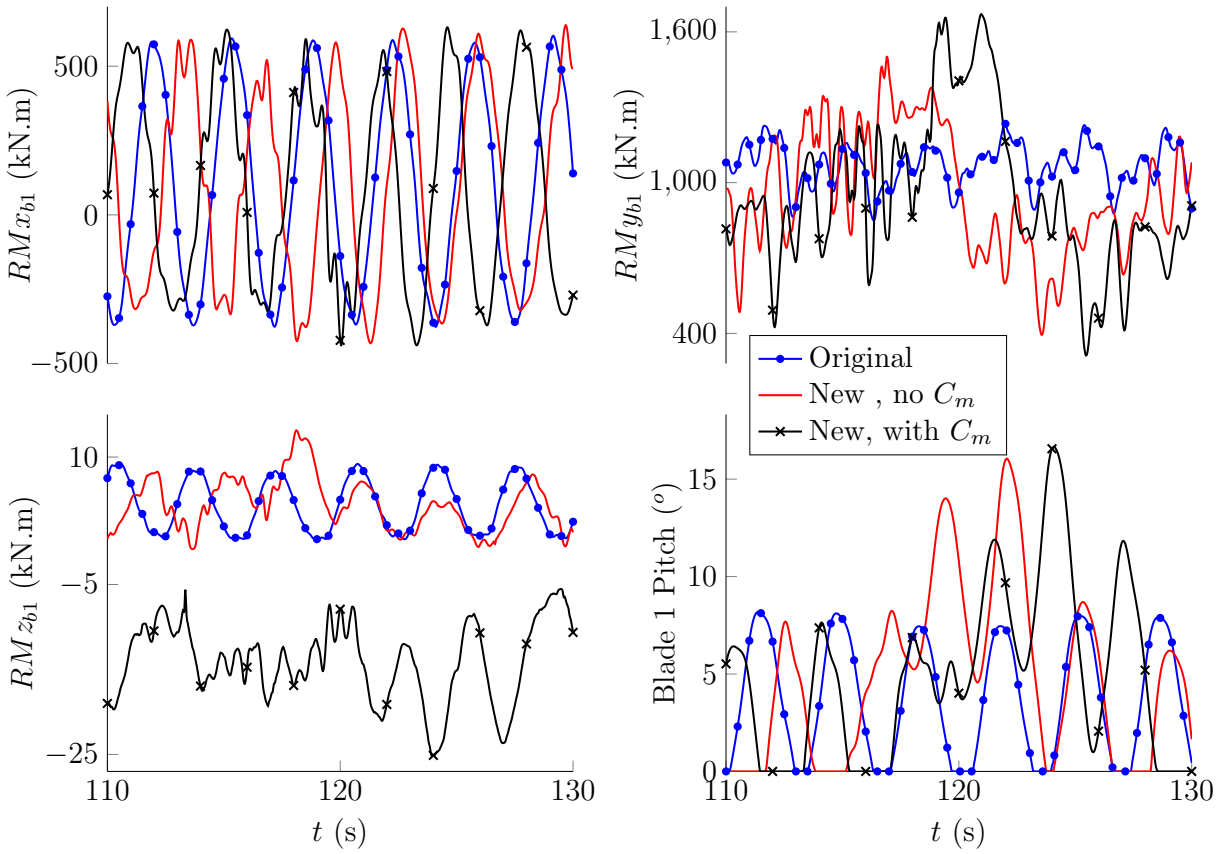

Source: Author.

As blade root, tilt and yaw rotor moments intensity of original coefficients simulations keeps under similar limits compared to previous results, new coefficients response have much higher amplitudes. The frequency response of the tilt and yaw rotor moments seen in Figure 5.12 also indicates that the mean rotor speed changed, because the peaks of M_{tilt} and M_{yaw} do not concentrate at 1 Hz, as it was pointed in case 1 analysis.

Under case 4 simulations, the wind turbine is free to move in the yaw direction. Any change in rotor plane angle relative to the wind may cause significant aerodynamic effects. It was observed that the angles of attack variation alongside the blade in this case study was much higher. Using original coefficients, AoA was going from $-8°$ at the tip to more than $70°$ at the blade root. In new coefficients response, tip and blade root angles of attack respectively surpassed $-20°$ and $90°$ in some simulation time intervals. Nonetheless, blade pitch angles are reaching its minimum range value, which may indicate that some controller gains must be adjusted to the IPC be able to reduce blade section angles of attack and make the controller reliable in turbine free yaw condition.

As no yaw misalignment correction controller was available and its development is outside the scope of this work, no further investigation about the use of Morim (2019) IPC for different simulation conditions was made.

Figure 5.11 – 14.5 m/s MWS M_{tilt} and M_{yaw} for case 4 in time domain.

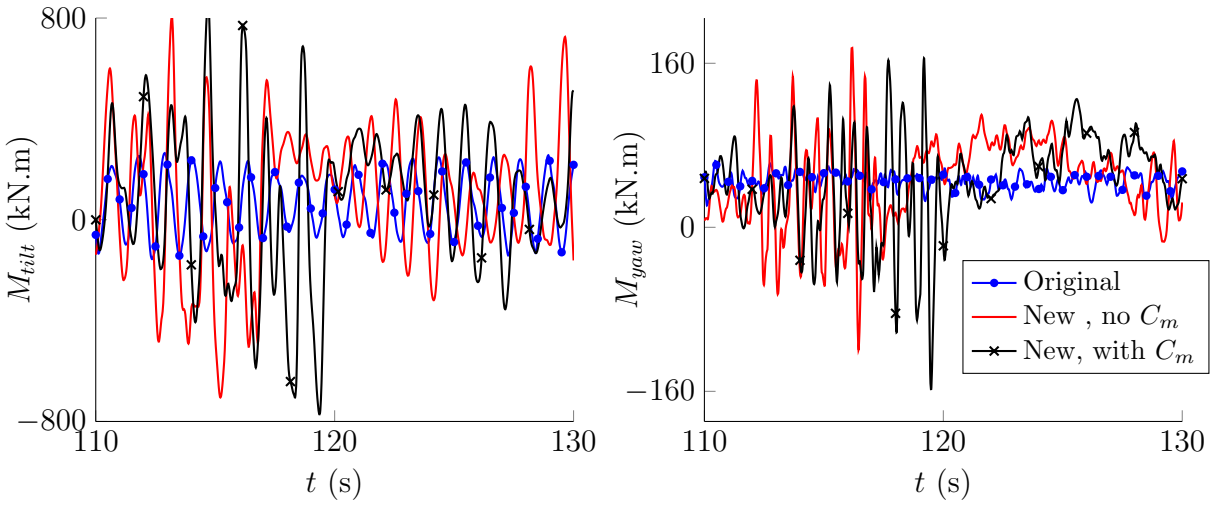

Source: Author.

Figure 5.12 – 14.5 m/s MWS M_{tilt} and M_{yaw} for case 4 in frequency domain.

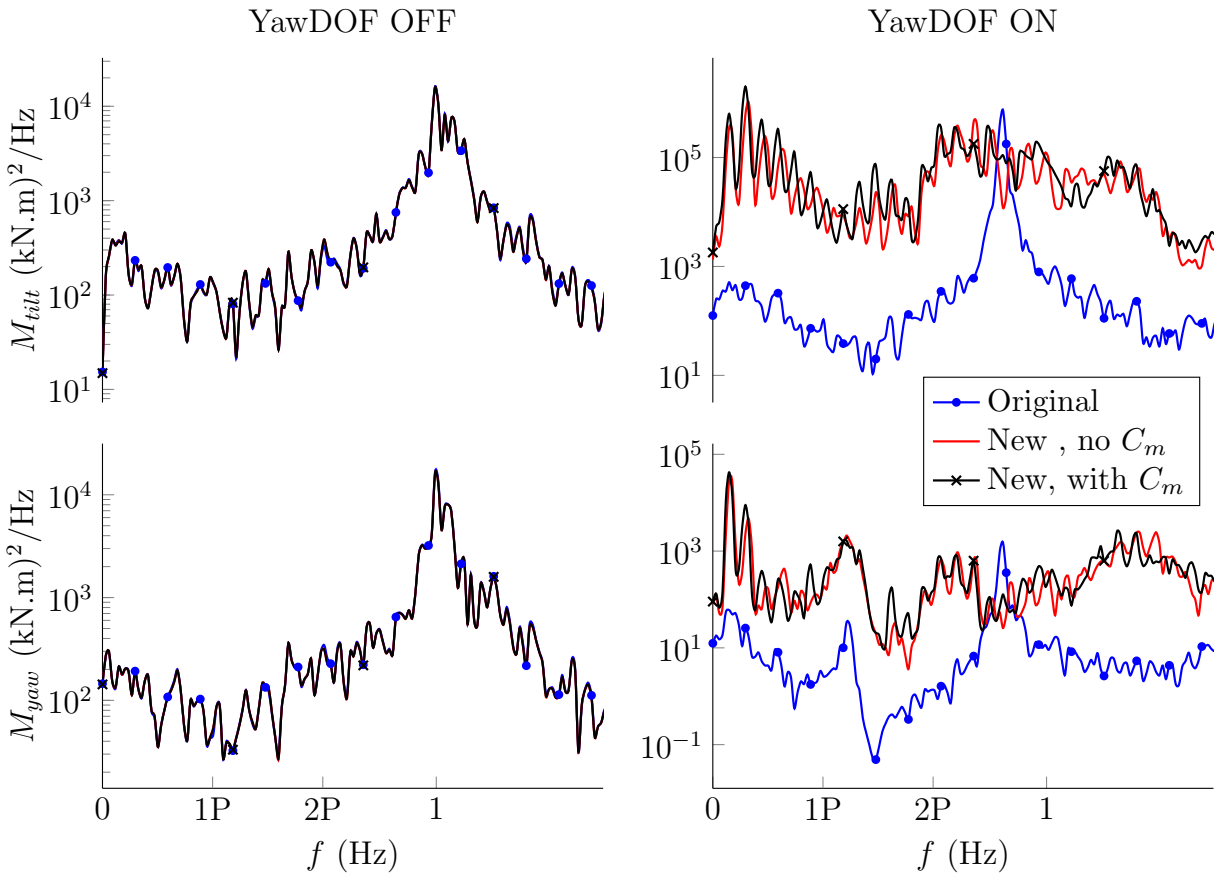

Source: Author.

6 CONCLUSION

This work comprehends a literature review regarding wind turbines simulations, a theoretical review about wind turbines main topics and other subjects around the main work theme: an investigation about the pitching moment coefficient influence in Morim (2019) Individual Pitch Controller.

After developing a seemingly compatible new set of aerodynamic coefficients to take the C_m into account and study its influence on the IPC, simulation results showed small impact in blade root edgewise (RMx) and flatwise (RMy) bending moments, but a big difference in blade root torsional moment (RMz). Despite that, tilt and yaw rotor moments were little affected. As these values are the inputs for the IPC, blade pitch angles commanded by the controller were also little affected. New M_{tilt} and M_{yaw} calculations were developed by considering the torsional component of the blade root moments in the loads coordinates transformation to the hub, but the modified equations did not change the dynamics of the controller relative to Morim's equations due to the low magnitude of RMz compared to the other two blade root moment components.

From an implementation and costs point of view, as the IPC needs load monitoring to work, the present work results indicates that may not be necessary to take RMz into consideration in rotor load calculation equations, as this would imply in more sensors to measure this root moment, besides RMx and RMy. This would raise production and maintenance costs of the pitch control system. To confirm this hypothesis, more scenarios should be considered and more simulations should be made with a large set of wind profiles and turbine conditions, specially taking into consideration the mentioned flags that was set to false in this work (tower and nacelle aerodynamic influence, "YawDOF").

On the other hand, from a simulation and design point of view, both C_m and RMz certainly plays a big role as it approximates the turbine model dynamics to a real turbine behavior. As shown, taking the pitching moment coefficient into consideration in the simulations changed significantly RMz intensity and orientation. The engineer that would design this pitch control system without considering this coefficient could cause a long history of flaws and a significant time and monetary loss for any project.

After enabling the "YawDOF" flag, simulation results showed a great turbine and controller dynamics change relative to previous cases. The blade pitch angles commanded by the controller reached its minimal range value, not being able to reduce large angles of attack during the simulation. Also, original and new coefficients results were very different, which imply in a deeper study about the yaw misalignment aerodynamic effects occurring in case 4 simulations, but this is outside the scope of this work. Although being very unlikely that the turbine will experience this kind of situation, since batteries and accumulators are responsible for feathering the blades and shutting off rotation in case of any failure, case

4 results may indicate that some controller gains must be further investigated to assess IPC reliability. To follow IPC studies, other approach besides estimating new coefficients may be change the simulated turbine model in OpenFAST to one that already have pitching moment coefficients in its original files (such as the ”5MW_Land_DLL_WTurb” or ”Test18”).

Finally, after a reliable aerodynamic coefficients development or a new choice of turbine model, introducing the pitching moment coefficient in OpenFAST IPC simulations would certainly provide more realistic results, open up space for more aerodynamic analysis, improvements and an even more robust controller.

6.1 POSSIBLE UPCOMING WORKS

- Investigation about tower and nacelle aerodynamic influence;
- Nacelle/yaw controller development;
- IPC gains adjustment for yaw misaligned condition;
- Simulations with a great amount of wind profiles;
- IPC and OpenFAST coupled with QBlade (LLFVW) aerodynamic simulations;
- Study about other aerodynamic coefficients estimation methods;
- Development of more reliable aerodynamic coefficients;
- Use of UFSM wind tunnel to calculate new aerodynamic coefficients and replace the ones used in this work;
- Use of AI to identify blade damage and overload.

BIBLIOGRAPHY

ABEEólica. **Números ABEEólica - Fevereiro 2019**. São Paulo, 2019.

ANDERSON, J. D. **Fundamentals of Aerodynamics**. 6. ed. New York: McGraw-Hill, 2016.

ANNONI, J. et al. Evaluating tilt for wind plants. **2017 American Control Conference (ACC)**, p. 717–722, 2017. DOI:10.23919/ACC.2017.7963037.

BAUCHAU, O. A. **Flexible Multibody Dynamics**. Atlanta: Springer, 2011. 751 p. ISBN 9789400703346.

BELTRAN, B.; BENBOUZID, M.; AHMED-ALI, T. Second-order sliding mode control of a doubly fed induction generator driven wind turbine. **IEEE Transactions on Energy Conversion**, v. 27, n. 2, p. 261–269, 2012. DOI:10.1109/TEC.2011.21815150.

BERTIN, J.; CUMMINGS, R. **Aerodynamics for Engineers**. 6. ed. Upper Saddle River: Pearson Prentice-Hall, 2013.

BOSSANYI, E. A. The design of closed loop controllers for wind turbines. **Wind Energy**, v. 3, n. 3, p. 149–163, 2000. DOI:10.1002/we.34.

____. Wind turbine control for load reduction. **Wind Energy**, v. 6, n. 3, p. 229–244, 2003. ISSN 10954244. DOI:10.1002/we.95.

____. Further load reductions with individual pitch control. **Wind Energy**, v. 8, n. 4, p. 481–485, 2005. DOI:10.1002/we.166.

BRETON, S.-P. **Study of the stall delay phenomenon and of wind turbine blade dynamics using numerical approaches and NREL's wind tunnel tests** . 2008. Tese (PhD Thesis) — Norwegian University of Science and Technology, 2008.

British Standards Institution. **BS EN 61400 Part 1 : Wind turbines - Design requirements**. [S.l.]: BSI Standards Limited, 2014.

____. **BS EN 61400 Part 13 : Wind turbines - Measurement of mechanical loads**. [S.l.]: BSI Standards Limited, 2016.

BURTON, T. et al. **Wind Energy Handbook**. 2. ed. New Delhi: Wiley, 2011. ISBN 9780470699751.

CIANG, C. C.; LEE, J.-R.; BANG, H.-J. Structural health monitoring for a wind turbine system: a review of damage detection methods. **Measurement Science and Technology**, IOP Publishing, v. 19, n. 12, p. 122001, oct 2008. DOI:10.1088/0957-0233/19/12/122001.

COOPERMAN, A.; MARTINEZ, M. Load monitoring for active control of wind turbines. **Renewable and Sustainable Energy Reviews**, Elsevier, Vol. 41, p. 189–201, 09 2015. DOI:10.1016/j.rser.2014.08.029.

DAM, C. P. van; BERG, D. E.; JOHNSON, S. J. **Active load control techniques for wind turbines.** [S.l.], 2008. DOI:10.2172/943932.

DU, Z.; SELIG, M. S. A 3-D stall-delay model for horizontal axis wind turbine performance prediction. **1998 ASME Wind Energy Symposium**, p. 9–19, 1998. DOI:10.2514/6.1998-21.

DURAND, W. F. et al. **Aerodynamic Theory**. Berlin: Springer, 1935. ISBN 9783642896309.

EGGERS, A.; CHANEY, K.; DIGUMARTHI, R. An assessment of approximate modeling of aerodynamic loads on the uae rotor. In: ____. **41st Aerospace Sciences Meeting and Exhibit**. [S.l.: s.n.], 2003. DOI:10.2514/6.2003-868.

Enerfín do Brasil. **Complexo Eólico de Osório**. Grupo Elencor, 2019. Acesso em 07 dez. 2019. Disponível em: <http://complexoeolicodeosorio.com.br>.

EPE. **Relatório Síntese do Balanço Energético Nacional 2019**. [S.l.], 2019. 67 p. Disponível em: <http://www.epe.gov.br/>.

FAULSTICH, S.; HAHN, B.; TAVNER, P. J. Wind turbine downtime and its importance for offshore deployment. **Wind Energy**, v. 14, n. 3, p. 327–337, 2011. DOI:10.1002/we.421.

GE Energy. **GE Energy 1.5MW Wind Turbine**. [S.l.], 2009. 1–12 p. Disponível em: <https://geosci.uchicago.edu/~moyer/GEOS24705/Readings/GEA14954C15-MW-Broch.pdf>.

HANSEN, M. O. L. **Aerodynamics of Wind Turbines.** 3. ed. New York: Routledge, 2015. 189 p. ISSN 0143702X. ISBN 9781138775077.

HAYES, M. H. **Statistical Digital Signal Processing and Modeling**. 1st. ed. USA: John Wiley amp; Sons, Inc., 1996. DOI:10.2307/1271141. ISBN 0471594318.

HE, K. et al. Combined pitch and trailing edge flap control for load mitigation of wind turbines. **Energies**, MDPI AG, v. 11, n. 10, p. 2519, Sep 2018. ISSN 1996-1073. DOI:10.3390/en11102519.

IEA. **Key world energy statistics**. [s.n.], 2019. Disponível em: <https://webstore.iea.org/key-world-energy-statistics-2019>.

____. **World Energy Outlook 2019**. Paris: [s.n.], 2019. Disponível em: <https://www.iea.org/reports/world-energy-outlook-2019>.

IRENA. **Renewable Capacity Statistics 2020, International Renewable Energy Agency (IRENA)**. [S.l.: s.n.], 2020. 66 p. ISBN 978-92-9260-239-0.

____. **Renewable Power Generation Costs in 2019**. Abu Dhabi: [s.n.], 2020. ISSN 1476-4687. ISBN 978-92-9260-040-2.

JONKMAN, J. **Recent Aeroelastic Enhancements in OpenFAST**. 2018. Disponível em: <https://energyworkshops.sandia.gov/wp-content/uploads/2018/09/OpenFAST_Jonkman_Rev3.pdf>.

JONKMAN, J. et al. Validation of FAST.farm against large-eddy simulations. **Journal of Physics: Conference Series**, IOP Publishing, v. 1037, jun 2018. DOI:10.1088/1742-6596/1037/6/062005.

JONKMAN, J. M. et al. Development of fast.farm: A new multi-physics engineering tool for wind-farm design and analysis. In: ____. **35th Wind Energy Symposium**. [S.l.: s.n.], 2017. DOI:10.2514/6.2017-0454.

JOSE, A.; FALZARANO, J.; WANG, H. A Study of Negative Damping in Floating Wind Turbines Using Coupled Program FAST-SIMDYN. **ASME 2018 1st International Offshore Wind Technical Conference**, v. 1, 11 2018. DOI:10.1115/IOWTC2018-1112.

KATZ, J.; PLOTKIN, A. **Low-Speed Aerodynamics**. 2. ed. New York: Cambridge University Press, 2001. ISBN 9780521665520.

LARSEN, T. J.; MADSEN, H. A.; THOMSEN, K. Active load reduction using individual pitch, based on local blade flow measurements. **Wind Energy**, v. 8, n. 1, p. 67–80, 2005. DOI:10.1002/we.141.

LI, D. et al. A review of damage detection methods for wind turbine blades. **Smart Materials and Structures**, IOP Publishing, v. 24, n. 3, p. 033001, feb 2015. DOI:10.1088/0964-1726/24/3/033001.

LIAO, C.; ZHAO, X.; XU, J. Blade layers optimization of wind turbines using fast and improved pso algorithm. **Renewable Energy**, v. 42, p. 227 – 233, 2012. ISSN 0960-1481. DOI:10.1016/j.renene.2011.08.011.

MANWELL, J.; MCGOWAN, J.; ROGERS, A. **Wind Energy Explained: Theory, Design and Application**. 2. ed. United Kingdom: Wiley, 2010. ISBN 9780470015001.

MATLAB. **Welch's power spectral density estimate**. The MathWorks Inc., 2020. Acesso em 20 sept. 2020. Disponível em: <https://www.mathworks.com/help/signal/ref/pwelch.html>.

MORIM, R. B. **CONTROLE INDIVIDUAL DE PASSO PARA TURBINAS EÓLICAS UTILIZANDO CONTROLADOR ADAPTATIVO**. 2019. 148 p. Tese (Mestrado em Engenharia Elétrica), Santa Maria, 2019.

MORIM, R. B. et al. Analysis of Wind Turbine Power Generation with Individual Pitch Control. **2019 IEEE PES Innovative Smart Grid Technologies Conference - Latin America (ISGT Latin America)**, IEEE, p. 1–6, 2019. DOI:10.1109/ISGT-LA.2019.8895292.

NREL. **Index of Airfoil Coefficients**. NREL, 2004. Acesso em 07 dez. 2019. Disponível em: <https://wind.nrel.gov/airfoils/Coefficients/>.

NREL. **OpenFAST Documentation**. Lakewood, Estados Unidos, 2019. Release v2.1.0, 105 p. Acesso em 04 out. 2019.

ONS. **Boletim Mensal de Geração Eólica Outubro** / **2019**. [S.l.], 2019. 44 p.

____. **Boletim Mensal de Geração Eólica Fevereiro** / **2020**. [S.l.], 2020.

Peng K Y. **Horizontal Axis Wind Turbine**. PengPeng Science and Art, 2009. Acesso em 01 sept. 2020. Disponível em: <http://www.pengky.cn/zz-horizontal-axis-turbine/horizontal-axis-turbine.html>.

PEREZ-BECKER, S. et al. Is the blade element momentum theory overestimating wind turbine loads? – an aeroelastic comparison between openfast's aerodyn and qblade's lifting-line free vortex wake method. **Wind Energy Science**, v. 5, n. 2, p. 721–743, 2020. DOI:10.5194/wes-5-721-2020.

ROOIJ, R. V. **Terminology , Reference Systems and Conventions**. TU Delft: [s.n.], 2001.

SANTONI, C. et al. Effect of tower and nacelle on the flow past a wind turbine. **Wind Energy**, v. 20, n. 12, p. 1927–1939, 2017. ISSN 10991824. DOI:10.1002/we.2130.

SCHAFFARCZYK, A. P. **Introduction to Wind Turbine Aerodynamics**. Berlin: Springer, 2014. ISSN 18653529. ISBN 9781849961745.

SPERA, D. (Ed.). **Wind turbine technology.** 2. ed. New York: ASME, 2009. ISSN 0038092X.

US DOE. **2017 Wind Technologies Market Report**. [S.l.], 2017.

VISBAL, M. On the formation and control of the dynamic stall vortex on a pitching airfoil. In: ____. **29th Aerospace Sciences Meeting**. [S.l.: s.n.], 1991. DOI:10.2514/6.1991-6.

VITERNA, L.; JANETZKE, D. Theoretical and experimental power from large horizontal-axis wind turbines. **NASA Technical Memorandum**, 10 1982. DOI:10.2172/6763041.

WANG, L.; LIU, X.; KOLIOS, A. State of the art in the aeroelasticity of wind turbine blades: Aeroelastic modelling. **Renewable and Sustainable Energy Reviews**, Elsevier, 2016. DOI:10.1016/j.rser.2016.06.007.

WANG, Y.; WANG, J.; ZHANG, J. Effects of Wind Rotor Tilt Angle on Aerodynamic Power of Wind Turbine under Typical Periodic Disturbances. **IFToMM WC 2019**, Springer International Publishing, v. 73, 2019. DOI:10.1007/978-3-030-20131-9$_3$41.

WINDEUROPE. **Wind energy in Europe in 2018**. [S.l.], 2018.

XIAO, S.; YANG, G.; GENG, H. Individual Pitch Control Design of Wind Turbines for Load Reduction Using Sliding Mode Method. **IEEE ECCE Asia Downunder**, 2013. DOI:10.1109/ECCE-Asia.2013.6579101.

APPENDIX A – AERODYNAMIC COEFFICIENTS

A.1 – NREL DATABASE COEFFICIENTS OF GE 1.5SLE AIRFOILS

	S818			S825			S826		
α	C_l	C_d	C_m	C_l	C_d	C_m	C_l	C_d	C_m
-7				-0.097	0.0088	-0.1764	-0.053	0.0089	-0.1787
-6	-0.09	0.0082	-0.1621	0.013	0.0062	-0.1788	0.057	0.0086	-0.1807
-5	0.019	0.0083	-0.1657	0.123	0.0065	-0.1811	0.167	0.0084	-0.1828
-4	0.127	0.0083	-0.169	0.233	0.0068	-0.1834	0.277	0.0065	-0.1848
-3	0.235	0.0084	-0.1722	0.343	0.0071	-0.1857	0.387	0.0065	-0.1868
-2	0.343	0.0084	-0.1753	0.452	0.0074	-0.1879	0.497	0.0066	-0.1889
-1	0.450	0.0085	-0.1781	0.56	0.0076	-0.1896	0.607	0.0068	-0.1909
0	0.558	0.0086	-0.1805	0.668	0.0078	-0.1912	0.715	0.0069	-0.1925
1	0.665	0.0088	-0.1832	0.776	0.0080	-0.1929	0.823	0.0071	-0.1939
2	0.772	0.0090	-0.1857	0.883	0.0083	-0.1944	0.931	0.0073	-0.1954
3	0.879	0.0092	-0.1880	0.991	0.0086	-0.1958	1.038	0.0075	-0.1968
4	0.985	0.0095	-0.1901	1.098	0.0089	-0.1972	1.146	0.0078	-0.1982
5	1.090	0.0099	-0.1920	1.205	0.0093	-0.1983	1.251	0.0088	-0.199
6	1.196	0.0102	-0.1937	1.306	0.0118	-0.1981	1.348	0.0127	-0.1978
7	1.300	0.0106	-0.1952	1.404	0.0145	-0.1973	1.448	0.015	-0.1974
8	1.404	0.0111	-0.1965	1.503	0.0167	-0.1965	1.545	0.0175	-0.1965
9	1.475	0.0176	-0.1903						
10	1.562	0.0202	-0.1878						
11	1.646	0.0225	-0.1848						
12	1.724	0.0246	-0.1807						
13	1.770	0.0270	-0.1712						

Source: Copied from NREL (2004)

A.2 – S818 ORIGINAL DATA

α	C_l	C_d	α	C_l	C_d
-180	-0.170	0.0200	4	0.990	0.0096
-170	0.640	0.0500	5	1.100	0.0099
-160	0.840	0.3100	6	1.200	0.0103
-150	1.080	0.6200	7	1.310	0.0108
-140	1.150	0.9600	8	1.410	0.0113
-130	1.090	1.3000	9	1.510	0.0118
-120	0.880	1.5200	10	1.560	0.0194
-110	0.600	1.6600	11	1.610	0.0221
-100	0.310	1.7600	12	1.650	0.0245
-90	0.000	1.8000	13	1.650	0.0269
-80	-0.310	1.7600	14	1.630	0.0296
-70	-0.600	1.6600	15	1.620	0.0520
-60	-0.880	1.5200	30	1.080	0.6200
-50	-1.090	1.3000	40	1.150	0.9600
-40	-1.150	0.9600	50	1.090	1.3000
-30	-1.080	0.6200	60	0.880	1.5200
-20	-0.840	0.3100	70	0.600	1.6600
-10	-0.640	0.0144	80	0.310	1.7600
-8	-0.480	0.0124	90	0.000	1.8000
-6	-0.090	0.0082	100	-0.310	1.7600
-5	0.020	0.0082	110	-0.600	1.6600
-4	0.130	0.0082	120	-0.880	1.5200
-3	0.240	0.0082	130	-1.090	1.3000
-2	0.350	0.0086	140	-1.150	0.9600
-1	0.460	0.0086	150	-1.080	0.6200
0	0.570	0.0087	160	-0.840	0.3100
1	0.670	0.0088	170	-0.640	0.0500
2	0.780	0.0090	180	-0.170	0.0200
3	0.890	0.0093			

A.3 – S818 NEW DATA

α	C_l	C_d	C_m
-180	0.0000	0.0100	0.0000
-170	0.9929	0.0100	0.4000
-160	1.0256	0.1565	0.5785
-150	0.9062	0.4001	0.5084
-140	0.8399	0.6996	0.5125
-130	0.7501	1.0193	0.5411
-120	0.6150	1.3212	0.5757
-110	0.4349	1.5697	0.6046
-100	0.2228	1.7357	0.6196
-90	0.0000	1.8000	0.6150
-80	-0.2228	1.7357	0.5845
-70	-0.4349	1.5697	0.5374
-60	-0.6150	1.3212	0.4803
-50	-0.7501	1.0193	0.4205
-40	-0.8399	0.6996	0.3642
-30	-0.9062	0.4001	0.3141
-20	-1.0256	0.1565	0.2603
-10	-0.7756	0.0234	0.1091
-6	-0.0886	0.0079	-0.1621
-5	0.0197	0.0082	-0.1657
-4	0.1274	0.0082	-0.1690
-3	0.2351	0.0084	-0.1722
-2	0.3428	0.0084	-0.1753
-1	0.4499	0.0085	-0.1781
0	0.5576	0.0086	-0.1805
1	0.6648	0.0088	-0.1832
2	0.7719	0.0090	-0.1857
3	0.8790	0.0092	-0.1880
4	0.9855	0.0095	-0.1901
5	1.0914	0.0099	-0.1920
6	1.1980	0.0102	-0.1937
7	1.3033	0.0106	-0.1952
8	1.4086	0.0112	-0.1965
9	1.4944	0.0183	-0.1903
10	1.5897	0.0217	-0.1878
11	1.6831	0.0252	-0.1848
12	1.7730	0.0290	-0.1807
13	1.8440	0.0350	-0.1712
20	1.4652	0.1565	-0.2989
30	1.2946	0.4001	-0.3651
40	1.1999	0.6996	-0.4144
50	1.0716	1.0193	-0.4622
60	0.8786	1.3212	-0.5089
70	0.6213	1.5697	-0.5520
80	0.3183	1.7357	-0.5885
90	0.0000	1.8000	-0.6150
100	-0.2228	1.7357	-0.6196
110	-0.4349	1.5697	-0.6046
120	-0.6150	1.3212	-0.5757
130	-0.7501	1.0193	-0.5411
140	-0.8399	0.6996	-0.5125
150	-0.9062	0.4001	-0.5084
160	-1.0256	0.1565	-0.5785
170	-0.9929	0.0100	-0.5000
180	0.0000	0.0100	0.0000

A.4 – S825 ORIGINAL DATA

α	C_l	C_d	α	C_l	C_d
-180	-0.170	0.0200	4	1.090	0.0095
-170	0.640	0.0500	5	1.200	0.0098
-160	0.840	0.3100	6	1.300	0.0102
-150	1.080	0.6200	7	1.410	0.0107
-140	1.150	0.9600	8	1.490	0.0155
-130	1.090	1.3000	9	1.580	0.0179
-120	0.880	1.5200	10	1.660	0.0203
-110	0.600	1.6600	11	1.680	0.0250
-100	0.310	1.7600	12	1.700	0.0273
-90	0.000	1.8000	13	1.700	0.0297
-80	-0.310	1.7600	14	1.680	0.0324
-70	-0.600	1.6600	15	1.660	0.0520
-60	-0.880	1.5200	30	1.080	0.6200
-50	-1.090	1.3000	40	1.150	0.9600
-40	-1.150	0.9600	50	1.090	1.3000
-30	-1.080	0.6200	60	0.880	1.5200
-20	-0.840	0.3100	70	0.600	1.6600
-10	-0.640	0.0144	80	0.310	1.7600
-8	-0.480	0.0124	90	0.000	1.8000
-6	0.010	0.0074	100	-0.310	1.7600
-5	0.120	0.0075	110	-0.600	1.6600
-4	0.230	0.0077	120	-0.880	1.5200
-3	0.340	0.0078	130	-1.090	1.3000
-2	0.440	0.0080	140	-1.150	0.9600
-1	0.550	0.0082	150	-1.080	0.6200
0	0.660	0.0084	160	-0.840	0.3100
1	0.770	0.0086	170	-0.640	0.0500
2	0.880	0.0089	180	-0.170	0.0200
3	0.980	0.0091			

A.5 – S825 NEW DATA

α	C_l	C_d	C_m	α	C_l	C_d	C_m
-180	0.0000	0.0100	0.0000	1	0.7760	0.0080	-0.1929
-170	0.9116	0.0362	0.4000	2	0.8830	0.0083	-0.1944
-160	0.7268	0.1933	0.4346	3	0.9910	0.0086	-0.1958
-150	0.7326	0.4341	0.4407	4	1.0980	0.0089	-0.1972
-140	0.7342	0.7297	0.4775	5	1.2050	0.0093	-0.1983
-130	0.6877	1.0445	0.5239	6	1.3059	0.0118	-0.1981
-120	0.5816	1.3408	0.5695	7	1.4038	0.0145	-0.1973
-110	0.4205	1.5832	0.6062	8	1.5027	0.0167	-0.1965
-100	0.2193	1.7425	0.6274	10	1.3023	0.0362	-0.2563
-90	0.0000	1.8000	0.6285	20	1.0382	0.1933	-0.3432
-80	-0.2193	1.7425	0.6067	30	1.0465	0.4341	-0.3943
-70	-0.4205	1.5832	0.5665	40	1.0489	0.7297	-0.4459
-60	-0.5816	1.3408	0.5135	50	0.9824	1.0445	-0.4962
-50	-0.6877	1.0445	0.4542	60	0.8308	1.3408	-0.5422
-40	-0.7342	0.7297	0.3953	70	0.6007	1.5832	-0.5812
-30	-0.7326	0.4341	0.3421	80	0.3133	1.7425	-0.6107
-20	-0.7268	0.1933	0.2970	90	0.0000	1.8000	-0.6285
-10	-0.9116	0.0362	0.2331	100	-0.2193	1.7425	-0.6274
-7	-0.0971	0.0088	-0.1764	110	-0.4205	1.5832	-0.6062
-6	0.0129	0.0062	-0.1788	120	-0.5816	1.3408	-0.5695
-5	0.1230	0.0065	-0.1811	130	-0.6877	1.0445	-0.5239
-4	0.2330	0.0068	-0.1834	140	-0.7342	0.7297	-0.4775
-3	0.3430	0.0071	-0.1857	150	-0.7326	0.4341	-0.4407
-2	0.4520	0.0074	-0.1879	160	-0.7268	0.1933	-0.4346
-1	0.5600	0.0076	-0.1896	170	-0.9116	0.0362	-0.5000
0	0.6680	0.0078	-0.1912	180	0.0000	0.0100	0.0000

A.6 – S826 ORIGINAL DATA

α	C_l	C_d	α	C_l	C_d
-180	-0.170	0.0200	4	1.140	0.0082
-170	0.640	0.0500	5	1.250	0.0087
-160	0.840	0.3100	6	1.350	0.0104
-150	1.080	0.6200	7	1.440	0.0146
-140	1.150	0.9600	8	1.530	0.0184
-130	1.090	1.3000	9	1.630	0.0200
-120	0.880	1.5200	10	1.650	0.0219
-110	0.600	1.6600	11	1.670	0.0239
-100	0.310	1.7600	12	1.680	0.0262
-90	0.000	1.8000	13	1.670	0.0288
-80	-0.310	1.7600	14	1.650	0.0316
-70	-0.600	1.6600	15	1.630	0.0520
-60	-0.880	1.5200	30	1.080	0.6200
-50	-1.090	1.3000	40	1.150	0.9600
-40	-1.150	0.9600	50	1.090	1.3000
-30	-1.080	0.6200	60	0.880	1.5200
-20	-0.840	0.3100	70	0.600	1.6600
-10	-0.640	0.0144	80	0.310	1.7600
-8	-0.480	0.0124	90	0.000	1.8000
-6	0.060	0.0092	100	-0.310	1.7600
-5	0.170	0.0082	110	-0.600	1.6600
-4	0.280	0.0067	120	-0.880	1.5200
-3	0.390	0.0068	130	-1.090	1.3000
-2	0.500	0.0069	140	-1.150	0.9600
-1	0.600	0.0070	150	-1.080	0.6200
0	0.710	0.0072	160	-0.840	0.3100
1	0.820	0.0074	170	-0.640	0.0500
2	0.930	0.0076	180	-0.170	0.0200
3	1.040	0.0078			

A.7 – S826 NEW DATA

α	C_l	C_d	C_m	α	C_l	C_d	C_m
-180	0.0000	0.0100	0.0000	1	0.8231	0.0071	-0.1939
-170	0.9331	0.0369	0.4000	2	0.9310	0.0073	-0.1954
-160	0.7367	0.1940	0.4393	3	1.0379	0.0075	-0.1968
-150	0.7383	0.4348	0.4437	4	1.1458	0.0078	-0.1982
-140	0.7377	0.7302	0.4797	5	1.2505	0.0088	-0.1990
-130	0.6897	1.0450	0.5257	6	1.3464	0.0127	-0.1978
-120	0.5827	1.3412	0.5711	7	1.4456	0.0150	-0.1974
-110	0.4210	1.5834	0.6076	8	1.5414	0.0174	-0.1965
-100	0.2194	1.7427	0.6286	10	1.3330	0.0369	-0.2582
-90	0.0000	1.8000	0.6297	20	1.0524	0.1940	-0.3461
-80	-0.2194	1.7427	0.6079	30	1.0548	0.4348	-0.3966
-70	-0.4210	1.5834	0.5677	40	1.0539	0.7302	-0.4477
-60	-0.5827	1.3412	0.5147	50	0.9853	1.0450	-0.4977
-50	-0.6897	1.0450	0.4556	60	0.8324	1.3412	-0.5435
-40	-0.7377	0.7302	0.3969	70	0.6014	1.5834	-0.5824
-30	-0.7383	0.4348	0.3440	80	0.3134	1.7427	-0.6118
-20	-0.7367	0.1940	0.2993	90	0.0000	1.8000	-0.6297
-10	-0.9331	0.0369	0.2347	100	-0.2194	1.7427	-0.6286
-7	-0.0536	0.0091	-0.1787	110	-0.4210	1.5834	-0.6076
-6	0.0565	0.0087	-0.1807	120	-0.5827	1.3412	-0.5711
-5	0.1666	0.0085	-0.1828	130	-0.6897	1.0450	-0.5257
-4	0.2768	0.0065	-0.1848	140	-0.7377	0.7302	-0.4797
-3	0.3869	0.0065	-0.1868	150	-0.7383	0.4348	-0.4437
-2	0.4971	0.0066	-0.1889	160	-0.7367	0.1940	-0.4393
-1	0.6072	0.0068	-0.1909	170	-0.9331	0.0369	-0.5000
0	0.7152	0.0069	-0.1925	180	0.0000	0.0100	0.0000

APPENDIX B – WIND FILES

B.1 – 14.5 M/S MEAN WIND SPEED FILE

```
This summary file was generated by TurbSim (v1.06.00, 21-Sep-2012) on 10-Feb-2020 at 11:18:19.

Runtime Options:

   2318573  Random seed #1
    RANLUX  Type of random number generator
         F  Output binary HH turbulence parameters?
         F  Output formatted turbulence parameters?
         F  Output AeroDyn HH files?
         F  Output AeroDyn FF files?
         T  Output BLADED FF files?
         F  Output tower data?
         F  Output formatted FF files?
         T  Output coherent turbulence time step file?
         T  Clockwise rotation when looking downwind?
 0 -  NONE  IEC turbulence models scaled to exact specified standard deviation

Turbine/Model Specifications:

        13  Vertical grid-point matrix dimension
        13  Horizontal grid-point matrix dimension
     0.050  Time step [seconds]
   600.000  Analysis time [seconds]
   600.000  Usable output time [seconds]
    84.288  Hub height [m]
    80.000  Grid height [m]
    80.000  Grid width [m]
     0.000  Vertical flow angle [degrees]
     0.000  Horizontal flow angle [degrees]

Meteorological Boundary Conditions:

    IECKAI  IEC Kaimal spectral model
         1  IEC standard: IEC 61400-1 Ed. 3: 2005
     3.000  Percent turbulence intensity, IEC 61400-1 Ed. 3: 2005
       NTM  IEC Normal Turbulence Model
       N/A  IEC Extreme Turbulence Model (ETM) "c" parameter [m/s]
       IEC  Wind profile type
    84.288  Reference height [m]
    14.500  Reference wind speed [m/s]
       N/A  Jet height [m]
     0.200  Power law exponent
     0.030  Surface roughness length [m]

Coherent turbulence time step files are not available for IEC or TIDAL spectral models.

WARNING:   A coherent turbulence time step file cannot be generated with the IECKAI model.

You have requested that the following file(s) be generated:
TurbSim.wnd (AeroDyn/BLADED full-field wnd file)

Turbulence Simulation Scaling Parameter Summary:

   Turbulence model used                             =  IEC Kaimal
   Turbulence characteristic                         =  User-specified
   IEC standard                                      =  IEC 61400-1 Ed. 3: 2005
   Mean wind speed at hub height                     =   14.500 m/s
   Characteristic value of standard deviation        =    0.435 m/s
   Turbulence scale                                  =   42.000 m
   u-component integral scale                        =  340.200 m
   Coherency scale                                   =  340.200 m
   Characteristic value of hub turbulence intensity =    3.000%
   Gradient Richardson number                        =    0.000
   Wind profile type                                 =  Power law on rotor disk, logarithmic elsewhere
   Power law exponent                                =    0.200
   Mean shear across rotor disk                      =    0.037 (m/s)/m
   Assumed rotor diameter                            =   80.000 m
   Surface roughness length                          =    0.030 m
   Number of time steps in the FFT                   =    12144
   Number of time steps output                       =    12111

   Mean Flow Angles:

   Vertical   =   0.0 degrees
   Horizontal =   0.0 degrees
```

```
   Mean Wind Speed Profile:

   Height    Wind Speed   Horizontal Angle  U-comp (X)   V-comp (Y)   W-comp (Z)
     (m)        (m/s)         (degrees)       (m/s)        (m/s)        (m/s)
   ------    ----------   ----------------  ----------   ----------   ----------
    124.3       15.67           0.00          15.67         0.00         0.00
    117.6       15.50           0.00          15.50         0.00         0.00
    111.0       15.32           0.00          15.32         0.00         0.00
    104.3       15.13           0.00          15.13         0.00         0.00
     97.6       14.93           0.00          14.93         0.00         0.00
     91.0       14.72           0.00          14.72         0.00         0.00
     84.3       14.50           0.00          14.50         0.00         0.00
     77.6       14.26           0.00          14.26         0.00         0.00
     71.0       14.01           0.00          14.01         0.00         0.00
     64.3       13.74           0.00          13.74         0.00         0.00
     57.6       13.44           0.00          13.44         0.00         0.00
     51.0       13.11           0.00          13.11         0.00         0.00
     44.3       12.75           0.00          12.75         0.00         0.00



Harvested Random Seeds after Generation of the Random Numbers:

     28604433 K1
            0 K2

Hub-Height Simulated Turbulence Statistical Summary:

   Type of Wind        Min (m/s)   Mean (m/s)    Max (m/s)  Sigma (m/s)       TI (%)
   ----------------    ---------   ----------    ---------  -----------       ------
   Longitudinal (u)        13.23        14.50        15.78        0.367        2.533
   Lateral (v)             -1.17         0.00         1.23        0.341        2.349
   Vertical (w)            -0.85         0.00         0.70        0.212        1.463
   U component             13.23        14.50        15.78        0.367        2.533
   V component             -1.17         0.00         1.23        0.341        2.349
   W component             -0.85         0.00         0.70        0.212        1.463
   Horizontal (U&V)        13.23        14.50        15.78        0.367        2.528
   Total                   13.23        14.51        15.78        0.367        2.528

                       Min Reynolds     Mean Reynolds    Max Reynolds    Correlation
   Product             Stress (m/s)^2   Stress (m/s)^2   Stress (m/s)^2  Coefficient
   ----------------    -------------    -------------    -------------   -----------
   u'w'                     -0.536           -0.007           0.429        -0.093
   u'v'                     -0.755           -0.007           0.530        -0.053
   v'w'                     -0.496           -0.005           0.504        -0.065

Friction Velocity (Ustar)  =      0.085 m/s
Maximum Instantaneous TKE  =      0.907 (m/s)^2
Maximum Instantaneous CTKE =      0.468 (m/s)^2

U-component (X) statistics from the hub grid point:

   Mean =  14.5000 m/s
   TI   =   2.5333 %

Normalizing Parameters for Binary Data (approximate statistics):

   UBar  =  14.5000 m/s
   TI(u) =   2.5333 %
   TI(v) =   2.3494 %
   TI(w) =   1.4633 %
   Height Offset =   0.0000 m
   Grid Base     =  44.2876 m

Nyquist frequency of turbulent wind field =        10.000 Hz
Processing complete.  2.8281 CPU seconds used.
```

B.2 – 18 M/S MEAN WIND SPEED FILE

```
This summary file was generated by TurbSim (v1.06.00, 21-Sep-2012) on 15-Mar-2020 at 23:11:13.

Runtime Options:

   2318573  Random seed #1
    RANLUX  Type of random number generator
```

```
         F  Output binary HH turbulence parameters?
         F  Output formatted turbulence parameters?
         F  Output AeroDyn HH files?
         F  Output AeroDyn FF files?
         F  Output BLADED FF files?
         F  Output tower data?
         F  Output formatted FF files?
         T  Output coherent turbulence time step file?
         T  Clockwise rotation when looking downwind?
 0 -  NONE  IEC turbulence models scaled to exact specified standard deviation



Turbine/Model Specifications:

        13  Vertical grid-point matrix dimension
        13  Horizontal grid-point matrix dimension
     0.050  Time step [seconds]
   600.000  Analysis time [seconds]
   600.000  Usable output time [seconds]
    84.288  Hub height [m]
    80.000  Grid height [m]
    80.000  Grid width [m]
     0.000  Vertical flow angle [degrees]
     0.000  Horizontal flow angle [degrees]

Meteorological Boundary Conditions:

    NWTCUP  NREL National Wind Technology Center spectral model
       N/A  IEC standard
    KHTEST  Kelvin-Helmholtz billow test case
       N/A  IEC turbulence type
       N/A  IEC Extreme Turbulence Model (ETM) "c" parameter [m/s]
       IEC  Wind profile type
    84.288  Reference height [m]
    18.000  Reference wind speed [m/s]
       N/A  Jet height [m]
     0.300  Power law exponent
     0.021  Surface roughness length [m]

Non-IEC Meteorological Boundary Conditions:

    45.000  Site latitude [degrees]
     0.020  Gradient Richardson number
     0.878  Friction or shear velocity [m/s]
       N/A  Mixing layer depth [m]
    -0.727  Mean hub u'w' Reynolds stress
     1.129  Mean hub u'v' Reynolds stress
     0.418  Mean hub v'w' Reynolds stress
(   13.886, 0.199E-03)  u-component coherence parameters
(    9.719, 0.490E-03)  v-component coherence parameters
(    6.541, 0.399E-02)  w-component coherence parameters
     0.000  Coherence exponent

Coherent Turbulence Scaling Parameters:
C:\Users\AUGUSTO\Documents\PROGRAMAS\nrel_turbsim\Test\EventData
            Name of the path containing the coherent turbulence data files
       les  Type of coherent turbulence data files
         F  Randomize the disturbance scale and location?
     1.000  Disturbance scale (ratio of wave height to rotor diameter)
     0.500  Fractional location of tower centerline from right
     0.500  Fractional location of hub height from the bottom of the dataset
    30.000  Minimum start time for coherent structures [seconds]

You have requested that the following file(s) be generated:
   TurbSim.wnd (AeroDyn/BLADED full-field wnd file)
   TurbSim.cts (AeroDyn coherent turbulence time step file)

Turbulence Simulation Scaling Parameter Summary:

   Turbulence model used                          =  NREL National Wind Technology Center
   Gradient Richardson number                     =    0.020
   Monin-Obukhov (M-O) z/L parameter              =    0.058
   Monin-Obukhov (M-O) length scale               = 1454.601 m
   Mean wind speed at hub height                  =   18.000 m/s
   Wind profile type                              =  Power law on rotor disk, logarithmic elsewhere
   Power law exponent                             =    0.300
   Mean shear across rotor disk                   =    0.067 (m/s)/m
   Assumed rotor diameter                         =   80.000 m
   Surface roughness length                       =    0.021 m
   Number of time steps in the FFT                =    12096
   Number of time steps output                    =    12089
```

KH Billow Test Parameters:

Gradient Richardson number	=	0.020
Power law exponent	=	0.300
Length of coherent structures	=	300.000 s
Minimum coherent TKE	=	30.000 (m/s)^2

Mean Flow Angles:

Vertical = 0.0 degrees
Horizontal = 0.0 degrees

Mean Wind Speed Profile:

Height (m)	Wind Speed (m/s)	Horizontal Angle (degrees)	U-comp (X) (m/s)	V-comp (Y) (m/s)	W-comp (Z) (m/s)
124.3	20.22	0.00	20.22	0.00	0.00
117.6	19.89	0.00	19.89	0.00	0.00
111.0	19.55	0.00	19.55	0.00	0.00
104.3	19.19	0.00	19.19	0.00	0.00
97.6	18.81	0.00	18.81	0.00	0.00
91.0	18.42	0.00	18.42	0.00	0.00
84.3	18.00	0.00	18.00	0.00	0.00
77.6	17.56	0.00	17.56	0.00	0.00
71.0	17.09	0.00	17.09	0.00	0.00
64.3	16.60	0.00	16.60	0.00	0.00
57.6	16.06	0.00	16.06	0.00	0.00
51.0	15.48	0.00	15.48	0.00	0.00
44.3	14.84	0.00	14.84	0.00	0.00

Harvested Random Seeds after Generation of the Random Numbers:

28491372 K1
0 K2

Scaling statistics from the hub grid point:

Cross-Component	Scaling Factor
u'w'	-0.12385E+00
u'v'	-0.12680E-01
v'w'	0.29924E+00

Hub-Height Simulated Turbulence Statistical Summary:

Type of Wind	Min (m/s)	Mean (m/s)	Max (m/s)	Sigma (m/s)	TI (%)
Longitudinal (u)	10.98	18.00	24.98	2.757	15.315
Lateral (v)	-6.32	0.00	5.96	1.813	10.070
Vertical (w)	-4.05	0.00	4.08	1.233	6.849
U component	10.98	18.00	24.98	2.757	15.315
V component	-6.32	0.00	5.96	1.813	10.070
W component	-4.05	0.00	4.08	1.233	6.849
Horizontal (U&V)	11.15	18.09	25.43	2.741	15.150
Total	11.21	18.14	25.44	2.740	15.110

Product	Min Reynolds Stress (m/s)^2	Mean Reynolds Stress (m/s)^2	Max Reynolds Stress (m/s)^2	Correlation Coefficient
u'w'	-21.990	-0.727	16.391	-0.214
u'v'	-23.092	1.129	39.537	0.226
v'w'	-10.652	0.418	15.741	0.187

Friction Velocity (Ustar) = 0.853 m/s
Maximum Instantaneous TKE = 40.124 (m/s)^2
Maximum Instantaneous CTKE = 19.959 (m/s)^2

Mean standard deviation across all grid points:
u component: 2.623 m/s
v component: 1.875 m/s
w component: 1.287 m/s

Number of coherent events = 1
Predicted length of coherent events = 300.000 seconds
Length of coherent events = 307.039 seconds
Maximum predicted event CTKE = 35.875 (m/s)^2

U-component (X) statistics from the hub grid point:

```
   Mean =  18.0000 m/s
   TI   =  15.3152 %


Normalizing Parameters for Binary Data (approximate statistics):

   UBar  =  18.0000 m/s
   TI(u) =  15.3152 %
   TI(v) =  10.0704 %
   TI(w) =   6.8491 %
   Height Offset =   0.0000 m
   Grid Base     =  44.2876 m

Nyquist frequency of turbulent wind field =        10.000 Hz
Nyquist frequency of coherent turbulent events =   25.005 Hz

Processing complete.  5.8906 CPU seconds used.
```

APPENDIX C – INPUT FILES FOR OPENFAST ANALYSIS

C.1 – MAIN (WP VSP WTURB CM)

```
------- OpenFAST example INPUT FILE -------------------------------------------
FAST Certification Test #13: WindPACT 1.5 MW Baseline with many DOFs with VS and VP and FF turbulence.
---------------------- SIMULATION CONTROL --------------------------------------
True           Echo            - Echo input data to <RootName>.ech (flag)
"FATAL"        AbortLevel      - Error level when simulation should abort (string){"WARNING","SEVERE","FATAL"}
        400    TMax            - Total run time (s)
      0.005    DT              - Recommended module time step (s)
          2    InterpOrder     - Interpolation order for input/output time history (-) {1=linear, 2=quadratic}
          0    NumCrctn        - Number of correction iterations(-){0=explicit calculation,i.e.,no corrections}
      99999    DT_UJac         - Time between calls to get Jacobians (s)
      1E+06    UJacSclFact     - Scaling factor used in Jacobians (-)
---------------------- FEATURE SWITCHES AND FLAGS ------------------------------
          1    CompElast       - Compute structural dynamics (switch) {1=ElastoDyn; 2=ElastoDyn + BeamDyn for
blades}
          1    CompInflow      - Compute inflow wind velocities (switch) {0=still air; 1=InflowWind; 2=external
from OpenFOAM}
          2    CompAero        - Compute aerodynamic loads (switch) {0=None; 1=AeroDyn v14; 2=AeroDyn v15}
          1    CompServo       - Compute control and electrical-drive dynamics (switch) {0=None; 1=ServoDyn}
          0    CompHydro       - Compute hydrodynamic loads (switch) {0=None; 1=HydroDyn}
          0    CompSub         - Compute sub-structural dynamics (switch) {0=None; 1=SubDyn; 2=External
Platform MCKF}
          0    CompMooring     - Compute mooring system (switch) {0=None; 1=MAP++; 2=FEAMooring; 3=MoorDyn;
4=OrcaFlex}
          0    CompIce         - Compute ice loads (switch) {0=None; 1=IceFloe; 2=IceDyn}
---------------------- INPUT FILES ---------------------------------------------
"WP_VSP_WTurb_ElastoDyn.dat"    EDFile          - Name of file containing ElastoDyn input parameters (quoted
string)
"unused"       BDBldFile(1)    - Name of file containing BeamDyn input parameters for blade 1 (quoted string)
"unused"       BDBldFile(2)    - Name of file containing BeamDyn input parameters for blade 2 (quoted string)
"unused"       BDBldFile(3)    - Name of file containing BeamDyn input parameters for blade 3 (quoted string)
"WP_Baseline_InflowWind_14p5mps_ric.dat"    InflowFile  - Name of file containing inflow wind input parameters
(quoted string)
"WP_Baseline_AeroDyn15_Dynin_cm.dat"    AeroFile   - Name of file containing aerodynamic input parameters
(quoted string)
"WP_VSP_WTurb_ServoDyn_ric.dat"    ServoFile     - Name of file containing control and electrical-drive input
parameters (quoted string)
"unused"       HydroFile       - Name of file containing hydrodynamic input parameters (quoted string)
"unused"       SubFile         - Name of file containing sub-structural input parameters (quoted string)
"unused"       MooringFile     - Name of file containing mooring system input parameters (quoted string)
"unused"       IceFile         - Name of file containing ice input parameters (quoted string)
---------------------- OUTPUT --------------------------------------------------
True           SumPrint        - Print summary data to "<RootName>.sum" (flag)
          1    SttsTime        - Amount of time between screen status messages (s)
      99999    ChkptTime       - Amount of time between creating checkpoint files for potential restart (s)
       0.05    DT_Out          - Time step for tabular output (s) (or "default")
          0    TStart          - Time to begin tabular output (s)
          0    OutFileFmt      - Format for tabular (time-marching) output file (switch) {1: text file
[<RootName>.out], 2: binary file [<RootName>.outb], 3: both}
True           TabDelim        - Use tab delimiters in text tabular output file? (flag) {uses spaces if false}
"ES10.3E2"     OutFmt          - Format used for text tabular output, excluding the time channel.  Resulting
field should be 10 characters. (quoted string)
---------------------- LINEARIZATION -------------------------------------------
False          Linearize       - Linearization analysis (flag)
          2    NLinTimes       - Number of times to linearize (-) [>=1] [unused if Linearize=False]
         30,         60    LinTimes        - List of times at which to linearize (s) [1 to NLinTimes] [unused
if Linearize=False]
          1    LinInputs       - Inputs included in linearization (switch) {0=none; 1=standard; 2=all module
inputs (debug)} [unused if Linearize=False]
          1    LinOutputs      - Outputs included in linearization (switch) {0=none; 1=from OutList(s); 2=all
module outputs (debug)} [unused if Linearize=False]
False          LinOutJac       - Include full Jacobians in linearization output (for debug) (flag) [unused if
Linearize=False; used only if LinInputs=LinOutputs=2]
False          LinOutMod       - Write module-level linearization output files in addition to output for full
system? (flag) [unused if Linearize=False]
---------------------- VISUALIZATION -------------------------------------------
          0    WrVTK           - VTK visualization data output: (switch) {0=none; 1=initialization data only;
2=animation}
          2    VTK_type        - Type of VTK visualization data: (switch) {1=surfaces; 2=basic meshes
(lines/points); 3=all meshes (debug)} [unused if WrVTK=0]
false          VTK_fields      - Write mesh fields to VTK data files? (flag) {true/false} [unused if WrVTK=0]
         15    VTK_fps         - Frame rate for VTK output (frames per second){will use
closest integer multiple of DT} [used only if WrVTK=2]
```

C.2 – AERODYN

```
------- AERODYN v15 for OpenFAST INPUT FILE ------------------------------------------------
1.5 MW baseline aerodynamic parameters for FAST certification tests #11-#13.
======  General Options  ============================================================================
False         Echo                - Echo the input to "<rootname>.AD.ech"?  (flag)
"default"     DTAero              - Time interval for aerodynamic calculations {or "default"} (s)
          1   WakeMod             - Type of wake/induction model (switch) {0=none, 1=BEMT, 2=DBEMT}
[WakeMod cannot be 2 when linearizing]
          2   AFAeroMod           - Type of blade airfoil aerodynamics model (switch) {1=steady model,
2=Beddoes-Leishman unsteady model} [AFAeroMod must be 1 when linearizing]
          0   TwrPotent           - Type tower influence on wind based on potential flow around the
tower (switch) {0=none, 1=baseline potential flow, 2=potential flow with Bak correction}
False         TwrShadow           - Calculate tower influence on wind based on downstream
tower shadow? (flag)
False         TwrAero             - Calculate tower aerodynamic loads? (flag)
False         FrozenWake          - Assume frozen wake during linearization? (flag) [used only when
WakeMod=1 and when linearizing]
False         CavitCheck          - Perform cavitation check? (flag) [AFAeroMod must be 1 when
CavitCheck=true]
======  Environmental Conditions  ===================================================================
      1.225   AirDens             - Air density (kg/m^3)
 1.4639E-05   KinVisc             - Kinematic air viscosity (m^2/s)
        335   SpdSound            - Speed of sound (m/s)
     103500   Patm                - Atmospheric pressure (Pa) [used only when CavitCheck=True]
       1700   Pvap                - Vapour pressure of fluid (Pa) [used only when CavitCheck=True]
        0.5   FluidDepth          - Water depth above mid-hub height (m) [used only when CavitCheck=True]
======  Blade-Element/Momentum Theory Options  ========================== [unused when WakeMod=0]
          2   SkewMod             - Type of skewed-wake correction model (switch) {1=uncoupled,
2=Pitt/Peters, 3=coupled} [unused when WakeMod=0]
"default"     SkewModFactor       - Constant used in Pitt/Peters skewed wake model {or "default" is
15/32*pi} (-) [used only when SkewMod=2; unused when WakeMod=0]
True          TipLoss             - Use the Prandtl tip-loss model? (flag) [unused when WakeMod=0]
True          HubLoss             - Use the Prandtl hub-loss model? (flag) [unused when WakeMod=0]
true          TanInd              - Include tangential induction in BEMT calculations? (flag)
[unused when WakeMod=0]
False         AIDrag              - Include the drag term in the axial-induction calculation? (flag)
[unused when WakeMod=0]
False         TIDrag              - Include the drag term in the tangential-induction calculation?
(flag) [unused when WakeMod=0 or TanInd=FALSE]
"Default"     IndToler            - Convergence tolerance for BEMT nonlinear solve residual equation
{or "default"} (-) [unused when WakeMod=0]
        100   MaxIter             - Maximum number of iteration steps (-) [unused when WakeMod=0]
======  Dynamic Blade-Element/Momentum Theory Options  ==================== [used only when WakeMod=2]
          2   DBEMT_Mod           - Type of dynamic BEMT (DBEMT) model {1=constant tau1,
2=time-dependent tau1} (-) [used only when WakeMod=2]
          4   tau1_const          - Time constant for DBEMT (s) [used only when WakeMod=2
and DBEMT_Mod=1]
======  Beddoes-Leishman Unsteady Airfoil Aerodynamics Options  =========== [used only when AFAeroMod=2]
          3   UAMod               - Unsteady Aero Model Switch (switch) {1=Baseline model (Original),
2=Gonzalez's variant (changes in Cn,Cc,Cm), 3=Minemma/Pierce variant (changes in Cc and Cm)}
[used only when AFAeroMod=2]
True          FLookup             - Flag to indicate whether a lookup for f' will be calculated (TRUE)
or whether best-fit exponential equations will be used (FALSE); if FALSE S1-S4 must be provided in
airfoil input files (flag) [used only when AFAeroMod=2]
======  Airfoil Information ==========================================================================
          1   InCol_Alfa          - The column in the airfoil tables that contains the angle of attack (-)
          2   InCol_Cl            - The column in the airfoil tables that contains the lift coefficient (-)
          3   InCol_Cd            - The column in the airfoil tables that contains the drag coefficient (-)
          4   InCol_Cm            - The column in the airfoil tables that contains the pitching-moment
coefficient; use zero if there is no Cm column (-)
          0   InCol_Cpmin         - The column in the airfoil tables that contains the Cpmin coefficient;
use zero if there is no Cpmin column (-)
          4   NumAFfiles          - Number of airfoil files used (-)
"../WP_Baseline/Airfoils/cylinder.dat"    AFNames             - Airfoil file names (NumAFfiles lines)
(quoted strings)
"../WP_Baseline/Airfoils/s818_2703_cm2.dat"
"../WP_Baseline/Airfoils/s825_2103_cm2.dat"
"../WP_Baseline/Airfoils/s826_1603_cm2.dat"
======  Rotor/Blade Properties  =====================================================================
False        UseBlCm             - Include aerodynamic pitching moment in calculations?  (flag)
"../WP_Baseline/WP_Baseline_AeroDyn_blade.dat"    ADBlFile(1) - Name of file containing distributed
aerodynamic properties for Blade #1 (-)
"../WP_Baseline/WP_Baseline_AeroDyn_blade.dat"    ADBlFile(2) - Name of file containing distributed
aerodynamic properties for Blade #2 (-) [unused if NumBl < 2]
"../WP_Baseline/WP_Baseline_AeroDyn_blade.dat"    ADBlFile(3) - Name of file containing distributed
aerodynamic properties for Blade #3 (-) [unused if NumBl < 3]
======  Tower Influence and Aerodynamics ============================== [used only when TwrPotent/=0,
TwrShadow=True, or TwrAero=True]
          2   NumTwrNds           - Number of tower nodes used in the analysis  (-) [used only when
```

```
TwrPotent/=0, TwrShadow=True, or TwrAero=True]
TwrElev        TwrDiam        TwrCd
(m)              (m)           (-)
0.0000000E+00  5.6200000E+00  0.0000000E+00
8.2390000E+01  2.8200000E+00  0.0000000E+00



======  Outputs  ======================================================================================
True          SumPrint            - Generate a summary file listing input options and interpolated
properties to "<rootname>.AD.sum"?  (flag)
          9   NBlOuts             - Number of blade node outputs [0 - 9] (-)
          3, 5, 7, 9, 11, 13, 15, 16, 17    BlOutNd - Blade nodes whose values will be output  (-)
          0   NTwOuts             - Number of tower node outputs [0 - 9]  (-)
          1,          2,          3,          4,          5    TwOutNd  - Tower nodes whose values will
be output  (-)
                  OutList             - The next line(s) contains a list of output parameters.
                  See OutListParameters.xlsx for a listing of available output channels, (-)
"RtSkew"
"B1N1Alpha"
"B1N2Alpha"
"B1N3Alpha"
"B1N4Alpha"
"B1N5Alpha"
"B1N6Alpha"
"B1N7Alpha"
"B1N8Alpha"
"B1N9Alpha"
"B2N1Alpha"
"B2N2Alpha"
"B2N3Alpha"
"B2N4Alpha"
"B2N5Alpha"
"B2N6Alpha"
"B2N7Alpha"
"B2N8Alpha"
"B2N9Alpha"
"B3N1Alpha"
"B3N2Alpha"
"B3N3Alpha"
"B3N4Alpha"
"B3N5Alpha"
"B3N6Alpha"
"B3N7Alpha"
"B3N8Alpha"
"B3N9Alpha"
"B1N1Fl"
"B1N2Fl"
"B1N3Fl"
"B1N4Fl"
"B1N5Fl"
"B1N6Fl"
"B1N7Fl"
"B1N8Fl"
"B1N9Fl"
"B2N1Fl"
"B2N2Fl"
"B2N3Fl"
"B2N4Fl"
"B2N5Fl"
"B2N6Fl"
"B2N7Fl"
"B2N8Fl"
"B2N9Fl"
"B3N1Fl"
"B3N2Fl"
"B3N3Fl"
"B3N4Fl"
"B3N5Fl"
"B3N6Fl"
"B3N7Fl"
"B3N8Fl"
"B3N9Fl"
"B1N1Mm"
"B1N2Mm"
"B1N3Mm"
"B1N4Mm"
"B1N5Mm"
"B1N6Mm"
"B1N7Mm"
"B1N8Mm"
"B1N9Mm"
```

```
"B2N1Mm"
"B2N2Mm"
"B2N3Mm"
"B2N4Mm"
"B2N5Mm"
"B2N6Mm"
"B2N7Mm"
"B2N8Mm"
"B2N9Mm"
"B3N1Mm"
"B3N2Mm"
"B3N3Mm"
"B3N4Mm"
"B3N5Mm"
"B3N6Mm"
"B3N7Mm"
"B3N8Mm"
"B3N9Mm"
END of input file (the word "END" must appear in the first 3 columns of this last OutList line)
---------------------------------------------------------------------------------------
```

C.3 – ELASTODYN

```
------- ELASTODYN v1.03.* INPUT FILE -------------------------------------------
FAST certification Test #13: WindPACT 1.5 MW Baseline with many DOFs with VS and VP and FF turbulence. Model
properties from "InputData1.5A08V07adm.xls" (from C. Hansen) with bugs removed.
---------------------- SIMULATION CONTROL --------------------------------------
False         Echo        - Echo input data to "<RootName>.ech" (flag)
          3   Method      - Integration method: {1: RK4, 2: AB4, or 3: ABM4} (-)
      0.005   DT          - Integration time step (s)
---------------------- ENVIRONMENTAL CONDITION ---------------------------------
    9.80665   Gravity     - Gravitational acceleration (m/s^2)
---------------------- DEGREES OF FREEDOM --------------------------------------
True          FlapDOF1    - First flapwise blade mode DOF (flag)
True          FlapDOF2    - Second flapwise blade mode DOF (flag)
True          EdgeDOF     - First edgewise blade mode DOF (flag)
False         TeetDOF     - Rotor-teeter DOF (flag) [unused for 3 blades]
True          DrTrDOF     - Drivetrain rotational-flexibility DOF (flag)
True          GenDOF      - Generator DOF (flag)
False         YawDOF      - Yaw DOF (flag)
True          TwFADOF1    - First fore-aft tower bending-mode DOF (flag)
True          TwFADOF2    - Second fore-aft tower bending-mode DOF (flag)
True          TwSSDOF1    - First side-to-side tower bending-mode DOF (flag)
True          TwSSDOF2    - Second side-to-side tower bending-mode DOF (flag)
False         PtfmSgDOF   - Platform horizontal surge translation DOF (flag)
False         PtfmSwDOF   - Platform horizontal sway translation DOF (flag)
False         PtfmHvDOF   - Platform vertical heave translation DOF (flag)
False         PtfmRDOF    - Platform roll tilt rotation DOF (flag)
False         PtfmPDOF    - Platform pitch tilt rotation DOF (flag)
False         PtfmYDOF    - Platform yaw rotation DOF (flag)
---------------------- INITIAL CONDITIONS --------------------------------------
          0   OoPDefl     - Initial out-of-plane blade-tip displacement (meters)
          0   IPDefl      - Initial in-plane blade-tip deflection (meters)
        7.5   BlPitch(1)  - Blade 1 initial pitch (degrees)
        7.5   BlPitch(2)  - Blade 2 initial pitch (degrees)
        7.5   BlPitch(3)  - Blade 3 initial pitch (degrees) [unused for 2 blades]
          0   TeetDefl    - Initial or fixed teeter angle (degrees) [unused for 3 blades]
          0   Azimuth     - Initial azimuth angle for blade 1 (degrees)
         10   RotSpeed    - Initial or fixed rotor speed (rpm)
          0   NacYaw      - Initial or fixed nacelle-yaw angle (degrees)
          0   TTDspFA     - Initial fore-aft tower-top displacement (meters)
          0   TTDspSS     - Initial side-to-side tower-top displacement (meters)
          0   PtfmSurge   - Initial or fixed horizontal surge translational displacement of platform (meters)
          0   PtfmSway    - Initial or fixed horizontal sway translational displacement of platform (meters)
          0   PtfmHeave   - Initial or fixed vertical heave translational displacement of platform (meters)
          0   PtfmRoll    - Initial or fixed roll tilt rotational displacement of platform (degrees)
          0   PtfmPitch   - Initial or fixed pitch tilt rotational displacement of platform (degrees)
          0   PtfmYaw     - Initial or fixed yaw rotational displacement of platform (degrees)
---------------------- TURBINE CONFIGURATION -----------------------------------
          3   NumBl       - Number of blades (-)
         35   TipRad      - The distance from the rotor apex to the blade tip (meters)
       1.75   HubRad      - The distance from the rotor apex to the blade root (meters)
          0   PreCone(1)  - Blade 1 cone angle (degrees)
          0   PreCone(2)  - Blade 2 cone angle (degrees)
          0   PreCone(3)  - Blade 3 cone angle (degrees) [unused for 2 blades]
          0   HubCM       - Distance from rotor apex to hub mass [positive downwind] (meters)
          0   UndSling    - Undersling length [distance from teeter pin to the rotor apex](meters)[unused for
```

```
3 blades]
          0   Delta3      - Delta-3 angle for teetering rotors (degrees) [unused for 3 blades]
          0   AzimB1Up    - Azimuth value to use for I/O when blade 1 points up (degrees)
       -3.3   OverHang    - Distance from yaw axis to rotor apex [3 blades] or teeter pin [2 blades] (meters)
       0.99   ShftGagL    - Distance from rotor apex [3 blades] or teeter pin [2 blades] to shaft strain gages
[positive for upwind rotors] (meters)
         -5   ShftTilt    - Rotor shaft tilt angle (degrees)
    -0.1449   NacCMxn     - Downwind distance from the tower-top to the nacelle CM (meters)
          0   NacCMyn     - Lateral  distance from the tower-top to the nacelle CM (meters)
      1.389   NacCMzn     - Vertical distance from the tower-top to the nacelle CM (meters)
          0   NcIMUxn     - Downwind distance from the tower-top to the nacelle IMU (meters)
          0   NcIMUyn     - Lateral  distance from the tower-top to the nacelle IMU (meters)
          0   NcIMUzn     - Vertical distance from the tower-top to the nacelle IMU (meters)
       1.61   Twr2Shft    - Vertical distance from the tower-top to the rotor shaft (meters)
      82.39   TowerHt     - Height of tower above ground level [onshore] or MSL [offshore] (meters)
          0   TowerBsHt   - Height of tower base above ground level [onshore] or MSL [offshore] (meters)
          0   PtfmCMxt    - Downwind distance from the ground level [onshore] or MSL [offshore] to the
platform CM (meters)
          0   PtfmCMyt    - Lateral distance from the ground level [onshore] or MSL [offshore] to the
platform CM (meters)
         -0   PtfmCMzt    - Vertical distance from the ground level [onshore] or MSL [offshore] to the
platform CM (meters)
         -0   PtfmRefzt   - Vertical distance from the ground level [onshore] or MSL [offshore] to the
platform reference point (meters)


---------------------- MASS AND INERTIA ----------------------------------------
          0   TipMass(1)  - Tip-brake mass, blade 1 (kg)
          0   TipMass(2)  - Tip-brake mass, blade 2 (kg)
          0   TipMass(3)  - Tip-brake mass, blade 3 (kg) [unused for 2 blades]
      15148   HubMass     - Hub mass (kg)
      34600   HubIner     - Hub inertia about rotor axis [3 blades] or teeter axis [2 blades] (kg m^2)
     53.036   GenIner     - Generator inertia about HSS (kg m^2)
      51170   NacMass     - Nacelle mass (kg)
      49130   NacYIner    - Nacelle inertia about yaw axis (kg m^2)
          0   YawBrMass   - Yaw bearing mass (kg)
          0   PtfmMass    - Platform mass (kg)
          0   PtfmRIner   - Platform inertia for roll tilt rotation about the platform CM (kg m^2)
          0   PtfmPIner   - Platform inertia for pitch tilt rotation about the platform CM (kg m^2)
          0   PtfmYIner   - Platform inertia for yaw rotation about the platform CM (kg m^2)
---------------------- BLADE ---------------------------------------------------
         15   BldNodes    - Number of blade nodes (per blade) used for analysis (-)
"../WP_Baseline/Baseline_Blade.dat"    BldFile(1)  - Name of file containing properties for blade 1
(quoted string)
"../WP_Baseline/Baseline_Blade.dat"    BldFile(2)  - Name of file containing properties for blade 2
(quoted string)
"../WP_Baseline/Baseline_Blade.dat"    BldFile(3)  - Name of file containing properties for blade 3
(quoted string) [unused for 2 blades]
---------------------- ROTOR-TEETER --------------------------------------------
          0   TeetMod     - Rotor-teeter spring/damper model {0: none, 1: standard, 2: user-defined from
routine UserTeet} (switch) [unused for 3 blades]
          0   TeetDmpP    - Rotor-teeter damper position (degrees) [used only for 2 blades and when
TeetMod=1]
          0   TeetDmp     - Rotor-teeter damping constant (N-m/(rad/s)) [used only for 2 blades
and when TeetMod=1]
          0   TeetCDmp    - Rotor-teeter rate-independent Coulomb-damping moment (N-m) [used only for 2 blades
and when
TeetMod=1]
          0   TeetSStP    - Rotor-teeter soft-stop position (degrees) [used only for 2 blades and when
TeetMod=1]
          0   TeetHStP    - Rotor-teeter hard-stop position (degrees) [used only for 2 blades
and when TeetMod=1]
          0   TeetSSSp    - Rotor-teeter soft-stop linear-spring constant (N-m/rad) [used only for 2 blades
and when TeetMod=1]
          0   TeetHSSp    - Rotor-teeter hard-stop linear-spring constant (N-m/rad) [used only for 2 blades
and when TeetMod=1]
---------------------- DRIVETRAIN ----------------------------------------------
        100   GBoxEff     - Gearbox efficiency (%)
     87.965   GBRatio     - Gearbox ratio (-)
    5.6E+09   DTTorSpr    - Drivetrain torsional spring (N-m/rad)
      1E+07   DTTorDmp    - Drivetrain torsional damper (N-m/(rad/s))
---------------------- FURLING -------------------------------------------------
False         Furling     - Read in additional model properties for furling turbine (flag) [must currently be
FALSE)
"unused"      FurlFile    - Name of file containing furling properties (quoted string) [unused when Furling=
False]
---------------------- TOWER ---------------------------------------------------
         10   TwrNodes    - Number of tower nodes used for analysis (-)
"../WP_Baseline/Baseline_Tower.dat"    TwrFile     - Name of file containing tower properties (quoted string)
---------------------- OUTPUT --------------------------------------------------
True          SumPrint    - Print summary data to "<RootName>.sum" (flag)
          1   OutFile     - Switch to determine where output will be placed: {1: in module output file only;
```

```
2: in glue code output file only; 3: both} (currently unused)
True          TabDelim    - Use tab delimiters in text tabular output file? (flag) (currently unused)
"ES10.3E2"    OutFmt      - Format used for text tabular output (except time).  Resulting field should be 10
characters. (quoted string) (currently unused)
          0   TStart      - Time to begin tabular output (s) (currently unused)
         10   DecFact     - Decimation factor for tabular output {1: output every time step} (-) (currently
unused)
          2   NTwGages    - Number of tower nodes that have strain gages for output [0 to 9] (-)
          4,          7    TwrGagNd    - List of tower nodes that have strain gages [1 to TwrNodes](-)[unused
if NTwGages=0]
          0   NBlGages    - Number of blade nodes that have strain gages for output [0 to 9] (-)
          0   BldGagNd    - List of blade nodes that have strain gages [1 to BldNodes] (-) [unused if
NBlGages=0]
              OutList     - The next line(s) contains a list of output parameters.  See OutListParameters.xlsx
for a listing of available output channels, (-)
"Azimuth"                 - LSSTipPxa = Azimuth angle
"YawPzn"                  - Nacelle yaw angle (position) about the zn-zp axis
"BldPitch1"               - Blade 1 pitch angle
"BldPitch2"               - Blade 2 pitch angle
"BldPitch3"               - Blade 3 pitch angle
"IPDefl1"                 - IP blade 1,2 tip deflections
"IPDefl2"                 - IP blade 1,2 tip deflections
"TwstDefl1"               - Blade torsional tip twist deflections
"TwstDefl2"               - Blade torsional tip twist deflections
"TwstDefl3"               - Blade torsional tip twist deflections
"RootMxb1"                - Blade 1 root moments
"RootMyb1"                - Blade 1 root moments
"RootMzb1"                - Blade 1 root moments
"RootMxb2"                - Blade 2 root moments
"RootMyb2"                - Blade 2 root moments
"RootMzb2"                - Blade 2 root moments
"RootMxb3"                - Blade 3 root moments
"RootMyb3"                - Blade 3 root moments
"RootMzb3"                - Blade 3 root moments
"LSShftFys"               - Non-rotating LSS shear forces
"LSShftFzs"               - Non-rotating LSS shear forces
"LSShftMxa"               - (RotTorq) Rotor Torque Mx
"LSSTipMys"               - Non-rotating LSS bending moments at the shaft tip
"LSSTipMzs"               - Non-rotating LSS bending moments at the shaft tip
"LSSTipMya"               - Rotating LSS bending moments at the shaft tip
"LSSTipMza"               - Rotating LSS bending moments at the shaft tip
"YawBrTDxp"               - Fore Aft (FA) tower-top deflections wrt tilted tower
"YawBrTDyp"               - Side-Side (SS) tower-top deflections wrt tilted tower
"YawBrMxn"                - Tower-top / yaw bearing roll, pitch, and yaw moments
"YawBrMyn"                - Tower-top / yaw bearing roll, pitch, and yaw moments
"YawBrMzn"                - Tower-top / yaw bearing roll, pitch, and yaw moments
"LSSGagPxa"               - Low Speed Shaft
"RotSpeed"                - Rotor speed RPM
"PtfmPitch"               - Platform displacement around y axis (deg).
"PtfmYaw"                 - Platform displacement around z axis (deg).
"TwrBsMzt"                - Tower base yaw moment (kNm)
"TwrBsMyt"                - Tower base tilt moment (kNm)
"TwrBsMxt"                - Tower base roll moment
"TwrBsFxt"
"TwrBsFyt"
"TwrBsFzt"
"RootFxb1"
"RootFxb2"
"RootFxb3"
"RootFyb1"
"RootFyb2"
"RootFyb3"
"RootFzb1"
"RootFzb2"
"RootFzb3"
"LSSGagFys"
"YawBrTAxp"               - Tower top fore-aft acceleration
"YawBrTAyp"               - Tower top side-to-side acceleration
"NcIMUTAxs"               - Tower top axial acceleration
"NcIMUTAys"
"TipDxb1"                 - Blade tip xB deflection relative to the pitch axis
"TipDyb1"                 - Blade tip yB deflection relative to the pitch axis
"TipDxb2"                 - Blade tip xB deflection relative to the pitch axis
"TipDyb2"                 - Blade tip yB deflection relative to the pitch axis
"TipDxb3"                 - Blade tip xB deflection relative to the pitch axis
"TipDyb3"                 - Blade tip yB deflection relative to the pitch axis
"RotPwr"
END of input file (the word "END" must appear in the first 3 columns of this last OutList line)
---------------------------------------
```

C.4 – SERVODYN

```
------- SERVODYN v1.05.* INPUT FILE -------------------------------------------
FAST certification Test #13: WindPACT 1.5 MW Baseline with many DOFs with VS and VP and FF turbulence. Model
properties from "InputData1.5A08VO7adm.xls" (from C. Hansen) with bugs removed.
---------------------- SIMULATION CONTROL --------------------------------------
False         Echo          - Echo input data to <RootName>.ech (flag)
      0.005   DT            - Communication interval for controllers (s) (or "default")
---------------------- PITCH CONTROL -------------------------------------------
          4   PCMode        - Pitch control mode {0: none, 3: user-defined from routine PitchCntrl, 4: user-
defined from Simulink/Labview, 5: user-defined from Bladed-style DLL} (switch)
          5   TPCOn         - Time to enable active pitch control (s) [unused when PCMode=0]
     9999.9   TPitManS(1)   - Time to start override pitch maneuver for blade 1 and end standard pitch control
(s)
     9999.9   TPitManS(2)   - Time to start override pitch maneuver for blade 2 and end standard pitch control
(s)
     9999.9   TPitManS(3)   - Time to start override pitch maneuver for blade 3 and end standard pitch control
(s) [unused for 2 blades]
          2   PitManRat(1) - Pitch rate at which override pitch maneuver heads toward final pitch angle for
blade 1 (deg/s)
          2   PitManRat(2) - Pitch rate at which override pitch maneuver heads toward final pitch angle for
blade 2 (deg/s)
          2   PitManRat(3) - Pitch rate at which override pitch maneuver heads toward final pitch angle for
blade 3 (deg/s) [unused for 2 blades]
        2.6   BlPitchF(1)   - Blade 1 final pitch for pitch maneuvers (degrees)
        2.6   BlPitchF(2)   - Blade 2 final pitch for pitch maneuvers (degrees)
        2.6   BlPitchF(3)   - Blade 3 final pitch for pitch maneuvers (degrees) [unused for 2 blades]
---------------------- GENERATOR AND TORQUE CONTROL ----------------------------
          4   VSContrl      - Variable-speed control mode {0: none, 1: simple VS, 3: user-defined from routine
UserVSCont, 4: user-defined from Simulink/Labview, 5: user-defined from Bladed-style DLL} (switch)
          1   GenModel      - Generator model {1: simple, 2: Thevenin, 3: user-defined from routine UserGen}
(switch) [used only when VSContrl=0]
         95   GenEff        - Generator efficiency [ignored by the Thevenin and user-defined generator models]
(%)
True          GenTiStr      - Method to start the generator {T: timed using TimGenOn, F: generator speed using
SpdGenOn} (flag)
True          GenTiStp      - Method to stop the generator {T: timed using TimGenOf, F: when generator power =
0} (flag)
     9999.9   SpdGenOn      - Generator speed to turn on the generator for a startup (HSS speed) (rpm) [used
only when GenTiStr=False]
          0   TimGenOn      - Time to turn on the generator for a startup (s) [used only when GenTiStr=True]
     9999.9   TimGenOf      - Time to turn off the generator (s) [used only when GenTiStp=True]
---------------------- SIMPLE VARIABLE-SPEED TORQUE CONTROL --------------------
       1800   VS_RtGnSp     - Rated generator speed for simple variable-speed generator control (HSS side)
(rpm) [used only when VSContrl=1]
    8376.58   VS_RtTq       - Rated generator torque/constant generator torque in Region 3 for simple variable-
speed generator control (HSS side) (N-m) [used only when VSContrl=1]
   0.002585   VS_Rgn2K      - Generator torque constant in Region 2 for simple variable-speed generator control
(HSS side) (N-m/rpm^2) [used only when VSContrl=1]
 9.9999E-06   VS_SlPc       - Rated generator slip percentage in Region 2 1/2 for simple variable-speed
 generator control (%) [used only when VSContrl=1]
---------------------- SIMPLE INDUCTION GENERATOR ------------------------------
     9999.9   SIG_SlPc      - Rated generator slip percentage (%) [used only when VSContrl=0 and GenModel=1]
     9999.9   SIG_SySp      - Synchronous (zero-torque) generator speed (rpm) [used only when VSContrl=0 and
GenModel=1]
     9999.9   SIG_RtTq      - Rated torque (N-m) [used only when VSContrl=0 and GenModel=1]
     9999.9   SIG_PORt      - Pull-out ratio (Tpullout/Trated) (-) [used only when VSContrl=0 and GenModel=1]
---------------------- THEVENIN-EQUIVALENT INDUCTION GENERATOR -----------------
     9999.9   TEC_Freq      - Line frequency [50 or 60] (Hz) [used only when VSContrl=0 and GenModel=2]
       9998   TEC_NPol      - Number of poles [even integer > 0] (-) [used only when VSContrl=0 and GenModel=2]
     9999.9   TEC_SRes      - Stator resistance (ohms) [used only when VSContrl=0 and GenModel=2]
     9999.9   TEC_RRes      - Rotor resistance (ohms) [used only when VSContrl=0 and GenModel=2]
     9999.9   TEC_VLL       - Line-to-line RMS voltage (volts) [used only when VSContrl=0 and GenModel=2]
     9999.9   TEC_SLR       - Stator leakage reactance (ohms) [used only when VSContrl=0 and GenModel=2]
     9999.9   TEC_RLR       - Rotor leakage reactance (ohms) [used only when VSContrl=0 and GenModel=2]
     9999.9   TEC_MR        - Magnetizing reactance (ohms) [used only when VSContrl=0 and GenModel=2]
---------------------- HIGH-SPEED SHAFT BRAKE ----------------------------------
          0   HSSBrMode     - HSS brake model {0: none, 1: simple, 3: user-defined from routine UserHSSBr, 4:
user-defined from Simulink/Labview, 5: user-defined from Bladed-style DLL} (switch)
     9999.9   THSSBrDp      - Time to initiate deployment of the HSS brake (s)
     9999.9   HSSBrDT       - Time for HSS-brake to reach full deployment once initiated (sec) [used only when
HSSBrMode=1]
     9999.9   HSSBrTqF      - Fully deployed HSS-brake torque (N-m) [unused when HSSBrMode=5]
---------------------- NACELLE-YAW CONTROL --------------------------------------
          0   YCMode        - Yaw control mode {0: none, 3: user-defined from routine UserYawCont,
4: user-defined from Simulink/Labview, 5: user-defined from Bladed-style DLL} (switch)
     9999.9   TYCOn         - Time to enable active yaw control (s) [unused when YCMode=0]
          0   YawNeut       - Neutral yaw position--yaw spring force is zero at this yaw (degrees)
          0   YawSpr        - Nacelle-yaw spring constant (N-m/rad)
          0   YawDamp       - Nacelle-yaw damping constant (N-m/(rad/s))
```

```
     9999.9   TYawManS     - Time to start override yaw maneuver and end standard yaw control (s)
          2   YawManRat    - Yaw maneuver rate (in absolute value) (deg/s)
          0   NacYawF      - Final yaw angle for override yaw maneuvers (degrees)
---------------------- TUNED MASS DAMPER ---------------------------------------
False         CompNTMD     - Compute nacelle tuned mass damper {true/false} (flag)
"unused"      NTMDfile     - Name of the file for nacelle tuned mass damper (quoted string) [unused when
CompNTMD is false]
False         CompTTMD     - Compute tower tuned mass damper {true/false} (flag)
"unused"      TTMDfile     - Name of the file for tower tuned mass damper (quoted string) [unused when
CompTTMD is false]
---------------------- BLADED INTERFACE ----------------------- [used only with Bladed Interface]
"unused"      DLL_FileName - Name/location of the dynamic library {.dll [Windows] or .so [Linux]} in the
Bladed-DLL format (-) [used only with Bladed Interface]
"DISCON.IN"    DLL_InFile   - Name of input file sent to the DLL (-) [used only with Bladed Interface]
"DISCON"      DLL_ProcName - Name of procedure in DLL to be called (-) [case sensitive; used only with
DLL Interface]
"default"     DLL_DT       - Communication interval for dynamic library (s) (or "default") [used only with
Bladed Interface]
false         DLL_Ramp     - Whether a linear ramp should be used between DLL_DT time steps [introduces time
shift when true] (flag) [used only with Bladed Interface]
     9999.9   BPCutoff     - Cuttoff frequency for low-pass filter on blade pitch from DLL (Hz) [used only
with Bladed Interface]
          0   NacYaw_North - Reference yaw angle of the nacelle when the upwind end points due North (deg)
[used only with Bladed Interface]
          0   Ptch_Cntrl   - Record 28: Use individual pitch control {0: collective pitch; 1: individual pitch
control} (switch) [used only with Bladed Interface]
          0   Ptch_SetPnt  - Record  5: Below-rated pitch angle set-point (deg) [used only with Bladed
Interface]
          0   Ptch_Min     - Record  6: Minimum pitch angle (deg) [used only with Bladed Interface]
          0   Ptch_Max     - Record  7: Maximum pitch angle (deg) [used only with Bladed Interface]
          0   PtchRate_Min - Record  8: Minimum pitch rate (most negative value allowed) (deg/s) [used only
with Bladed Interface]
          0   PtchRate_Max - Record  9: Maximum pitch rate  (deg/s) [used only with Bladed Interface]
          0   Gain_OM      - Record 16: Optimal mode gain (Nm/(rad/s)^2) [used only with Bladed Interface]
          0   GenSpd_MinOM - Record 17: Minimum generator speed (rpm) [used only with Bladed Interface]
          0   GenSpd_MaxOM - Record 18: Optimal mode maximum speed (rpm) [used only with Bladed Interface]
          0   GenSpd_Dem   - Record 19: Demanded generator speed above rated (rpm) [used only with Bladed
Interface]
          0   GenTrq_Dem   - Record 22: Demanded generator torque above rated (Nm) [used only with Bladed
Interface]
          0   GenPwr_Dem   - Record 13: Demanded power (W) [used only with Bladed Interface]
---------------------- BLADED INTERFACE TORQUE-SPEED LOOK-UP TABLE -------------
          0   DLL_NumTrq   - Record 26: No. of points in torque-speed look-up table {0 = none and use the
optimal mode parameters; nonzero = ignore the optimal mode PARAMETERs by setting Record 16 to 0.0} (-) [used
only with Bladed Interface]
 GenSpd_TLU   GenTrq_TLU
 (rpm)          (Nm)
---------------------- OUTPUT --------------------------------------------------
True          SumPrint     - Print summary data to <RootName>.sum (flag) (currently unused)
          1   OutFile      - Switch to determine where output will be placed: {1: in module output file only;
2: in glue code output file only; 3: both} (currently unused)
True          TabDelim     - Use tab delimiters in text tabular output file? (flag) (currently unused)
"ES10.3E2"    OutFmt       - Format used for text tabular output (except time).  Resulting field should be 10
characters. (quoted string) (currently unused)
          0   TStart       - Time to begin tabular output (s) (currently unused)
              OutList      - The next line(s) contains a list of output parameters. See OutListParameters.xlsx
for a listing of available output channels, (-)
"HSSBrTqC"
"GenTq"
"GenPwr"
END of input file (the word "END" must appear in the first 3 columns of this last OutList line)
---------------------------------------------------------------------------------------
```